Result & Discussion

Chapter 5

Result and Discussion

5.1 Preliminary phytochemical screening of crude extracts

In the present work, crude extract yield of TUME, CMME, and SIME was found to be 17.4, 13.44, and 12.4 % respectively (Table 5.1). However, TUME (Methanolic extract of *Tecomella undulata* bark) showed maximum yield among the extracts. Qualitative phytochemical screening of TUME, CMME, and SIME crude extracts has confirmed the presence of secondary metabolites such as carbohydrates, glycosides, saponins, flavonoids, triterpenoids, sterols, phenolic compounds/tannins, proteins, and amino acids in variable proportions.

Table 5.1: Yield (%) and phytochemical screening of crude extract of *Tecomella undulata* bark, *Citrus medica* fruit, and *Sesamum indicum* seed

Class	TUME	CMME	SIME
% Yield	17.4 %	13.44 %	12.4 %
Appearance	Dark blood red	Dark Brown	Brown
Phytochemical			
Alkaloid	+	-	-
Carbohydrates	+	+	+
Phytosterols	+	+	+
Tannins	+	+	+
Proteins & Amino Acids	-	+	+
Flavonoids	+	+	+
Glycosides	+	+	+
Saponins	+	-	-
Gum/Mucilage	-	+	-

TUME – *Tecomella undulata* methanolic extract, CMME – *Citrus medica* methanolic extract, SIME – *Sesamum indicum* methanolic extract

TUME is rich phytochemical composition and therapeutic potential are highlighted by phytochemical screening. Its traditional medical uses have a scientific basis thanks to the identified bioactive chemicals, which include alkaloids (Laghari, A.Q. et. Al 2014), flavonoids (Rohilla R, 2014), tannins (Khare CP 2007), saponins (Parveen, T., & Sharma, K. 2014), glycosides (Rohilla R, 2014), and terpenoids (Mohibb AM, 2000). To enable *Tecomella undulata* bark extract's development as a useful therapeutic agent in contemporary medicine, more research is required to clarify the precise pharmacological mechanisms and therapeutic advantages of the extract.

The phytochemical analysis of *Citrus medica* fruit extract (CMME) indicates a varied range of bioactive components, including phenolic and flavonoid compounds (Dadwal, V et.al. 2022), Coumarins (Chan, Y. Y., et.al. 2017), fatty acid and triterpenoids (Patil, S.J. 2009), amino acids (Dadwal, V et.al. 2022). CMME may have health benefits due to its phytoconstituents, which have been linked to antioxidant, anti-inflammatory, antibacterial, and other pharmacological actions. More study, including pharmacological investigations and clinical trials, is needed to better understand the specific mechanisms of action and therapeutic applications of *Citrus medica* fruit extract in human health and disease.

The phytochemical analysis of *Sesamum indicum* seed extract indicates a varied range of bioactive components, including phenolic compounds (Patel, K., et.al 2017), phytosterols (Meghwal, M., & Goswami, T. K. 2012), sesaminol glucosides (Hirata, F. et.al 1996), vitamin (Fasuan, T.O. et.al 2018), Protein (Hegde, D.M. 2012) and amino acids (Wang, R. et.al 2020). These phytoconstituents contribute to sesame seeds' nutritional and therapeutic qualities, including antioxidant, anti-inflammatory, and cardioprotective actions. More research is needed to determine the mechanisms of action and therapeutic potential of specific chemicals, opening the way for the development of sesame seed-derived products for health promotion and disease prevention.

5.2 Phytochemical Analysis of Crude Extract

The results of the Phytochemical analysis of crude extracts are shown in Table 5.2.

Table 5.2: Phytochemical analysis of a crude extract of *Tecomella undulata* bark, *Citrus medica* fruit, and *Sesamum indicum* seed

	Value (%w/w)

Sr. No.	Physicochemical Parameter	*T.undulata bark*	*C.medica* fruit	*S.indicum* seed
1.	Total Ash value	7.87± 1.38	4.66± 1.03	2.67 ± 0.32
2.	Water soluble ash	1.75 ± 0.08	2.66 ± 0.12	1.25 ± 0.06
3.	Acid insoluble ash	0.87 ± 0.04	0.17 ± 0.06	0.487 ± 0.03
4.	Cold water-soluble extractive	9.8 ± 0.23	21.00 ± 0.68	9.2 ± 0.45
5.	Hot water-soluble extractive	11.1 ± 0.66	51.5 ± 1.08	10.45 ± 0.78
6.	Ethanol soluble extractive	24.9 ± 0.89	25.66 ± 1.0	13.65 ± 1.1
7.	Loss on drying	6.97 ± 0.35	16.50 ± 0.47	3.45 ± 0.58
8.	Foreign matter	Nil	Nil	Nil
9.	Foaming index	<100	<100	<100
10.	Swelling index	5.32 ± 0.18 ml	1 ± 0.21 ml	2.10 ± 0.11 ml
11.	Solvent Residue	No	No	No

Values expressed as mean ± SEM with n = 3.

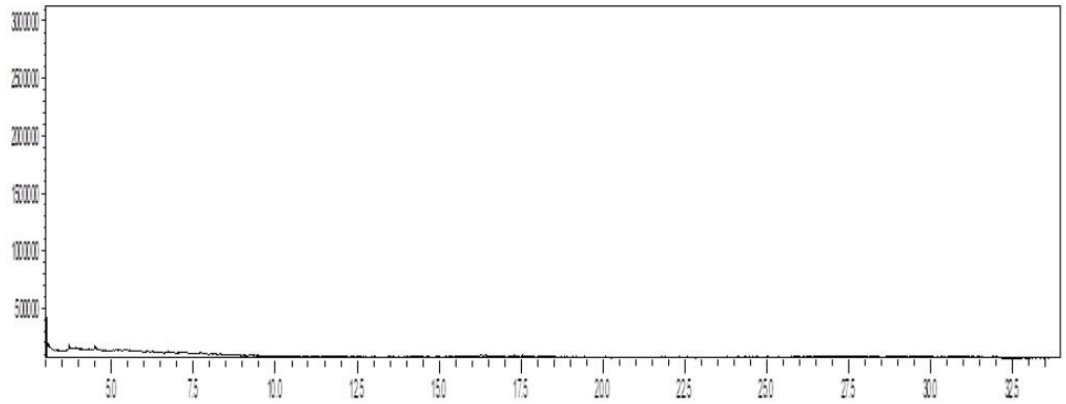

Figure. 5.1: Chromatogram of the solvent residue of *C.medica* methanolic extract

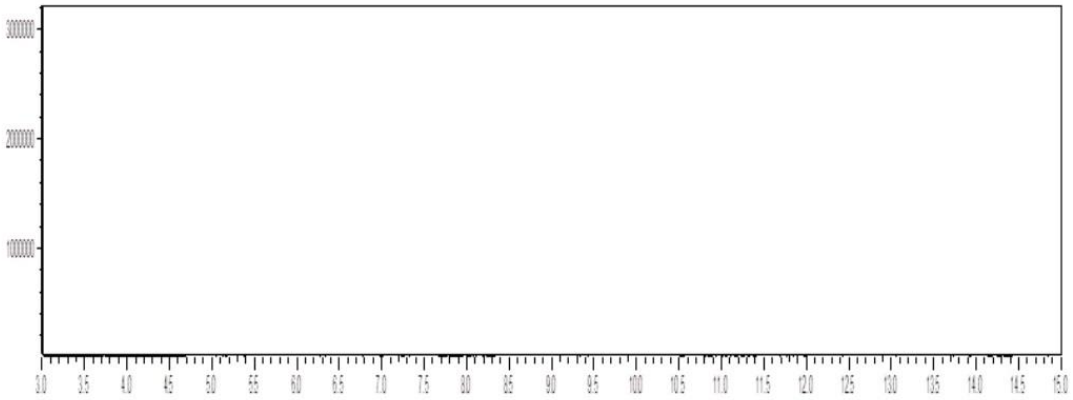

Figure 5.2: Chromatogram of the solvent residue of *T.undulata* methanolic extract

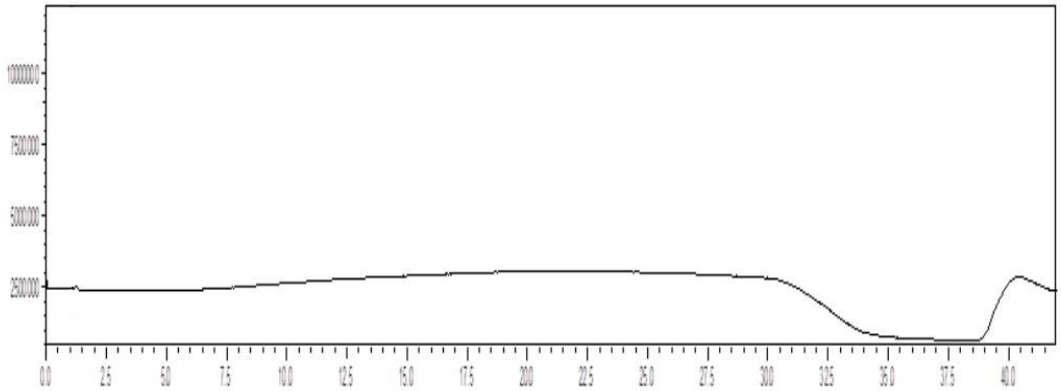

Figure 5.3: Chromatogram of the solvent residue of *S.indicum* methanolic extract

In Figures 5.1, 5.2, and 5.3, a typical chromatogram is displayed. It was noted from the chromatogram that there was no solvent peak. Thus, it was determined that there were no organic solvents present in any of the corresponding plant extracts.

5.3 Result of Total phenolic content of crude extract

From the results of the total phenolic content (TPC) analysis, the CMME contained a reasonable amount of TPC. The TPC was calculated using the regression equation of the standard curve plotted using tannic as standard (Figure 5.4B). Among the crude extracts, CMME possessed the highest levels of total phenolic (256.36 ± 9.38 mg TAE/g dry wt. of extract) while SIME possessed the lowest amount of total phenolics (155.65 ± 7.98 mg TAE/g dry wt. of extract). TUME contained 209.89 ± 8.64 mg TAE/g dry wt. extract (Figure 5.4A & Table 5.3).

Phenolics are one of the many varieties of phytochemicals that are secondary metabolites found in food and medicinal plants. The potential natural antioxidant

benefits of polyphenols and the role of reactive oxygen species in various pathobiological manifestations have been thoroughly examined and documented in earlier research works by Pietta P. G. (2000) and Møller, J.K. et al. (1999). CMME has the highest phenolic content 256.36 mg/TAE among the other crude extract. Similar findings of the total phenolic content of *Sesamum indicum* seeds, *Tecomella undulata*, and *C. medica* fruit have been published by Sharma, R.A. et al. (2013), Elhanafi, L. et al. (2019), and Gilani, F. et al. (2023).

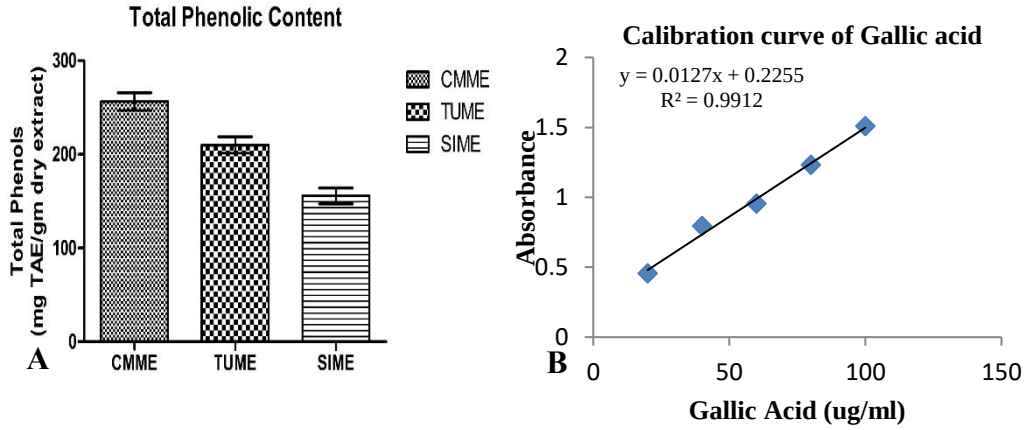

Figure 5.4: A) Total phenolic content of crude extracts B) Calibration curve of Gallic acid

Table 5.3: Total Phenolic content of crude extracts

Name of Extract	Total phenolic content (mg GAE/g)
CMME	256.36 ± 9.38
TUME	209.89 ± 8.64
SIME	155.65 ± 7.98

Values expressed as mean ± SEM with n = 3. TUME – *Tecomella undulata* methanolic extract, CMME – *Citrus medica* methanolic extract, SIME – *Sesamum indicum* methanolic extract

5.4 Result of Total flavonoid content of crude extract

From the results of the total Flavonoid content (TFC) analysis, the CMME contained a reasonable amount of TFC. The TFC was calculated using the regression equation of the standard curve plotted using Quercetin as standard (Figure 5.5B). Among the crude extracts, CMME possessed the highest levels of total phenolic (162.11 ± 0.74 mg QUE/g dry wt. of extract) while SIME possessed the lowest amount of total phenolics (84.13 ± 8.25 mg QUE/g dry wt. of extract). TUME contained 146.13 ± 0.83 mg QE/g dry wt. extract (Figure 5.5A & Table 5.4).

Fruits, vegetables, and medicinal plants are rich sources of flavonoids, a broad group of polyphenolic chemicals. They have a reputation for having anti-coagulant, anti-inflammatory, and antioxidant qualities, among other health-promoting qualities (Kim, H. et al. 2015). Therefore, when compared to other crude extracts, CMME had the highest quantity of flavonoids. According to research, phenolic compounds' primary sources of antioxidant activity include their redox characteristics, ability to donate hydrogen, singlet oxygen quenching capabilities, and chain breaking prowess (Rice-Evans, C. A., et al. 1995). Similar results about the total flavonoid content of *C. medica* fruit, *Tecomella undulata*, and *Sesamum indicum*seeds have been published by Elhanafi, L. et al. (2019), Gilani, F. et al. (2023), and Sharma, R.A. et al. (2013).

Table 5.4: Total Flavonoid content of crude extracts

Name of fractions	Total flavonoid content (mg QUE/g)
CMME	162.11 ± 0.74
TUME	146.13 ± 0.83
SIME	84.13 ± 8.25

Values expressed as mean ± SEM with n = 3. TUME – *Tecomella undulata* methanolic extract, CMME – *Citrus medica* methanolic extract, SIME – *Sesamum indicum* methanolic extract

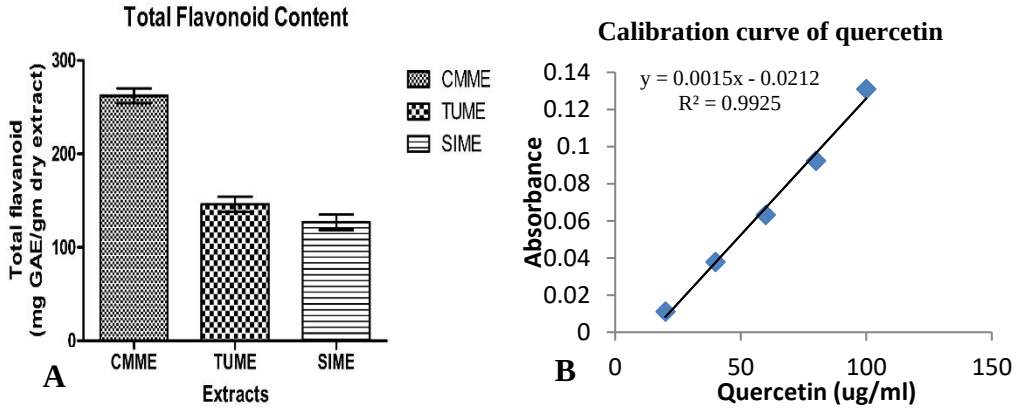

Figure 5.5: A) Total flavonoid content of crude extracts B) Calibration curve of Quercetin

5.5 Result of Total antioxidant capacity of crude Extract

The total antioxidant capacity (TAC) of crude extracts in the order of CMME>TUME>SIME is shown in Figure 5.6A. The total antioxidant activity is expressed as ascorbic acid equivalent (AAE). The CMME exhibited the highest total

antioxidant activity (278.32 ± 5.85 mg AAE) followed by TUME (157.55 ± 4.50 mg AAE), SIME (124.36 ± 8.33± 5.26 mg AAE).

The composition of the extract and the analytical test system both have a significant impact on the antioxidant capability of plant extracts and their fractions. To account for the diverse mechanisms of antioxidant activity, it is required to do many types of antioxidant capacity assays (Frankel and Meyer, 2000). This will yield more accurate results. Therefore, tests based on various methodologies are used to estimate the total phenolic content, total phenolic content, and total antioxidant activity to evaluate the antioxidant capabilities of CMME, TUME, and SIME. Due to the presence of a high concentration of phenolic and flavonoid groups, the findings indicate that CMME has a greater capacity for antioxidants than TUME, which has a comparable amount of these groups to exhibit antioxidant properties. These findings are consistent with those of other researchers, including Elhanafi, L. et al. (2019), Gilani, F. et al. (2023), and Sharma, R.A. et al. (2013).

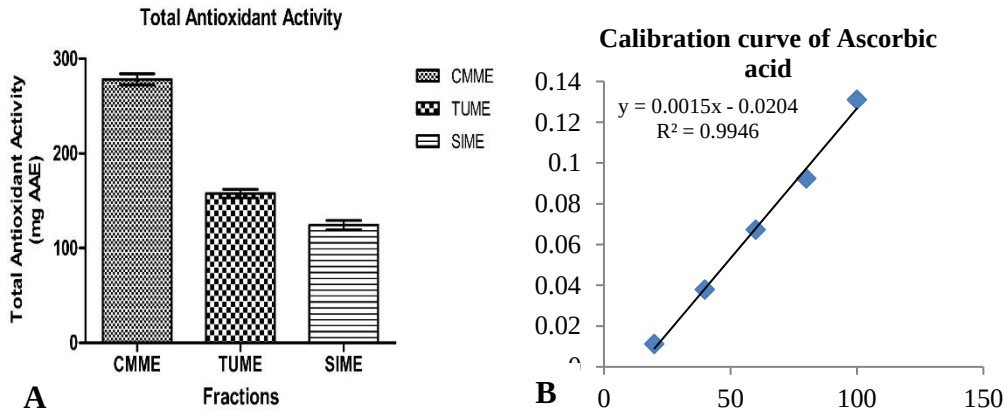

Figure 5.6: A) Total Antioxidant capacity of crude extracts B) Calibration curve of Ascorbic acid

Table 5.5: Total Antioxidant capacity of crude extracts

Name of fractions	Total Antioxidant capacity (mg AAE/g)
CMME	278.32 ± 5.85
TUME	157.55 ± 4.50
SIME	124.36 ± 8.33

Values expressed as mean ± SEM with n = 3. TUME – *Tecomella undulata* methanolic extract, CMME – *Citrus medica* methanolic extract, SIME – *Sesamum indicum* methanolic extract

5.6 *In-vitro* anticoagulant activity of crude extracts

5.6.1 Blood clotting time measurement

The crude extract of *Tecomella undulata* bark, *Citrus medica* fruit, and *Sesamum indicum* seed was discovered to affect clotting time. The experimental results showed that increasing the concentration of all extracts delayed the clotting time. Clotting time was highest at CMME (200 mg/ml) (18.29 ± 0.84), followed by 250 mg/ml of TUME (16.41 ± 0.94), and 300 mg/ml of SIME (16.41 ± 0.94). However, above this concentration, clotting time is reduced with increasing concentration. Figure 5.7 depicts these findings. This study indicates the existence of anticoagulants in CMME, TUME, and SIME, implying that their optimal function occurs within a certain range.

Table 5.6: *In-vitro* clotting time of varying concentrations of crude extracts

Concentration (mg/ml)	**Clotting Time (Minutes)**			
	NS	**CMME**	**TUME**	**SIME**
50	7.2 ± 0.54	8.12 ± 1.06^{ns}	7.34 ± 0.77^{ns}	7.27 ± 0.86^{ns}
100	7.2 ± 0.54	10.13 ± 0.95*	9.23 ± 1.06^{ns}	7.93 ± 0.74^{ns}
150	7.2 ± 0.54	16.54 ± 1.18**	14.3 ± 1.05**	8.25 ± 0.88^{ns}
200	7.2 ± 0.54	18.29 ± 0.84$^{\#}$	15.37 ± 0.91**	9.32 ± 0.85*
250	7.2 ± 0.54	18.08 ± 0.73$^{\#}$	16.41 ± 0.94**	11.28 ± 1.09*
300	7.2 ± 0.54	16.19 ± 1.03**	14.5 ± 0.95**	13.34 ± 0.85**
350	7.2 ± 0.54	15.05 ± 0.53**	13.33 ± 0.9**	12.23 ± 1.12*
400	7.2 ± 0.54	14.45 ± 0.59**	12.24 ± 0.85*	9.18 ± 1.01^{ns}
450	7.2 ± 0.54	14.15 ± 0.84**	12 ± 1.23*	8.98 ± 0.74^{ns}
500	7.2 ± 0.54	13.55 ± 0.64**	11.33 ± 1.15*	8.56 ± 0.78^{ns}

Results are expressed as Mean ± SE values (n=3). All extracts were suspended in saline. *p<0.05, **p<0.01, #p<0.001 significant when compared with Normal saline (vehicle control group) using one way ANOVA analysis. TUME – *Tecomella undulata* methanolic extract, CMME – *Citrus medica* methanolic extract, SIME – *Sesamum indicum* methanolic extract

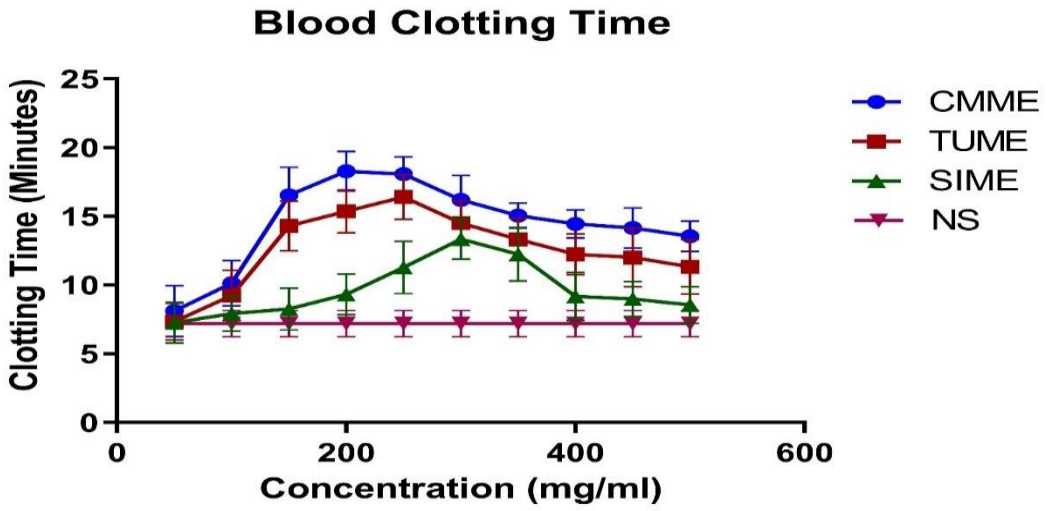

Figure 5.7: *In-vitro* Blood clotting time of varying concentration of Crude extracts

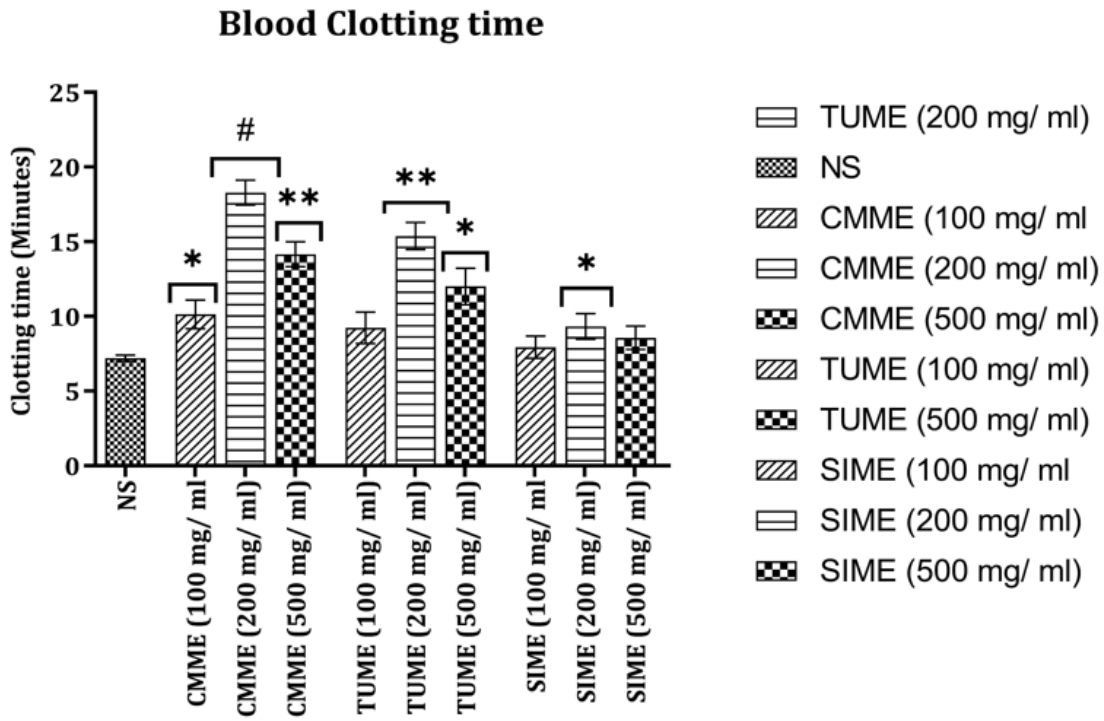

Figure 5.8: *In-vitro* Blood clotting time of Crude extracts at 100, 200 and 500 mg/ml concentration

To further examine the effect on blood clotting time, The extracts with the strongest effect on clotting time were tested at doses of 100, 200, and 500 mg/mL. At a dosage of 200 mg/mL, CMME significantly ($p>0.001$) delayed clotting time (18.29 ± 0.84) more than TUME ($P>0.01$) (15.37 ± 0.91) and SIME ($P>0.05$) (9.32 ± 0.85). At a dose of 100 mg/ml, only CMME was significant ($P>0.05$) at 10.13 ± 0.95 minutes. At a dosage of 500 mg/ml, CMME was significant ($P>0.01$) at 13.55 ± 0.64 minutes and

TUME (P>0.05) at 11.33 ± 1.15. SIME did not have a meaningful effect on blood clotting time at the same dosage level (Figure 5.8).

5.6.2 Prothrombin time (PT) activity assay

At a concentration of 200 mg/mL, all extracts of CMME, TUME, and SIME displayed a noteworthy (P < 0.05) increase in the Prothrombin Time (PT) compared to the control (Figure 5.9). To further study the effects on Prothrombin time (PT), the extracts with the greatest effect on clotting time were evaluated at doses of 100, 200, and 500 mg/mL. PT was significantly prolonged (P<0.001) at all tested concentrations (100, 200, and 500 mg/mL) compared to the control (Table 5.7).

Table 5.7: *In-vitro* prothrombin time (PT) and Activated prothrombin time (APTT) of crude extracts.

Group	PT Time (Seconds)	APPT Time (Seconds)
NS	12.93 ± 0.65	23.67 ± 2.08
CMME (100 mg/ml)	13.57333 ± 1.45	50.67 ± 6.81**
CMME (200 mg/ml)	20.12667 ± 1.06 #	93.67 ± 6.11#
CMME (500 mg/ml)	16.44 ± 1.06 **	72.00 ± 6.18#
TUME (100 mg/ml)	13.39 ± 1.13	44.33 ± 6.58*
TUME (200 mg/ml)	18.83 ± 1.39**	63.67 ± 7.02#
TUME (500 mg/ml)	15.97 ± 1.39*	50.33 ± 6.23**
SIME (100 mg/ml)	13.10 ± 1.44	38.67 ± 6.54
SIME (200 mg/ml)	16.25 ± 2.12 *	46.67 ± 7.64*
SIME (500 mg/ml)	14.66 ± 1.08	43.33 ± 6.43*

Results are expressed as Mean ± SE values (n=3). All extracts were suspended in saline. *p<0.05, **p<0.01, #p<0.001 significant when compared with Normal saline (vehicle control group) using one way ANOVA analysis. TUME – *Tecomella undulata* methanolic extract, CMME – *Citrus medica* methanolic extract, SIME – *Sesamum indicum* methanolic extract

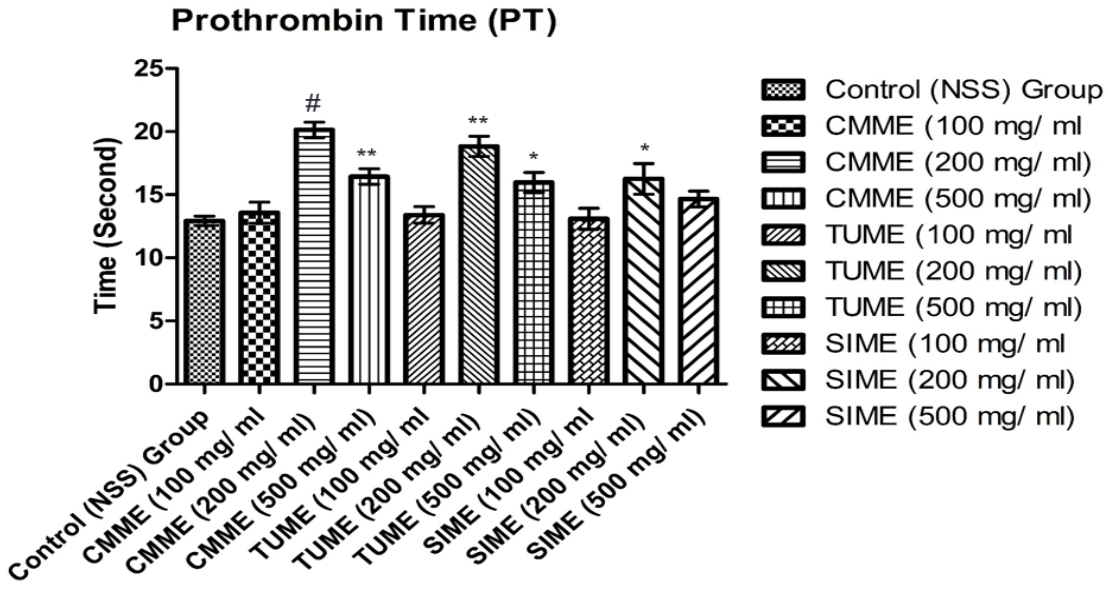

Figure 5.9: *In-vitro* Prothrombin time of Crude extracts

At all concentrations, the CMME consistently had a considerably longer PT than TUME and SIME ($P < 0.001$). At a concentration of 100 mg/ml, SIME, TUME, and CMME PTs were 13.10 ± 1.44, 13.39 ± 1.13, and 13.57 ± 1.45, respectively, with no significant difference from the normal group. At a concentration of 200 mg/mL, CMME had a significantly higher PT (20.12667 ± 1.06) than TUME (18.83 ± 1.39) or SIME (16.25 ± 2.12). At a concentration of 500 mg/ml, CMME was significant ($P<0.01$) at 13.55 ± 0.64 seconds and TUME ($P<0.05$) at 11.33 ± 1.15. SIME had no significant effect on prothrombin time at the same dosage level (Figure 5.9).

5.6.3 Activated Partial Thromboplastin time (APTT) activity assay.

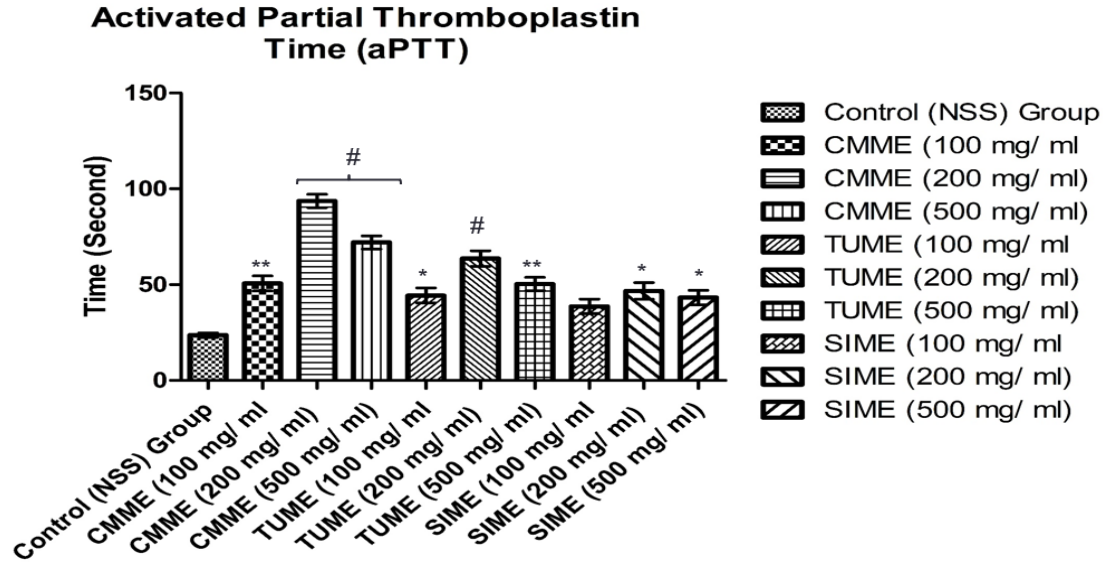

Figure 5.10: *In-vitro* Activated Partial Thromboplastin time of Crude extracts.

To further study the effects on Activated Partial Thromboplastin time (APPT), the extracts with the greatest effect on clotting time were evaluated at doses of 100, 200, and 500 mg/mL. APTT was significantly prolonged ($P< 0.001$) at all tested concentrations (100, 200, and 500 mg/mL) compared to the control (Table 5.7). At all concentrations, the CMME consistently had a considerably longer APPT than TUME and SIME ($P < 0.001$). At a concentration of 100 mg/ml, SIME, TUME, and CMME PTs were 38.67 ± 6.54, 44.33 ± 6.58, and 50.67 ± 6.81, respectively, with no significant difference from the normal group. At a concentration of 200 mg/mL, CMME had a significantly higher APPT (93.67 ± 6.11) than TUME (63.67 ± 7.02) or SIME (46.67 ± 7.64). At a concentration of 500 mg/ml, CMME was significant ($P>0.01$) at 72.00 ± 6.18 minutes, and TUME ($P>0.05$) at 50.33 ± 6.23. SIME (43.33 ± 6.43) had no significant effect on APTT at the same concentration (Figure 5.10).

To control blood coagulation in a variety of medical illnesses, including cardiovascular disease, diabetes mellitus, and bleeding disorders, a broad spectrum of anticoagulant and procoagulant drugs are frequently utilized. Nevertheless, a lot of these medications have unfavorable side effects. Finding and creating novel anticoagulant and procoagulant medications with fewer side effects is therefore necessary. The biological activities of carotenoids (Melo et al., 2013), polyphenols (Bojic et al., 2019), flavonoids (Guglielmonea et al., 2022), and polysaccharides (Amira M, 2017) are known to include antithrombotic, antiplatelet, anticoagulant, and antioxidant properties. While several terpenoids are known for their antioxidant qualities, researchers have shown that tannins have anticoagulant effects (Li, J., et al., 2014). Furthermore, saponins have been shown to have antiplatelet, anticoagulant, and fibrinolytic characteristics (Mosa et al., 2011).

The parameters for clotting to evaluate the clotting process, PT and aPTT are crucial. Whereas aPTT analyzes elements connected to the intrinsic and common routes, PT assesses the activity of components linked to the extrinsic coagulation pathway. While aPTT is usually used to assess the efficiency of heparin therapies, PT is frequently used to track the efficacy of coumarin therapy (vitamin K antagonists) (Davison C 2011). In a clinical assessment, abnormally prolonged PT and/or aPTT signal anomalies in the activity of clotting factors. For instance, if PT is normal but aPTT is protracted, this may indicate that factors VIII, IX, and XI associated with the contact pathways need

to be examined (Achneck et al., 2010). However, if prothrombin (factor II) and factors V, X, and PT are also impacted, problems with the common pathway are likely present. From the result, CMME and TUME have prolonged clotting time, PT, and aPTT suggesting that prothrombin, factors X, and V in the common coagulation pathway are inhibited. It will take more research to identify the precise mechanism underlying this suppression.

5.7 Preliminary phytochemical screening of Fractions

Based on the result of the *invitro* anticoagulant activity of the crude extract, Potent crude extracts of *C.medica* and *T.undualta* are partitioned using the liquid-liquid solvent extraction method.

5.7.1 Preliminary Phytochemical Screening of *C.medica* Fractions

In the present work, the fraction yield of CMPEF, CMBF, CMEAF, CMBUF, and CMWF was found to be 2, 1.4, 10.7, 23.1, and 7.7 % respectively (Table 5.8). However, CMBUF (butanol fraction of *C.medica*) showed maximum yield among the fractions. Qualitative phytochemical screening of CMPEF, CMBF, CMEAF, CMBUF, and CMWF has confirmed the presence of secondary metabolites such as carbohydrates, glycosides, saponins, flavonoids, triterpenoids, sterols, phenolic compounds/tannins, proteins, and amino acids in variable proportions.

Table 5.8: Yield (%) and phytochemical screening of fractions of *Citrus medica* fruit

Class	CMPEF	CMBF	CMEAF	CMBUF	CMWF
% Yield	2 %	1.4 %	10.7 %	23.1 %	7.7 %
Appearance	Cream	Pale Brown	Pale Brown	Dark Brown	Dark Brown
Phytochemical					
Alkaloid	-	-	-	+	+
Carbohydrates	-	-	+	+	+
Phytosterols	+	+	-	+	+
Tannins	+	+	-	+	+

Proteins & Amino Acids	-	-	-	+	+
Flavonoids	-	-	+	+	+
Glycosides	-	-	-	+	+
Saponins	-	-	+	+	+
Gum/Mucilage	-	-	-	+	+

CMPEF – *Citrus medica* petroleum ether fraction, CMBF - *Citrus medica* benzene fraction, CMEAF - *Citrus medica* ethyl acetate fraction, CMBUF - *Citrus medica* butanol fraction, CMWF - *Citrus medica* water fraction

5.7.2 Preliminary Phytochemical Screening of *T.undulata* Fractions

Table 5.9: Yield (%) and phytochemical screening of fractions of *Tecomella undulata* bark

Class	TUPEF	TUBF	TUEAF	TUBUF	TUWF
% Yield	0.5 %	1.9 %	6.7 %	17.1 %	7.4 %
Appearance	Light Yellow	Colourless	Red	Dark Red	Dark Red
Phytochemical					
Alkaloid	-	-	-	+	-
Carbohydrates	-	-	-	+	-
Phytosterols	+	+	+	+	-
Tannins	-	-	+	+	-
Proteins & Amino Acids	-	-	-	+	-
Flavonoids	-	-	+	+	+
Glycosides	-	-	-	+	+
Saponins	-	-	+	+	+
Gum/Mucilage	-	-	-	-	-

TUPEF – *Tecomella undulata* petroleum ether fraction, TUBF - *Tecomella undulata* benzene fraction, TUEAF - *Tecomella undulata* ethyl acetate fraction, TUBUF - *Tecomella undulata* butanol fraction, TUWF - *Tecomella undulata* water fraction

In the present work, the fraction yield of TUPEF, TUBF, TUEAF, TUBUF, and TUWF was found to be 0.5, 1.9, 6.7, 17.1, and 7.4 % respectively (Table 5.9). However, TUBUF (butanol fraction of *T.undulata*) showed maximum yield among the fractions. Qualitative phytochemical screening of TUPEF, TUBF, TUEAF, TUBUF, and TUWF has confirmed the presence of secondary metabolites such as carbohydrates, glycosides, saponins, flavonoids, triterpenoids, sterols, phenolic compounds/tannins, proteins, and amino acids in variable proportions.

Because plant fraction's antioxidant compounds have a higher affinity for polar solvents than non-polar ones, this could explain the polarity-dependent increases in fraction yield, presence of secondary metabolites, total phenolic content, total flavonoid content, antioxidant activity, reducing properties, and free radical scavenging activity (Nawaz, H. et.al 2020). In result finding, it shows variation in percentage yield and the presence of secondary metabolites in different fractions of CMME and TUME.

5.8 Result of Total phenolic content of fractions

5.8.1 Result of total phenolic content of fraction of *C.medica*

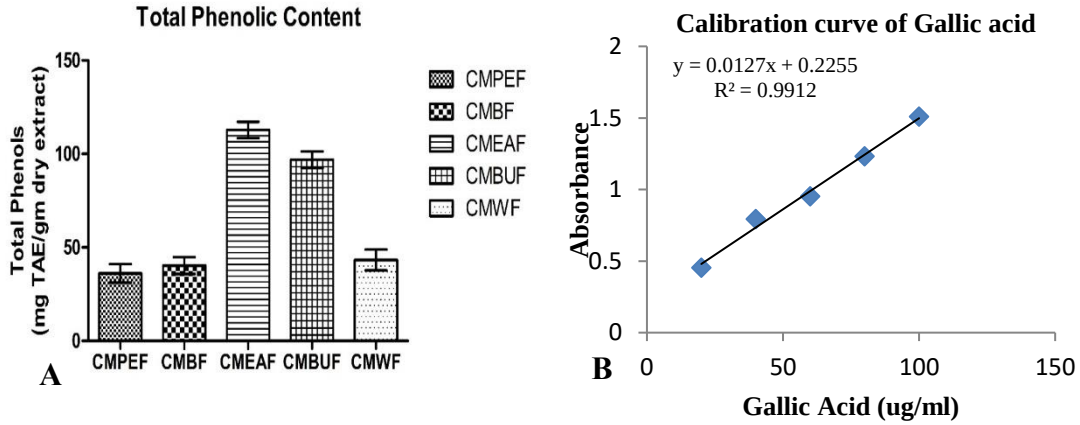

Figure 5.11: A) Total phenolic content of fraction of *C.medica* B) Calibration curve of Gallic acid

Table 5.10: Total Phenolic content of fractions of *Citrus medica* fruit

Name of fractions	Total phenolic content (mg GAE/g)
CMPEF	21.23 ± 2.97
CMBF	36.33 ± 2.74
CMEAF	175.77 ± 2.58
CMBUF	96.89 ± 2.67
CMWF	45.34 ± 2.82

Values expressed as mean ± SEM with n = 3. CMPEF – *Citrus medica* petroleum ether fraction, CMBF - *Citrus medica* benzene fraction, CMEAF - *Citrus medica* ethyl acetate fraction, CMBUF - *Citrus medica* butanol fraction, CMWF - *Citrus medica* water fraction

The total phenolic content of the fractions of *C.medica* was calculated and reported in milligrams of gallic acid equivalents per gram of dry weight. The results are shown in Table 5.10. CMEAF had the highest phenolic content of the fractions (175.77 ± 2.58 mg GAE/g), followed by CMBUF (96.89 ± 2.67 mg GAE/g), CMWF (45.34 ± 2.82 mg GAE/g), CMBF (36.33 ± 2.74mg GAE/g), CMPEF (21.23 ± 2.97 mg GAE/g) as shown in figure 5.11.

5.8.2 Result of total phenolic content of fraction of *T.undulata*

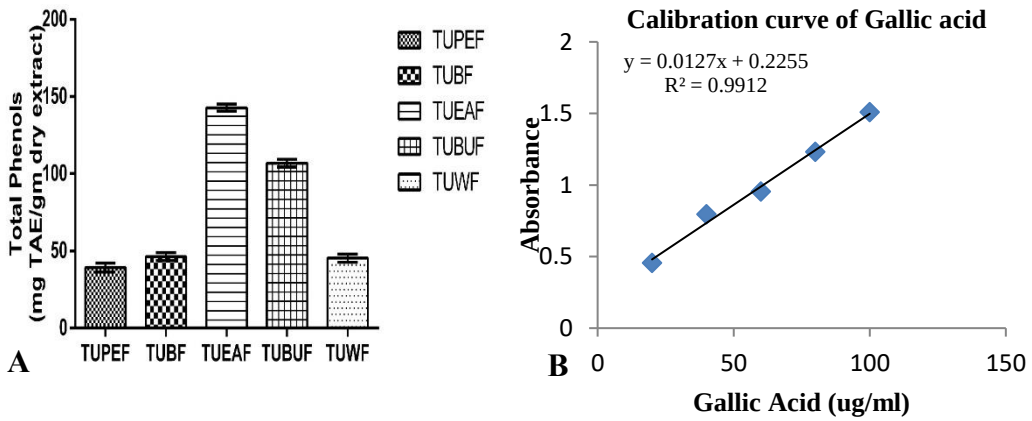

Figure 5.12: A) Total phenolic content of fraction of *T.undulata* B) Calibration curve of Gallic acid

Table 5.11: Total Phenolic content of fractions of *T.undulata* bark

Name of fractions	Total phenolic content (mg GAE/g)
TUPEF	39.23 ± 2.87
TUBF	46.33 ± 2.54
TUEAF	172.77 ± 2.38
TUBUF	106.89 ± 2.47

TUWF	45.34 ± 2.52

Values expressed as mean ± SEM with n = 3. TUPEF – *Tecomella undulata* petroleum ether fraction, TUBF - *Tecomella undulata* benzene fraction, TUEAF - *Tecomella undulata* ethyl acetate fraction, TUBUF - *Tecomella undulata* butanol fraction, TUWF - *Tecomella undulata* water fraction

The total phenolic content of the fractions of *T.undulata* was calculated and reported in milligrams of gallic acid equivalents per gram of dry weight. The results are shown in Table 5.11. TUEAF had the highest phenolic content of the fractions (172.77 ± 2.38 mg GAE/g), followed by TUBUF (106.89 ± 2.47 mg GAE/g), TUBF (46.33 ± 2.54 mg GAE/g), TUWF (45.34 ± 2.52 mg GAE/g), TUPEF (39.23 ± 2.87 mg GAE/g) as shown in figure 5.12A.

When evaluating plant extracts for possible health benefits and medicinal applications, one of the most important metrics to consider is their total phenolic content (TPC). Due to their demonstrated antioxidant activity, phenolic compounds have been connected to a number of health-promoting characteristics, including as anti-inflammatory, anti-cancer, and cardioprotective qualities (Rice-Evans et al., 1996). The total phenolic content of various fractions in *C.medica* and *T.undulata* offers important insights on the distribution of phenolic compounds within the plant and the possible uses of these fractions in nutritional and therapeutic contexts.

The total phenolic content of the *C.medica* and *T.undulata* fractions were calculated for the study and expressed as milligrams of gallic acid equivalents per gram of dry weight (mg GAE/g) (Soobrattee et al., 2005). Because gallic acid shares many structural similarities with phenolic compounds found in plants, it is frequently employed as a standard reference compound for the quantification of phenolic compounds.

The fractions of *C.medica* and *T.undulata* showed various degrees of total phenolic content, as shown by the data in Tables 5.9 and 5.10. CMEAF and TUEAF showed the highest phenolic content at 175.77 ± 2.58 and 172.77 ± 2.38 mg GAE/g. This suggests that, in comparison to other fractions, the ethyl acetate fraction of both plants is especially rich in phenolic chemicals. CMBU, and TUBUF showed a comparatively high phenolic content of 96.89 ± 2.67 and 106.89 ± 2.47 mg GAE/g, showing considerable phenolic content as well.

5.9 Result of Total flavonoid content of fractions

5.9.1 Result of total flavonoid content of fraction of *C.medica*

The total flavonoid content of the fractions of *C.medica* was calculated and reported in milligrams of quercetin equivalents per gram of dry weight. The results are shown in Table 5.12. CMEAF had the highest flavonoid content of the fractions (41.81 ± 0.91 mg QAE/g), followed by CMBUF (38.14 ± 0.88 mg QAE/g), CMWF (12.22 ± 0.89mg QAE/g), CMBF (10.26 ± 0.87 mg QAE/g), CMPEF (9.54 ± 0.84 mg QAE/g) as shown in figure 5.13A.

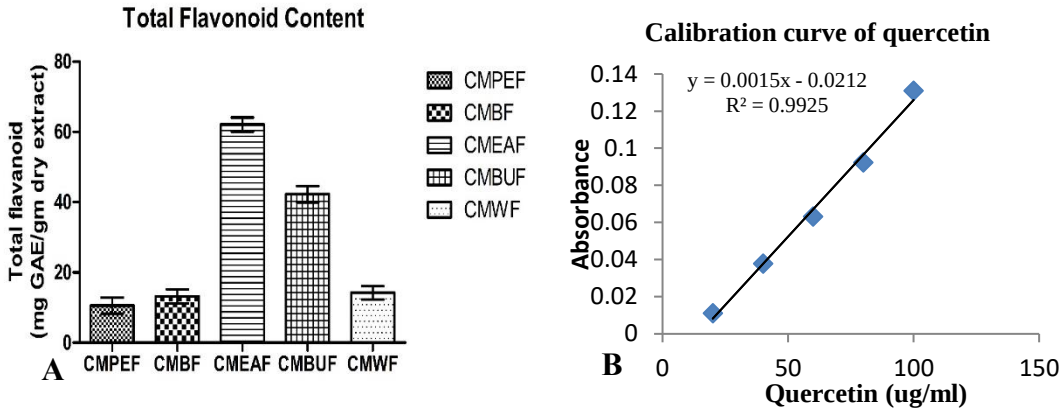

Figure 5.13: A) Total flavonoid content of fraction of *C.medica* B) Calibration curve of quercetin

Table 5.12: Total flavonoid content of fractions of *Citrus medica* fruit

Name of fractions	Total flavonoid content (mg QAE/g)
CMPEF	09.54 ± 0.84
CMBF	10.26 ± 0.87
CMEAF	41.81 ± 0.91
CMBUF	38.14 ± 0.88
CMWF	12.22 ± 0.89

Values expressed as mean ± SEM with n = 3. CMPEF – *Citrus medica* petroleum ether fraction, CMBF - *Citrus medica* benzene fraction, CMEAF - *Citrus medica* ethyl acetate fraction, CMBUF - *Citrus medica* butanol fraction, CMWF - *Citrus medica* water fraction

5.9.2 Result of total flavonoid content of fraction of *T.undulata*

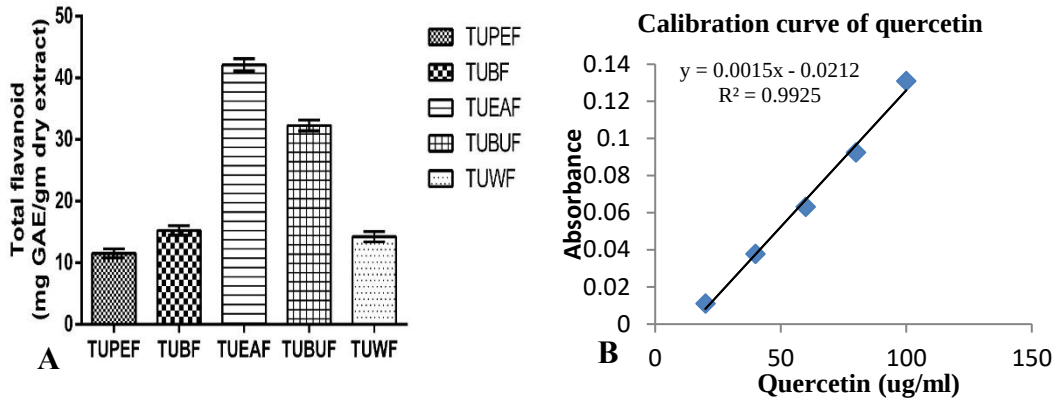

Figure 5.14: A) Total flavonoid content of fraction of *T.undulata* B) Calibration curve of quercetin

Table 5.13: Total flavonoid content of fractions of *Tecomella undulata* bark

Name of fractions	Total flavonoid content (mg QAE/g)
TUPEF	11.54 ± 0.74
TUBF	15.26 ± 0.83
TUEAF	42.11 ± 0.98
TUBUF	36.24 ± 0.81
TUWF	14.22 ± 0.79

Values expressed as mean ± SEM with n = 3. TUPEF – *Tecomella undulata* petroleum ether fraction, TUBF - *Tecomella undulata* benzene fraction, TUEAF - *Tecomella undulata* ethyl acetate fraction, TUBUF - *Tecomella undulata* butanol fraction, TUWF - *Tecomella undulata* water fraction

The total flavonoid content of the fractions of *T.undulata* was calculated and reported in milligrams of quercetin equivalents per gram of dry weight. The results are shown in Table 5.13. TUEAF had the highest flavonoid content of the fractions (42.11 ± 0.98 mg QAE/g), followed by TUBUF (36.24 ± 0.81 mg QAE/g), TUBF (15.26 ± 0.83 mg QAE/g), TUWF (14.22 ± 0.79 mg QAE/g), TUPEF (11.54 ± 0.74 mg QAE/g) as shown in figure 5.14A.

An important measure of plant extracts' potential health-promoting qualities is their total flavonoid content (TFC), which includes their anti-inflammatory, antioxidant, and other pharmacological effects. Plants contain a vast range of polyphenolic chemicals called flavonoids, which are recognized for their diverse range of bioactivities. The total flavonoid concentration of various fractions of *C.medica*, *T.undulata*, offers important information about the distribution of flavonoids within the plant and the possible uses of these fractions in nutritional and therapeutic applications. The

flavonoid concentration of CMEAF and TUEAF was found to be the highest among the fractions, with values of 41.81 ± 0.91 and 42.11 ± 0.98 mg QAE/g, respectively, as indicated by the results shown in Tables 5.12 and 5.13. Compared to other fractions, this suggests that the ethyl acetate fraction of both plants is especially rich in flavonoids. TUBUF, which came after CMBUF, also indicated a noteworthy flavonoid content, with a comparatively high flavonoid content of 38.14 ± 0.88 and 36.24 ± 0.81 mg QAE/g.

Overall, finding the total flavonoid content in various *T.undulata* and *C.medica*, fractions offers important new information about the distribution of flavonoids in these plants and their possible health advantages. To enable the creation of innovative dietary supplements and medicinal products using extracts from *T.undulata* and *C.medica*, more research is necessary to clarify the precise flavonoid molecules found in each fraction and their associated bioactivities.

5.10 Result of Total antioxidant capacity of fractions

5.10.1 Result of total antioxidant capacity of a fraction of *C.medica*

The total antioxidant capacity of the fractions of *C.medica* was calculated and reported in milligrams of ascorbic acid equivalents per gram of dry weight. The results are shown in Table 5.14. CMEAF had the highest antioxidant capacity (188.42 ± 4.75 mg AAE/g), followed by CMBUF (139.65 ± 5.35 mg AAE/g), CMWF (78.2 ± 4.11mg AAE/g), CMBF (58.22 ± 5.21 mg AAE/g), CMPEF (51.54 ± 4.75 mg AAE/g) as shown in figure 5.15A.

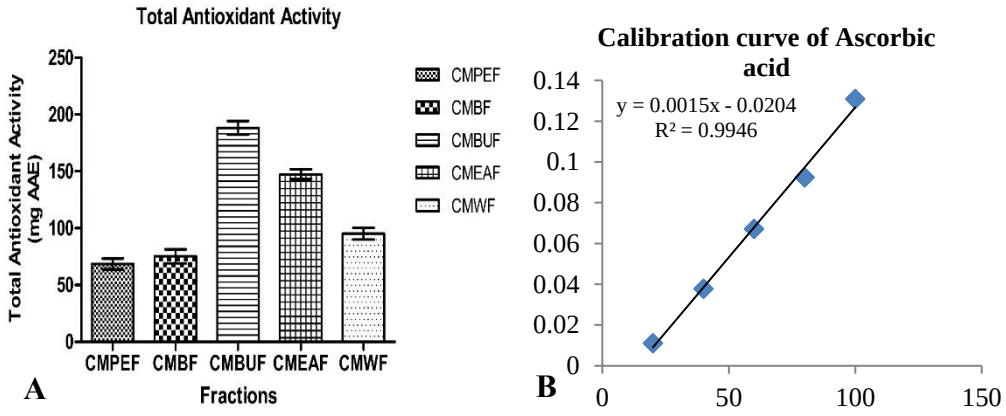

Figure 5.15: A) Total antioxidant capacity of a fraction of *C.medica* B) Calibration curve of ascorbic acid

Table 5.14: Total antioxidant capacity of fractions of *Citrus medica* fruit

Name of fractions	Total Antioxidant capacity (mg AAE/g)
CMPEF	51.54 ± 4.75
CMBF	58.22 ± 5.21
CMEAF	188.42 ± 4.75*
CMBUF	139.65 ± 5.35*
CMWF	78.2 ± 4.11

Values expressed as mean ± SEM with n = 3. CMPEF – *Citrus medica* petroleum ether fraction, CMBF - *Citrus medica* benzene fraction, CMEAF - *Citrus medica* ethyl acetate fraction, CMBUF - *Citrus medica* butanol fraction, CMWF - *Citrus medica* water fraction

5.10.2 Result of total antioxidant capacity of a fraction of *T.undulata*

The total antioxidant capacity of the fractions of *T.undulata* was calculated and reported in milligrams of quercetin equivalents per gram of dry weight. The results are shown in Table 5.15. TUEAF had the highest antioxidant capacity (178.32 ± 5.85 mg AAE/g), followed by TUBUF (137.43 ± 4.51 mg AAE/g), TUWF (91.2 ± 5.11 mg AAE/g), TUBF (78.22 ± 6.21 mg AAE/g), TUPEF (71.54 ± 4.85 mg AAE/g) as shown in figure 5.16A.

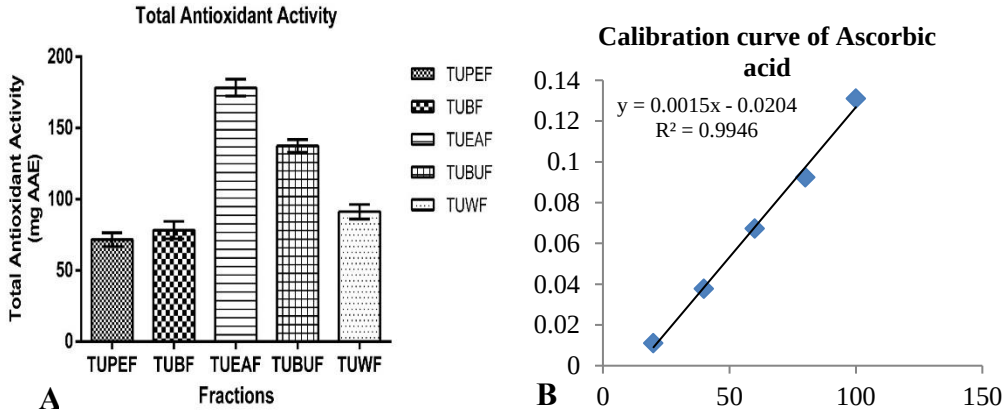

Figure 5.16: A) Total antioxidant capacity of a fraction of *T.undulata* B) Calibration curve of ascorbic acid

Table 5.15: Total antioxidant capacity of fractions of *T.undulata* Bark

Name of fractions	Total Antioxidant capacity (mg AAE/g)
TUPEF	71.54 ± 4.85
TUBF	78.22 ± 6.21
TUEAF	178.32 ± 5.85*
TUBUF	137.43 ± 4.51*
TUWF	91.2 ± 5.11

Values expressed as mean ± SEM with n = 3. Values expressed as mean ± SEM with n = 3. TUPEF – *Tecomella undulata* petroleum ether fraction, TUBF - *Tecomella undulata* benzene fraction, TUEAF - *Tecomella undulata* ethyl acetate fraction, TUBUF - *Tecomella undulata* butanol fraction, TUWF - *Tecomella undulata* water fraction

One of the most important metrics used to assess a substance's capacity to counteract oxidative stress and guard against oxidative damage is the evaluation of total antioxidant activity. To measure total antioxidant activity, many assays and methods have been developed, and these have provided insightful information on the possible health benefits of different chemicals and compounds (Agati et al., 2012). The antioxidative capabilities of phenolic compounds—particularly flavonoids—have been the subject of much research. These substances could contribute hydrogen atoms or electrons to free radicals, thereby counteracting their deleterious effects. The antioxidative activity of phenolic compounds is linked to the presence of hydroxyl (OH) groups, which improves their capacity to effectively scavenge free radicals. Higher concentrations frequently correspond with stronger antioxidative activity. Total phenolic concentration has been found to be a useful measure of a substance's antioxidative potential (Agati et al., 2012).

The total antioxidant capacity (measured in milligrams of ascorbic acid equivalents per gram of dry weight, or mg AAE/g) of the fractions of *C. medica* and *T.undulata* varied, as indicated by the data shown in Tables 5.14 and 5.15. To be more precise, CMBUF and TUBUF showed the lowest antioxidant capacity at 139.65 ± 5.35 and 137.43 ± 4.51 mg AAE/g, respectively, while CMEAF and TUEAF showed the highest antioxidant capacity at 188.42 ± 4.75 and 178.32 ± 5.85 mg AAE/g. These results imply that the butanol and ethyl acetate fractions of *C. medica* and *T.undulata* have strong antioxidant activity, which may be related to the presence of bioactive substances such as phenolic acids and flavonoids.

5.11 *In-vitro* antioxidant activity of fractions

5.11.1 DPPH free radical scavenging activity

5.11.1.1 DPPH free radical scavenging activity of fractions of *C.medica*

Figure 5.17A displays the relative potency of the fractions: CMEAF < CMBUF < CMWF < CMPEF < CMBF. Table 5.16 shows the appropriate IC50 values: 90.17±3.31, 104.25± 2.24, 173.37±2.22, 195.37±4.11, and 219.43± 3.3µg/ml,

respectively when compared with the positive control ascorbic acid (IC50=32.73± 1.71 µg/ml). The results reveal that the TUEAF and TUBUF fractions are the most effective at scavenging DPPH radicals in vitro. The IC50 for each fraction was determined using a linear regression equation.

Table 5.16: IC_{50} values of fractions of *C.medica* fruit on different *in vitro* antioxidant activity

Name of extracts	**DPPH radical scavenging activity (ug/ml)**	**Superoxide anion scavenging (ug/ml)**	**Ferric ion chelating (ug/ml)**	**Nitric oxide radical scavenging (ug/ml)**
CMPEF	195.37± 4.11	209.45± 2.1	211.27± 2.38	226.44± 3.33
CMBF	219.43± 3.3	196.08± 3.23	205.16± 5.22	232.42± 4.17
CMEAF	90.17± 3.31	121.13± 2.18	127.36± 3.22	142.16± 4.24
CMBUF	104.25± 2.24	130.26± 3.55	136.08± 3.24	156.37± 3.10
CMWF	173.37± 2.22	198.57± 2.67	208.24± 4.36	210.28± 2.92
Ascorbic Acid	32.73± 2.51	33.06± 2.31	56.54± 2.44	54.64± 2.78

Values expressed as mean ± SEM with n = 3. CMPEF – *Citrus medica* petroleum ether fraction, CMBF - *Citrus medica* benzene fraction, CMEAF - *Citrus medica* ethyl acetate fraction, CMBUF - *Citrus medica* butanol fraction, CMWF - *Citrus medica* water fraction

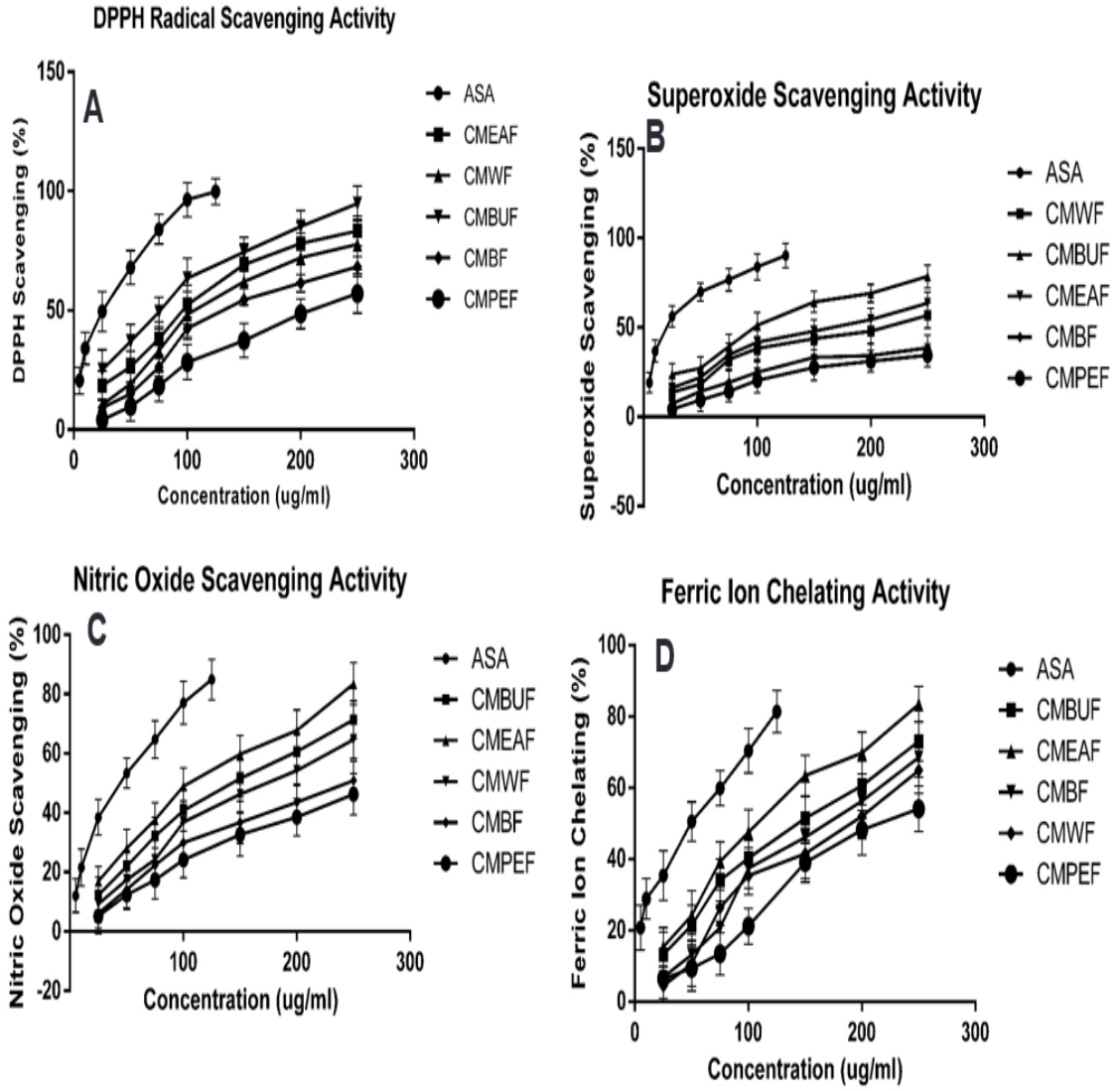

Figure 5.17: A) DPPH B) Superoxide C) Nitric oxide D) Ferric ion activity of *C.medica* fractions

5.11.1.2 DPPH free radical scavenging activity of fractions of *T.undulata*

Figure 5.18A displays the relative potency of the fractions: TUEAF < TUBUF < TUWF < TUBF < TUPEF. Table 5.17 shows the appropriate IC50 values: 100.29±2.11, 110.35±1.41, 133.97±2.62, 185.47±3.01, and 159.62±2.3 µg/ml, respectively when compared with the positive control ascorbic acid (IC50=32.73± 1.71 µg/ml). The results reveal that the TUEAF and TUBUF fractions are the most effective at scavenging DPPH radicals in vitro. The IC50 for each fraction was determined using a linear regression equation.

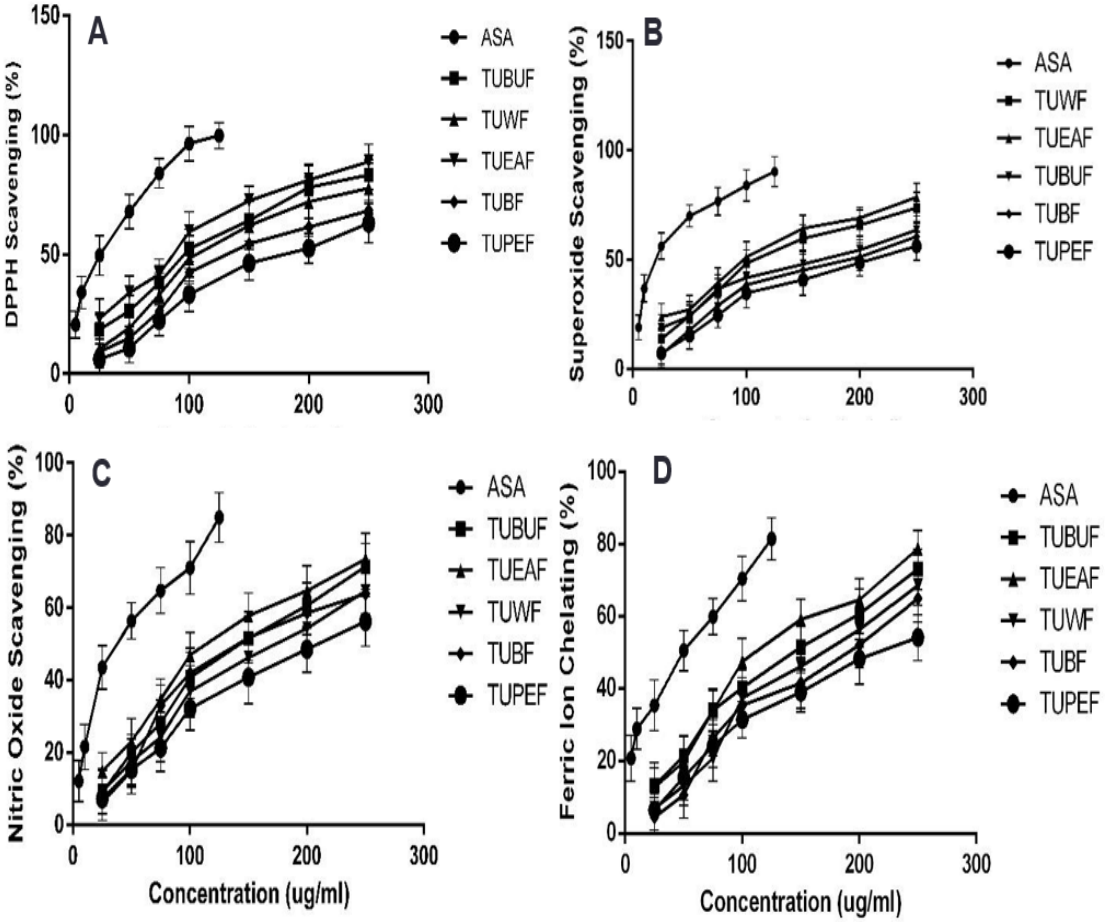

Figure 5.18: A) DPPH B) Superoxide C) Nitric oxide D) Ferric ion activity of *T.undulata* fractions

Table 5.17: IC_{50} values of fractions of *T.undulata* bark on different *in vitro* antioxidant activity

Name of extracts	DPPH radical scavenging activity (ug/ml)	Superoxide anion scavenging (ug/ml)	Ferric ion chelating (ug/ml)	Nitric oxide radical scavenging (ug/ml)
TUPEF	185.47± 3.01	204.75± 2.1	206.77± 3.41	212.54± 3.39
TUBF	159.62± 2.3	186.38± 3.33	195.27± 5.41	208.22± 4.17
TUEAF	100.29± 2.11	137.07± 2.28	137.68± 4.32	150.56± 4.44
TUBUF	110.35± 1.41	133.39± 3.25	142.98± 3.49	162.48± 3.21
TUWF	133.97± 2.62	168.67± 2.27	178.49± 4.20	187.58± 2.61
Ascorbic Acid	32.73± 1.71	33.06± 2.31	56.54± 2.44	54.64± 2.78

Values expressed as mean ± SEM with n = 3. Values expressed as mean ± SEM with n = 3. TUPEF – *Tecomella undulata* petroleum ether fraction, TUBF - *Tecomella undulata* benzene fraction, TUEAF -

Tecomella undulata ethyl acetate fraction, TUBUF - *Tecomella undulata* butanol fraction, TUWF - *Tecomella undulata* water fraction

In phytomedicine, 1,1-diphenyl 1-2-picrylhydrazyl, or DPPH, is a commonly used method for evaluating the scavenging abilities of bioactive fractions found in foods and plant extracts. As a stable nitrogen-centered radical, DPPH can take up an antioxidant's hydrogen atom to create a stable diamagnetic molecule. Thus, electrons are coupled off and the DPPH solution becomes discolored when an antioxidant and DPPH react. By giving up a hydrogen atom, this reaction produces the stable product 1,1-diphenyl-2-picryl hydrazine. The color of the process changes from purple to yellow, and this can be observed as a drop in absorbance at 517 nm (Yamaguchi, T. et al. 1998, Molyneux, P. 2004). The number of electrons absorbed determines whether the antioxidant's scavenging action or color bleaching is stochiometric (Molyneux, P. 2004). The scavenging activity of the antioxidant or the bleaching of the color stoichiometrically depends on the number of electrons taken up (Molyneux, P. 2004). These findings imply that the polyphenolic chemicals found in the CMEAF and TUBUF fractions may be responsible for the significant DPPH+ scavenging ability of its fractions.

5.11.2 Superoxide radical scavenging activity

5.11.2.1 Superoxide radical scavenging activity of fractions of *C.medica*

Figure 5.17B displays the relative potency of the fractions: CMEAF < CMBUF < CMBF < CMWF < CMPEF. Table 5.16 shows the appropriate IC50 values: 121.13± 2.18, 130.26± 3.55, 196.08± 3.23, 198.57± 2.67, and 209.45± 2.1 µg/ml, respectively when compared with the positive control ascorbic acid (IC50=33.06±2.31µg/ml). The results reveal that the CMEAF and CMBUF fractions are the most effective at scavenging superoxide radicals in vitro. The IC50 for each fraction was determined using a linear regression equation.

5.11.2.2 Superoxide radical scavenging activity of fractions of *T.undulata*

Figure 5.18B illustrates the patterns of fractions in their ability to quench superoxide anion. Table 5.17 presents the IC50 values for all fractions. TUBUF showed a higher IC50 value of 133.39±3.25 µg/ml, followed by TUEAF with an IC50 value of 137.07±2.28 µg/ml, TUWF (168.67± 2.27 ug/ml), TUBF (186.38±3.33 ug/ml) and TUPEF (204.75±2.1 ug/ml) when compared with the positive control ascorbic acid

(IC50=33.06±2.31µg/ml). The IC50 for each fraction was determined using a linear regression equation.

Nitro blue tetrazolium (NBT) reduction using riboflavin and light is the method used to quantify *in-vitro* super oxide radical scavenging activity. The process relies on riboflavin's autooxidation in the presence of light to produce super oxide radicals. Because super oxide can produce hydroxyl radicals and singlet oxygen, it is crucial to biology. Super oxide anion radical overproduction is linked to redox imbalance and has detrimental physiological effects. NBT is reduced by the super oxide radical to a blue formazan that has a wavelength of 560 nm. According to the findings, the CMEAF and TUBUF shown strong free radical scavenging action at low IC50 when compared to ascorbic acid (standard). Because these fractions have electron-donating substituent groups like -OH, -CL, and -CH3 at various locations along scaffold, they are electron donors. According to Wang et al. (2005), this chemical gave its electrons to the superoxide and scavenges them to stop them from interacting with NBT further. This inhibits the development of the blue-colored formazan result.

5.11.3 Nitric oxide radical scavenging activity

5.11.3.1 Nitric oxide radical scavenging activity of fractions of *C.medica*

The investigation (Figure 5.17C) revealed that the NO scavenging capabilities of the fractions and the positive control increased in a dose-dependent manner. These findings were verified by the IC50 analysis data shown in Table 5.16. CMEAF had the highest NO scavenging ability among the fractions, with an IC50 value of 142.16± 4.24 µg/ml, followed by CMBUF (IC50 = 156.37± 3.10 µg/ml), CMWF (IC50 = 210.28± 2.92 µg/ml), CMPEF (IC50 = 226.44± 3.33 µg/ml), and CMBF (IC50 = 232.42± 4.17 µg/ml). Only TUEAF and TUBUF showed greater NO scavenging efficacy than ascorbic acid (IC50 = 54.64± 2.78 µg/ml).

5.11.3.2 Nitric oxide radical scavenging activity of fractions of *T.undulata*

The investigation (Figure 5.18C) revealed that the NO scavenging capabilities of the fractions and the positive control increased in a dose-dependent manner. These findings were verified by the IC50 analysis data shown in Table 5.17. TUEAF had the highest NO scavenging ability among the fractions, with an IC50 value of 150.56± 4.44 µg/ml, followed by TUBUF (IC50 = 162.48± 3.21 µg/ml), TUWF (IC50 = 187.588± 2.61 µg/ml), TUBF (IC50 = 208.22± 4.17 µg/ml), and TUPEF (IC50 =

212.54± 3.39 µg/ml). Only TUEAF and TUBUF showed greater NO scavenging efficacy than ascorbic acid (IC50 = 54.64± 2.78 µg/ml).

Nitric oxide (NO) is a vital, multifaceted bioregulatory molecule that has a wide range of physiological applications as well as pathological consequences. According to Miller et al. (1993) and Malinski T. (2007), physiological effects include immunological response, blood pressure modulation, neuronal signal transmission, prevention of platelet aggregation, and smooth muscle relaxation. It may behave as an extremely unstable NO radical and has a very short half-life. While NO does not directly interact with biological macromolecules, in certain chronic diseases, superoxide anions in excess react with NO to form peroxynitrite anion ($ONOO^-$). This anion inhibits mitochondrial respiratory chain enzymes, reduces cellular oxygen consumption, blocks sodium transport across membranes, and can even cause DNA fragmentation and neuronal damage (Miller et al., 1993; Malinski T., 2007; Taira, J. et al., 2015). Additionally, $ONOO^-$ contributes to the pathogenesis of inflammation (Miller et al., 1993). Using the Greiss method, the nitric oxide radical scavenging activity of the *C. medica* and *T.undulata* fractions was determined. Sulphanilamide may become diazotized when NO, which is produced spontaneously in an aqueous solution of sodium nitroprusside at physiological pH, interacts with oxygen to produce nitrite ions. When naphthylethylenediamine dichloride and the diazotized product combine, an azo-dye intensity is formed, which is measured at 550 nm. Reduced absorbance at 550 nm would come from phytochemicals with nitric oxide radical scavenging activity competing with oxygen to react with nitric oxide and preventing the production of nitrite ions (Miller et al., 1993; Malinski T., 2007). Due to their significant NO scavenging effects, CMEAF and TUBUF may be used to scavenge excessive NO radicals produced by iNOS in atrial fibrillation and coronary atherothrombotic illness (Freedman, J. E., & Loscalzo, J. 2003).

5.11.4 Metal ion (Ferric ion) chelating activity:

5.11.4.1 Metal ion (Ferric ion) chelating activity of fractions of *C.medica*

The ferrous ion chelating ability of the various fractions was studied using the ferrozine-Fe^{2+} complex technique, as seen in Figure 5.17D. All the fractions indicated a reasonable ability to chelate iron (II) ions, with dose-dependent behavior. CMEAF had the highest iron chelating activity among all investigated fractions, with an IC50 value of 127.36± 3.22 µg/ml. CMBUF had an iron chelating activity with an IC50

value of 136.08± 3.24 µg/ml. Table 5.16 shows that CMBF, CMWF, and CMPEF required higher concentrations to chelate iron, with IC50 values of 205.16± 5.22, 208.24± 4.36 µg/ml, and 211.27± 2.38 µg/ml. Ascorbic acid, the reference standard, has the lowest IC50 value of 56.54 ± 2.44 µg/ml.

5.11.4.2 Metal ion (Ferric ion) chelating activity of fractions of *T.undulata*

The ferrous ion chelating ability of the various fractions was studied using the ferrozine-Fe2+ complex technique, as seen in Figure 5.18D. All the fractions indicated a reasonable ability to chelate iron (II) ions, with dose-dependent behavior. TUEAF had the highest iron chelating activity among all investigated fractions, with an IC50 value of 137.68± 4.32 µg/ml. TMBUF had an iron chelating activity with an IC50 value of 142.98± 3.49 µg/ml. Table 5.17 shows that TUWF, TUBF, and TUPEF required higher concentrations to chelate iron, with IC50 values of 178.49± 4.20 µg/ml, 195.27± 5.41 µg/ml, and 206.77± 3.41 µg/ml. Ascorbic acid, the reference standard, has the lowest IC50 value of 56.54 ± 2.44 µg/ml.

A compound's ability to remove excess catalyzing transition metals, which are essential for preventing lipid peroxidation, makes it a valuable component. Chelating compounds are known to lower the redox potential by establishing s-bonds with metals, which turns the oxidized metal ion into a non-reactive state. By breaking down hydrogen and lipid peroxides into reactive free radicals through the Fenton reaction, ferrous ions can start lipid peroxidation. It can also provide impetus to the chain reaction of lipid peroxidation by removing hydrogen atoms from other essential molecules and speed up peroxidation by breaking down lipid hydroperoxides into peroxyl and alkoxyl radicals (Halliwell B. 1991, Fridovich I. 1995). When ferrous ions and ferrozine combine, a purple substance is produced. There is a dose-dependent decrease in the intensity of the purple color complex when chelating chemicals or extracts are present. This implies that the constituents of the plant might either disrupt the development of the ferrozine-Fe2+ complex or engage in direct interactions with Fe2+. Accordingly, the intensity of the purple hue that forms can be used to measure the chelating effect of plant extracts as natural chelators (Liu & Yao 2007, Nagulendran, 2007). Higher metal chelating ability is quantitatively correlated with a decrease in color intensity. This study has established the involvement of CMEAF and TUBUF in metal chelating activity. They have demonstrated reasonable metal chelating activity, possibly in part due to their interference with the development of the

Ferrozine-Fe2+ complex. Chelating substances that establish bonds with metals function as secondary antioxidants by lowering their redox potential, which stabilizes the metal ion's oxidized state.

5.11.5 Reducing power capacity activity:

5.11.5.1 Reducing the power capacity of the fraction of *C. Medica*

Figure 5.19A shows the reductive power of various solvent fractions for *Citrus medica*. An increase in the reducing power activity was suggested by the absorbance rise. The extract fractions' and the positive control ascorbic acid's absorbance at 700 nm increased in a concentration-dependent manner, according to the results. Ascorbic acid demonstrated a potent reducing capacity. Once more, it was discovered that the CMEFA fraction had the largest reduction power among the others followed by CMBUF, CMWF, CMBF, and CMPEF.

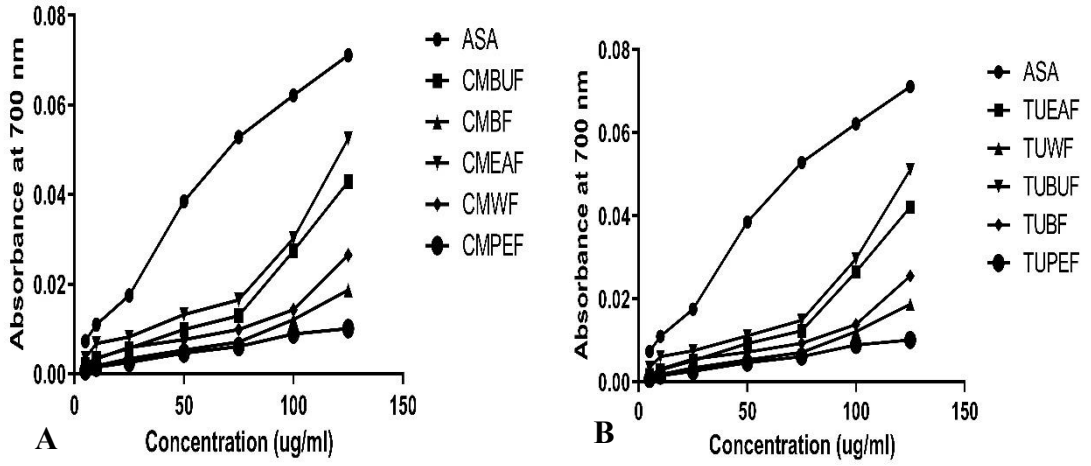

Figure 5.19: Reducing power capacity of A) *C.medica* B) *T.undulata* fractions

5.11.5.2 Reducing the power capacity of the fraction of *T.undulata*

Figure 5.19B illustrates how different solvent fractions of *T.undulata* were more effective in converting Fe3+ to Fe2+. The greatest reducing property was exhibited by TUBUF with a good concentration of TPC and TFC, followed by TUBUF, TUBF, TUWF, and TUPEF.

5.12 *In-vitro* anticoagulant activity of fractions

5.12.1 Blood clotting time measurement

5.12.1.1 Blood clotting time measurement of fractions of *C.medica*

The fractions of *Citrus medica* fruit were discovered to affect bleeding time. The experimental results showed that when the concentration of *C.medica* fractions rose, the clotting time lengthened. The maximum clotting time was achieved by CMEAF (21.85 ± 0.65) and CMBUF (16.89 ± 0.49) at a concentration of 7.5 mg/mL as compared to other concentrations. However, above this concentration, clotting time is reduced with increasing concentration. Figure 5.20 depicts these observations. This finding indicates the presence of anticoagulant(s) in *C.medica*, implying that they work optimally within a specified concentration range.

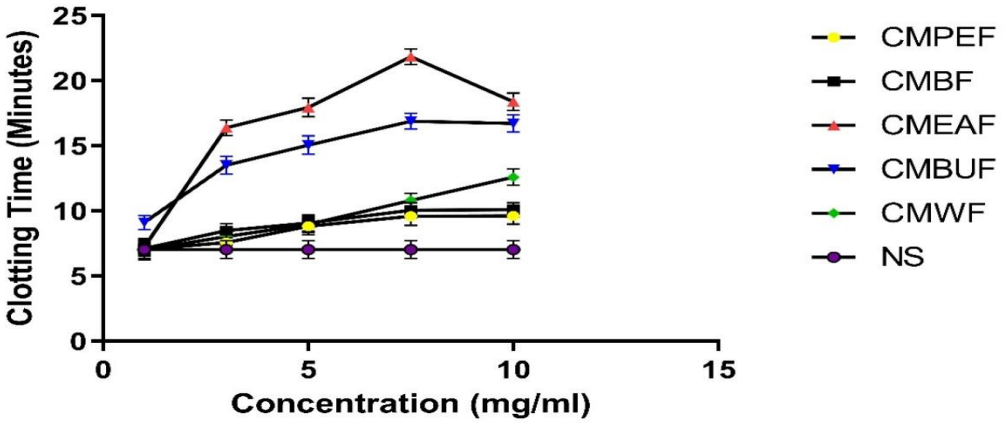

Figure 5.20: *In-vitro* blood clotting time of varying concentrations of fractions of *C.medica*

At the tested dose, all partitioned fractions of *C.medica* caused a significant increase in blood clotting time when compared to control samples. CMBUF (16.89 ± 0.49 minutes, ($p<0.001$)), CMEAF (21.85 ± 0.65 minutes, ($p<0.001$)), and CMWF (10.80 ± 0.52 minutes, ($p<0.001$)) had the longest clotting time at 7.5 mg/ml when compared to 10, 5, and 2.5 mg/ml concentrations. CMEAF had the greatest delay in blood clotting time (21.85 minutes, $p<0.001$), followed by CMBUF (16.89 ± 0.49 minutes) and CMWF (10.80 ± 0.52). At 2.5 and 5 mg/ml, CMWF, CMPEF, and CMBF had no significant effect on blood clotting time. However, at 7.5 and 10 mg/ml, they exhibited 10.80 ± 0.52, 10.05 ± 0.70, 9.59 ± 0.67, and 12.59 ± 0.72, 10.09 ± 0.90, 9.61 ± 0.46 minutes, respectively as shown in figure 5.21 and Table 5.18.

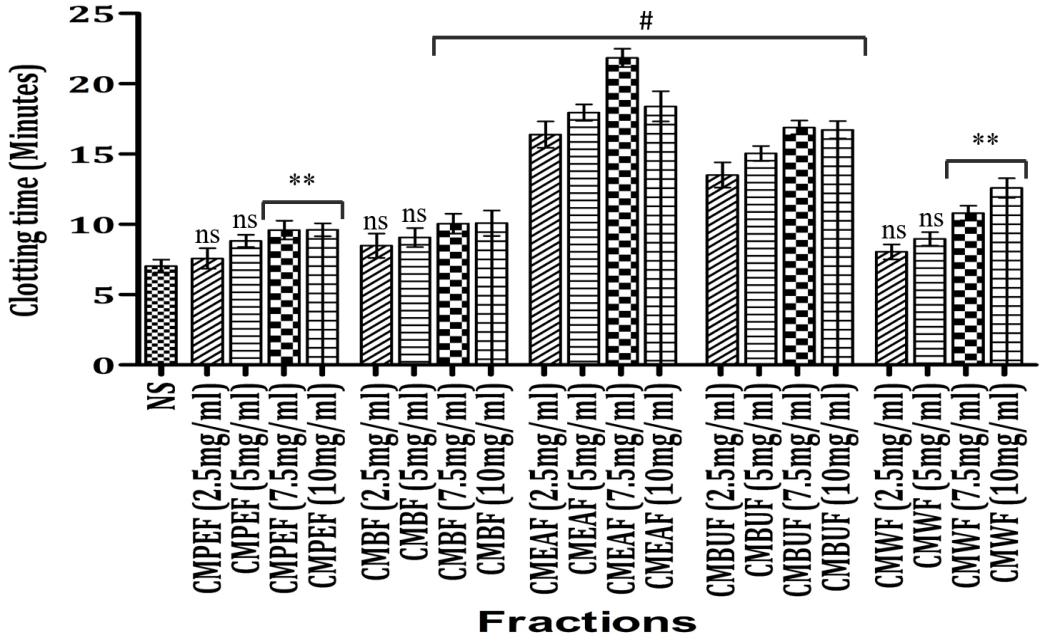

Figure 5.21: *In-vitro* blood clotting time of fractions of *C.medica* at 2.5, 5, 7.5, and 10 mg/ml

Table 5.18 *In-vitro* blood clotting time of fractions of *C.medica*

Group	Blood Clotting Time (Minutes)			
	2.5 mg/ml	**5 mg/ml**	**7.5 mg/ml**	**10 mg/ml**
NS	7.03 ± 0.46	7.03 ± 0.46	7.03 ± 0.46	7.03 ± 0.46
CMPEF	7.58 ± 0.73^{ns}	8.83 ± 0.44^{ns}	$9.59 \pm 0.67^{**}$	$9.61 \pm 0.46^{**}$
CMBF	8.49 ± 0.87^{ns}	9.07 ± 0.67^{ns}	$10.05 \pm 0.70^{\#}$	$10.09 \pm 0.90^{\#}$
CMEAF	$16.39 \pm 0.94^{\#}$	$17.95 \pm 0.58^{\#}$	$21.85 \pm 0.65^{\#}$	$18.39 \pm 1.08^{\#}$
CMBUF	$13.51 \pm 0.90^{\#}$	$15.05 \pm 0.54^{\#}$	$16.89 \pm 0.49^{\#}$	$16.72 \pm 0.61^{\#}$
CMWF	8.04 ± 0.53^{ns}	8.96 ± 0.47^{ns}	$10.80 \pm 0.52^{**}$	$12.59 \pm 0.72^{**}$

Results are expressed as Mean ± SE values (n=3). All fractions were suspended in saline. *p<0.05, **p<0.01, #p<0.001 significant when compared with Normal saline (vehicle control) using one way ANOVA analysis. NS- Normal saline, CMPEF – *Citrus medica* petroleum ether fraction, CMBF - *Citrus medica* benzene fraction, CMEAF - *Citrus medica* ethyl acetate fraction, CMBUF - *Citrus medica* butanol fraction, CMWF - *Citrus medica* water fraction.

5.12.1.2 Blood clotting time measurement of fractions of *T.undulata*

The fractions of *Tecomella undulata* fruit were discovered to affect bleeding time. The experimental results showed that when the concentration of *T.undualta* fractions increased, the clotting time increased. The highest clotting time was achieved by TUBUF (17.95 ± 0.59) and TUWF (16.89 ± 0.49) at a concentration of 7.5 mg/mL as compared to other concentrations. However, above this concentration, clotting time is

reduced with increasing concentration. Figure 5.22 depicts these observations. This finding indicates the presence of anticoagulant(s) in *T.undulata*, implying that they work optimally within a specified concentration range.

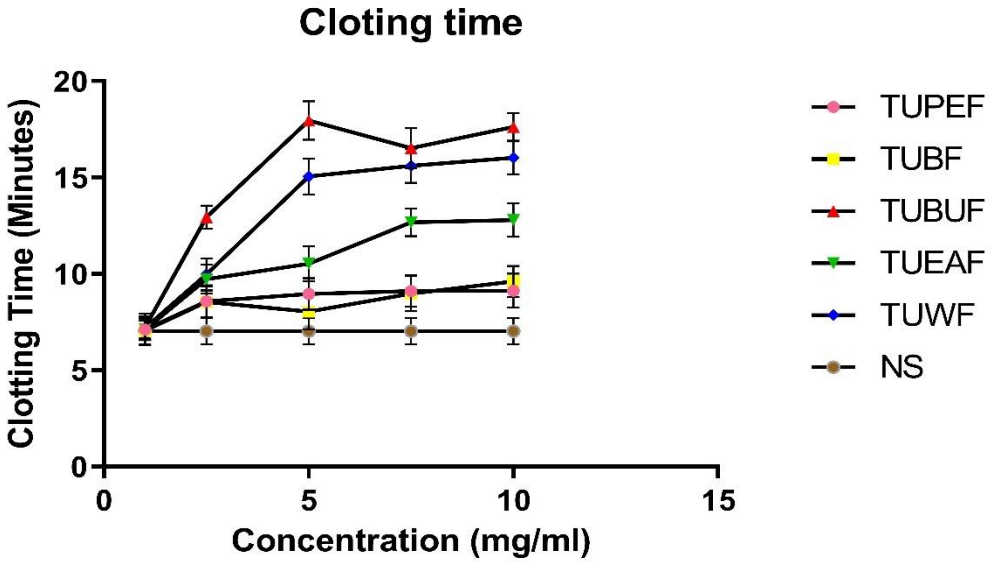

Figure 5.22: *In-vitro* blood clotting time of varying concentrations of fractions of *T.undulata*

When compared to control samples, all partitioned fractions of *T.undulata* significantly increased blood clotting time at the studied dosages. When compared to 10, 5, and 2.5 mg/ml concentrations, TUBUF (17.95 ± 0.59), TUWF (16.89 ± 0.49) ($p<0.001$), TUEAF (12.68 ± 0.65 minutes) ($p<0.001$), and CMWF (10.80 ± 0.52 minutes, ($p<0.001$) exhibited the longest clotting times at 7.5 mg/ml. Blood clotting time was not significantly affected by TUPEF and TUBF at 2.5 mg/ml concentration. TUPEF had a substantial ($p<0.01$) influence on clotting time, but TUBF had no effect at 5 mg/ml. Nevertheless, as indicated by Figure 5.23 and Table 5.19, at 7.5 and 10 mg/ml, they demonstrated 8.97 ± 0.63 ($p<0.01$), 9.10 ± 0.54 ($p<0.01$), and 9.61 ± 0.55 ($p<0.001$), 9.13 ± 0.51 ($p<0.01$) minutes, respectively.

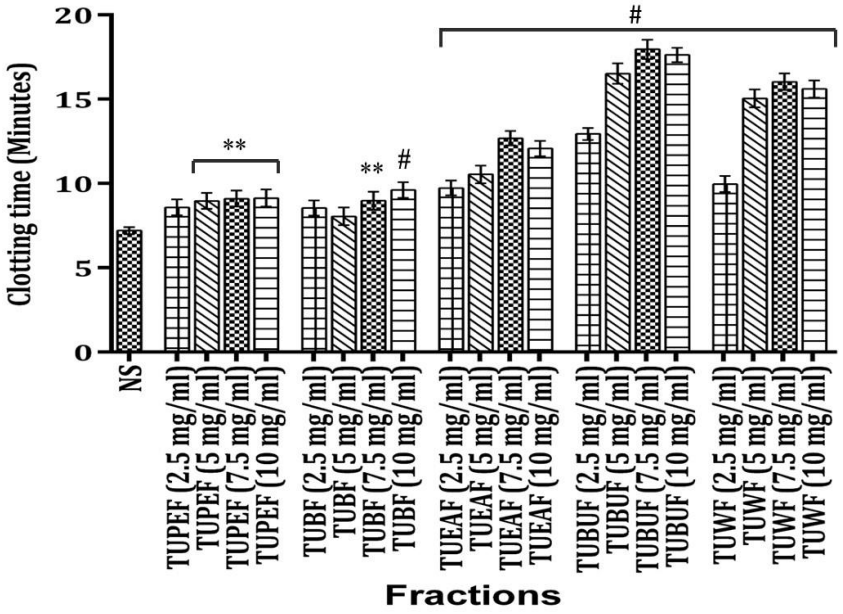

Figure 5.23: *In-vitro* blood clotting time of fractions of *T.undulata* at 2.5, 5, 7.5, and 10 mg/ml

Table 5.19: *In-vitro* blood clotting time of fractions of *T.undulata*

Group	Clotting Time (Minutes)			
	2.5 mg/ml	**5 mg/ml**	**7.5 mg/ml**	**10 mg/ml**
NS	7.03 ± 0.46	7.03 ± 0.46	7.03 ± 0.46	7.03 ± 0.46
TUPEF	8.58 ± 0.48^{ns}	$8.96 \pm 0.47^{**}$	$9.10 \pm 0.54^{**}$	$9.13 \pm 0.51^{**}$
TUBF	8.54 ± 0.46^{ns}	8.04 ± 0.53^{ns}	$8.97 \pm 0.63^{**}$	$9.61 \pm 0.55^{\#}$
TUEAF	$9.73 \pm 0.44^{\#}$	$10.53 \pm 0.52^{\#}$	$12.68 \pm 0.65^{\#}$	$12.07 \pm 0.80^{\#}$
TUBUF	$12.94 \pm 0.60^{\#}$	$16.52 \pm 0.49^{\#}$	$17.95 \pm 0.59^{\#}$	$17.62 \pm 0.61^{\#}$
TUWF	$9.97 \pm 0.51^{\#}$	$15.05 \pm 0.54^{\#}$	$16.03 \pm 0.57^{\#}$	$15.60 \pm 0.52^{\#}$

Results are expressed as Mean ± SE values (n=3). All fractions were suspended in saline. *p<0.05, **p<0.01, #p<0.001 significant when compared with Normal saline (vehicle control) using one way ANOVA analysis. NS- Normal saline, TUPEF – *Tecomella undulata* petroleum ether fraction, TUBF - *Tecomella undulata* benzene fraction, TUEAF - *Tecomella undulata* ethyl acetate fraction, TUBUF - *Tecomella undulata* butanol fraction, TUWF - *Tecomella undulata* water fraction.

5.12.2 Prothrombin time (PT) activity assay

5.12.2.1 Prothrombin time measurement of fractions of *C.medica*

It was found that prothrombin time was impacted by the different *citrus medica* fruit fractions. The experimental findings demonstrated that the clotting time increased with increasing *C. medica* fraction concentration. In comparison to other concentrations, the highest prothrombin time was obtained by CMEAF (91.33 ± 2.12) and CMBUF (79.43

± 2.18) seconds at a dose of 7.5 mg/mL. But prothrombin time decreases with increasing concentration above this point. Figure 5.24 illustrates these findings. This discovery suggests that *C. medica* contains anticoagulant(s), and that these anticoagulants function best within a certain concentration range.

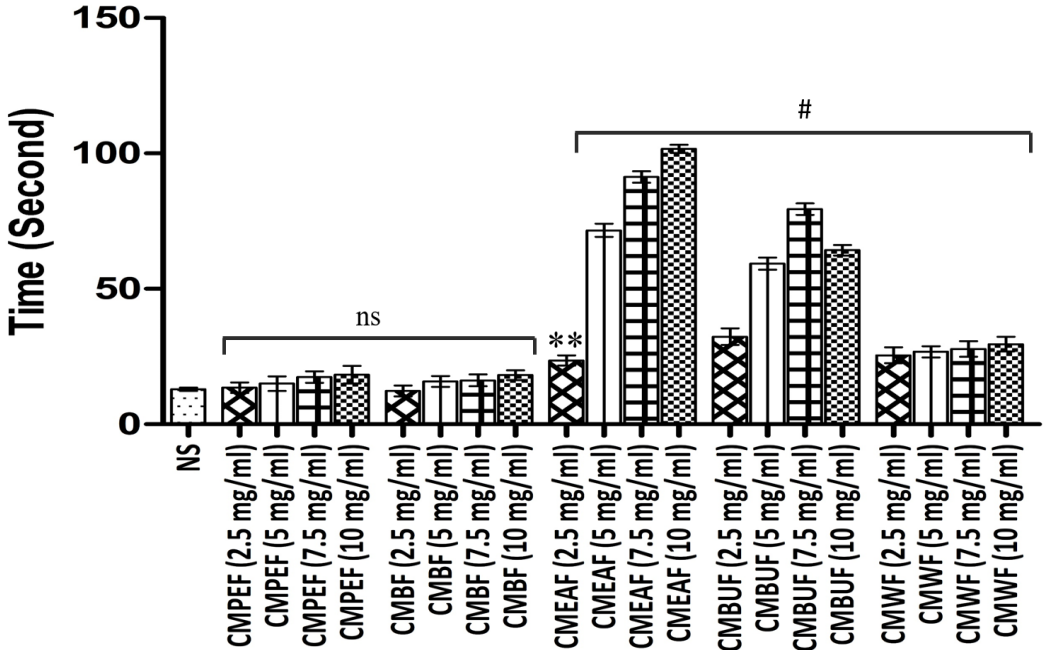

Figure 5.24: *In-vitro* prothrombin time of fractions of *C.medica*

Table 5.20: *In-vitro* prothrombin time of fractions of *C.medica*

Group	Prothrombin Time (Seconds)			
	2.5 mg/ml	**5 mg/ml**	**7.5 mg/ml**	**10 mg/ml**
NS	12.93 ± 0.65	12.93 ± 0.65	12.93 ± 0.65	12.93 ± 0.65
CMPEF	13.5 ± 1.95^{ns}	15 ± 2.65^{ns}	17.40 ± 2.13^{ns}	18.33 ± 3.21^{ns}
CMBF	12.33 ±2.02^{ns}	15.80 ± 2^{ns}	16.20 ± 2.19^{ns}	18.13 ± 1.82^{ns}
CMEAF	23.53 ±1.86**	71.60 ± 2.46$^{\#}$	91.33 ± 2.12$^{\#}$	101.67 ± 1.53$^{\#}$
CMBUF	32.33 ± 3.06$^{\#}$	59.30 ± 2.26$^{\#}$	79.43 ± 2.18$^{\#}$	64.27 ± 1.91$^{\#}$
CMWF	25.47 ± 2.94$^{\#}$	26.80 ± 2.07$^{\#}$	27.83 ± 2.91$^{\#}$	29.57 ± 2.68$^{\#}$

Results are expressed as Mean ± SE values (n=3). All fractions were suspended in saline. *p<0.05, **p<0.01, #p<0.001 significant when compared with Normal saline (vehicle control) using one way ANOVA analysis. NS- Normal saline, CMPEF – *Citrus medica* petroleum ether fraction, CMBF - *Citrus medica* benzene fraction, CMEAF - *Citrus medica* ethyl acetate fraction, CMBUF - *Citrus medica* butanol fraction, CMWF - *Citrus medica* water fraction.

All *C. medica* partitioned fractions increased prothrombin time significantly at the studied dose in comparison to control samples. Comparing 7.5 mg/ml concentrations to 5, 2.5 mg/ml concentrations, the longest prothrombin times were recorded by

CMBUF (91.33 ± 2.12 seconds, p<0.001), CMEAF (79.43 ± 2.18 seconds, p<0.001), and CMWF (27.83 ± 2.91 seconds, p<0.001) during the experiment. When CMEAF was compared to 7.5 mg/ml, it showed the most prothrombin time delay (101.67 seconds, p<0.001) at 10 mg/ml. CMPEF and CMBF showed no discernible impact on prothrombin time at 2.5 or 5 mg/ml. But as Figure 5.24 and Table 5.20 demonstrate, at 7.5 and 10 mg/ml, CMEAF, CMBUF, and CMWF demonstrated 91.33 ± 2.12, 79.43 ± 2.18, 27.83 ± 2.91, and 101.67 ± 1.53, 64.27 ± 1.91, 29.57 ± 2.68 seconds, respectively.

5.12.2.2 Prothrombin time measurement of fractions of *T.undulata*

It was discovered that the various *T.undulata* bark fractions affected prothrombin time. The results of the experiment showed that when the concentration of *T.undulata* fraction increased, so did the prothrombin time. TUBUF (58.67 ± 2.52) and TUWF (57.33 ± 2.08) seconds had the highest prothrombin times when compared to other fractions at a dose of 7.5 mg/mL. Above this threshold, however, prothrombin time falls as concentration increases. These results are illustrated in Figure 5.25. According to this finding, *T.undulata* may contain one or more anticoagulants, and it appears that these anticoagulants work best at specific concentrations.

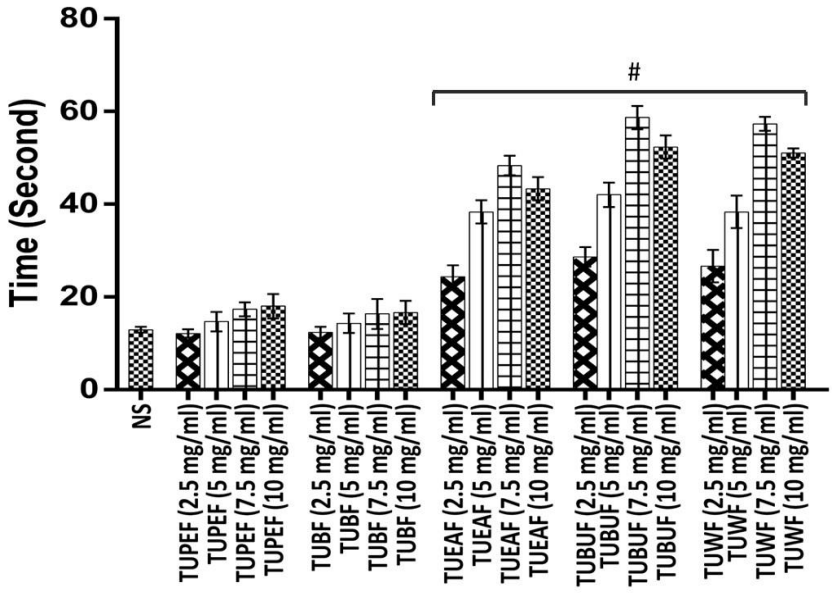

Figure 5.25: *In-vitro* Prothrombin time of fractions of *T.undulata*

Compared to control samples, all *T.undulata* partitioned fractions significantly increased prothrombin time at the tested dose. When 7.5 mg/ml concentrations were compared to 10, 5, and 2.5 mg/ml concentrations, TUBUF (58.67 ± 2.52 seconds,

p<0.001), TUWF (57.33 ± 2.08 seconds, p<0.001), and TUEAF (48.33 ± 2.08 seconds, p<0.001) showed the longest prothrombin time durations throughout the experiment. Figure 5.25 and Table 5.20 demonstrate that TUPEF and TUBF had no appreciable effect on prothrombin time at any concentration.

Table 5.21: *In-vitro* prothrombin time of fractions of *T.undulata*

Group	Prothrombin Time (Seconds)			
	2.5 mg/ml	**5 mg/ml**	**7.5 mg/ml**	**10 mg/ml**
NS	12.93 ± 0.65	12.93 ± 0.65	12.93 ± 0.65	12.93 ± 0.65
TUPEF	12.13 ±0.91^{ns}	14.67 ± 2.08^{ns}	17.33 ± 1.53^{ns}	18 ± 2.65^{ns}
TUBF	12.37 ±1.21^{ns}	14.33 ± 2.08^{ns}	16.33 ± 3.21^{ns}	16.67 ± 2.52^{ns}
TUEAF	24.33 ± 2.52$^{\#}$	38.33 ± 2.52$^{\#}$	48.33 ± 2.08$^{\#}$	43.33 ± 2.52$^{\#}$
TUBUF	28.67 ± 2.08$^{\#}$	42 ± 2.65$^{\#}$	58.67 ± 2.52$^{\#}$	52.33 ± 2.52$^{\#}$
TUWF	26.67 ± 3.51$^{\#}$	38.33 ± 3.51$^{\#}$	57.33 ± 2.08$^{\#}$	51 ± 2.65$^{\#}$

Results are expressed as Mean ± SE values (n=3). All fractions were suspended in saline. *p<0.05, **p<0.01, ***p<0.005, #p<0.001 significant when compared with Normal saline (vehicle control) Results are expressed as Mean ± SE values (n=3). All fractions were suspended in saline. *p<0.05, **p<0.01, #p<0.001 significant when compared with Normal saline (vehicle control) using one way ANOVA analysis. NS- Normal saline, TUPEF – *Tecomella undulata* petroleum ether fraction, TUBF - *Tecomella undulata* benzene fraction, TUEAF - *Tecomella undulata* ethyl acetate fraction, TUBUF - *Tecomella undulata* butanol fraction, TUWF - *Tecomella undulata* water fraction.

5.12.3 Activated Partial Thromboplastin time (APTT) activity assay

5.12.3.1 Activated Partial Thromboplastin time measurement of fractions of *C.medica*

It was discovered that the various *citrus medica* fruit fractions affected activated partial thromboplastin time. The results of the experiment showed that as the concentration of *C. medica* fraction grew, so did the activated partial thromboplastin time. When CMEAF and CMBUF were given a dose of 7.5 mg/mL, they obtained the maximum activated partial thromboplastin time (114.67 ± 3.51) seconds when compared to other concentrations. Above this threshold, however, APTT declines as concentration increases. These results are illustrated in Figure 5.26.

When compared to control samples, activated partial thromboplastin time rose considerably with all *C. medica* partitioned fractions at the tested dose. When 7.5 mg/ml concentrations were compared to 10, 5, and 2.5 mg/ml concentrations, CMEAF (114.67 ± 3.51 seconds, p<0.001), CMBUF (102.67 ± 3.51 seconds, p<0.001), and CMWF (27.83 ± 2.91 seconds, p<0.001) had the longest clotting durations throughout

the experiment. CMEAF demonstrated the greatest activated partial thromboplastin time delay (114.67 ± 3.51 seconds, p<0.001) at 7.5 mg/ml as compared to 10 mg/ml. At 2.5, 5, 7.5, and 10 mg/ml, CMPEF and CMBF had no appreciable effect on activated partial thromboplastin time. However, as Figure 5.26 and Table 5.22 show, CMEAF, CMBUF, and CMWF showed 32.33±3.21(p<0.01), 49.67 ±3.06 (p<0.001), 37.67±4.16 (p<0.01), and 72 ± 3, 71 ± 3 (p<0.001), and 37 ± 4 (p<0.001), seconds, respectively, at 2.5 and 5 mg/ml.

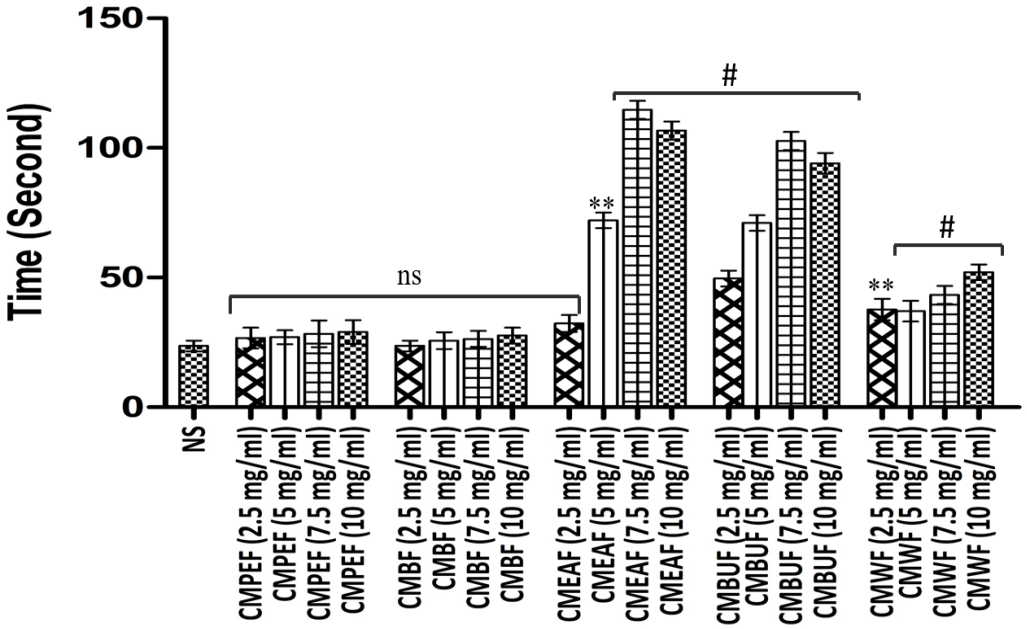

Figure 5.26: *In-vitro* Activated Partial Thromboplastin time of fractions of *C.medica*

Table 5.22: *In-vitro* Activated Partial Thromboplastin time of fractions of *C.medica*

Group	Activated Partial Thromboplastin Time (Seconds)			
	2.5 mg/ml	**5 mg/ml**	**7.5 mg/ml**	**10 mg/ml**
NS	23.67 ±2.08	23.67 ± 2.08	23.67 ± 2.08	23.67 ± 2.08
CMPEF	26.67 ± 4.04^{ns}	27 ± 2.65^{ns}	28.33 ± 5.13^{ns}	29 ± 4.58^{ns}
CMBF	23.67 ± 2.08^{ns}	25.67 ± 3.21^{ns}	26.33 ± 3.06^{ns}	27.67 ± 3.06^{ns}
CMEAF	$32.33\pm3.21^{**}$	$72 \pm 3^{\#}$	$114.67 \pm 3.51^{\#}$	$106.67 \pm 3.51^{\#}$
CMBUF	$49.67 \pm3.06^{\#}$	$71 \pm 3^{\#}$	$102.67 \pm 3.51^{\#}$	$94 \pm 4^{\#}$
CMWF	$37.67\pm4.16^{**}$	$37 \pm 4^{**}$	$43.33 \pm 3.51^{\#}$	$52 \pm 3^{\#}$

Results are expressed as Mean ± SE values (n=3). All fractions were suspended in saline. *p<0.05, **p<0.01, #p<0.001 significant when compared with Normal saline (vehicle control) using one way ANOVA analysis. NS- Normal saline, CMPEF – *Citrus medica* petroleum ether fraction, CMBF - *Citrus medica* benzene fraction, CMEAF - *Citrus medica* ethyl acetate fraction, CMBUF - *Citrus medica* butanol fraction, CMWF - *Citrus medica* water fraction.

5.12.3.2 Activated Partial Thromboplastin time measurement of fractions of *T.undulata*

It was discovered that the various *T.undulata* bark fractions affected activated partial thromboplastin time. The results of the experiment showed that when the concentration of *T.undulata* fraction increased, so did the activated partial thromboplastin time. TUBUF (114.67 ± 3.51) and TUWF (102.67 ± 3.51) seconds had the highest activated partial thromboplastin times when compared to other fractions at a dose of 7.5 mg/mL. Above this threshold, however, activated partial thromboplastin time falls as concentration increases. These results are illustrated in Figure 5.27. According to this finding, *T.undulata* may contain one or more anticoagulants, and it appears that these anticoagulants work best at specific concentrations.

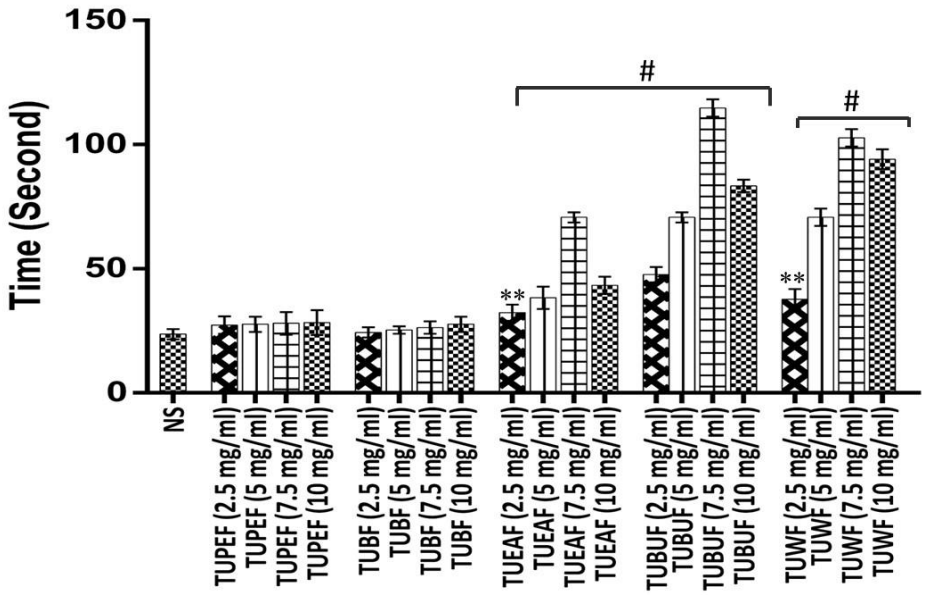

Figure 5.27: *In-vitro* Activated Partial Thromboplastin time of fractions of *T.undulata*

All *T.undulata* partitioned fractions enhanced activated partial thromboplastin time considerably at the tested dose when compared to control samples. TUBUF (114.67 ± 3.51 seconds, $p<0.001$), TUWF (102.67 ± 3.51 seconds, $p<0.001$), and TUEAF (70.67 ± 2.08 seconds, $p<0.001$) displayed the activated partial thromboplastin time lengths throughout the experiment when 7.5 mg/ml concentrations were compared to 10, 5, and 2.5 mg/ml concentrations. TUPEF and TUBF had no discernible influence on prothrombin time at any concentration, as shown by Figure 5.27 and Table 5.23. On

the other hand, demonstrate that at 2.5 and 5 mg/ml, TUBUF, TUWF, and TUEAF demonstrated 47.67 ± 3.06 ($p<0.001$), 37.67±4.16 ($p<0.01$), 32.33±3.21 ($p<0.01$), and 70.67 ± 2.08 ($p<0.001$), 70.67 ± 3.51 ($p<0.001$), and 38.33 ± 4.51 ($p<0.001$) seconds, individually.

Table 5.23: *In-vitro* Activated Partial Thromboplastin time of fractions of *T.undulata*

Group	Activated Partial Thromboplastin Time (Seconds)			
	2.5 mg/ml	5 mg/ml	7.5 mg/ml	10 mg/ml
NS	23.67 ± 2.08	23.67 ± 2.08	23.67 ± 2.08	23.67 ± 2.08
TUPEF	27.33 ±3.51^{ns}	27.67 ± 3.06^{ns}	28 ± 4.58^{ns}	28.33 ± 5.03^{ns}
TUBF	24.33 ±2.08^{ns}	25.33 ± 1.53^{ns}	26.33 ± 2.52^{ns}	27.67 ± 3.06^{ns}
TUEAF	32.33±3.21**	38.33 ± 4.51$^{\#}$	70.67 ± 2.08$^{\#}$	43.33 ± 3.51$^{\#}$
TUBUF	47.67 ± 3.06$^{\#}$	70.67 ± 2.08$^{\#}$	114.67 ± 3.51$^{\#}$	83.33 ± 2.52$^{\#}$
TUWF	37.67±4.16**	70.67 ± 3.51$^{\#}$	102.67 ± 3.51$^{\#}$	94 ± 4$^{\#}$

Results are expressed as Mean ± SE values (n=3). All fractions were suspended in saline. *p<0.05, **p<0.01, #p<0.001 significant when compared with Normal saline (vehicle control) Results are expressed as Mean ± SE values (n=3). All fractions were suspended in saline. *p<0.05, **p<0.01, #p<0.001 significant when compared with Normal saline (vehicle control) using one way ANOVA analysis. NS- Normal saline, TUPEF – *Tecomella undulata* petroleum ether fraction, TUBF - *Tecomella undulata* benzene fraction, TUEAF - *Tecomella undulata* ethyl acetate fraction, TUBUF - *Tecomella undulata* butanol fraction, TUWF - *Tecomella undulata* water fraction.

A complicated series of events involving numerous distinct protein pathways are involved in the coagulation system (Palta et al., 2014). These processes change fibrinogen into fibrin, which combines with platelets to form a thrombus. Intrinsic and extrinsic coagulation pathways are the two components that initiate coagulation cascades. Factor VIIa/tissue factor complex induces the first generation of activated factor X (Factor Xa), which is produced by the extrinsic coagulation pathway. Factors that contribute to the intrinsic pathway include XI, XII, IX, and VIII. Factor Xa, a key component of the coagulation cascade known as the common pathway, is amplified when the intrinsic pathway is activated (Palta et al., 2014). The ability to form a blood clot in a fair length of time is assessed by the APTT and PT tests; if any of these factors are hindered, the test results will be extended. The PT test is used to assess the extrinsic clotting factors, such as coagulation factor VII, whereas the APTT assesses coagulation factors VIII, IX, XI, and XII in the intrinsic coagulation pathway. Additionally, a

shared pathway including factors I, II, V, and X of the clotting cascade is assessed by these two tests.

As per result, with the exception of CMPEF, CMBF, TUPEF, and TUBF, all investigated fractions of *C.medica* and *T.undulata* prolonged PT and aPTT values concentration dependent, as shown in the data. Potent CMEAF, CMBUF, and CMWF fractions showed a minor reducing influence on the PT and aPTT at the 10 mg/ml concentration as compared to 7.5 mg/ml concentration, whereas CMEAF had prolonged PT and aPTT values at 7.5 mg/ml concentration. TUBUF showed a small reducing influence on the PT and aPTT at the 10 mg/ml concentration, but TUEAF, TUBUF, and TUWF fractions showed similar results at 7.5mg/ml. However, TUBUF had prolonged PT and aPTT values at 7.5 mg/ml concentration. The results of this bioactivity suggested that the butanol fraction of *T.undulata* and the ethyl acetate fraction of *C. medica* affected the common pathway in addition to the extrinsic and intrinsic pathways. As a result, their inhibition may be directed toward the common pathway factors, X, V, II, and I (Hood & Eby 2008). Based on these findings, the CMEAF and TUBUF fractions were employed for additional phytochemical research and *in-vitro* anticoagulant activity to determine the chemical constituents that were responsible.

5.13 Qualitative HPTLC Fingerprinting:

Thin layer chromatogram objects were scanned in reflectance or transmission mode using the CAMAG TLC scanner 3 and the LINOMAT-V densitometry assessment system with WINCAT software, either by absorbance or by fluorescence at 254 or 366 nm, respectively. The result was expressed in Rf value, peak area, and % peak area. The sample's Rf value was computed using the formula below:

$$R_f = \frac{\text{Distance travelled by sample from baseline}}{\text{Distance travelled by solvent from baseline}}$$

5.13.1 Qualitative HPTLC Fingerprinting of fractions of *C.medica*

Based on HPTLC fingerprinting, we discovered that various fractions of *C.medica* had a wide variety of secondary flavonoid metabolites, as seen by the various hues of the bands at 265 and 365 nm wavelengths (Figure 5.28A and B).

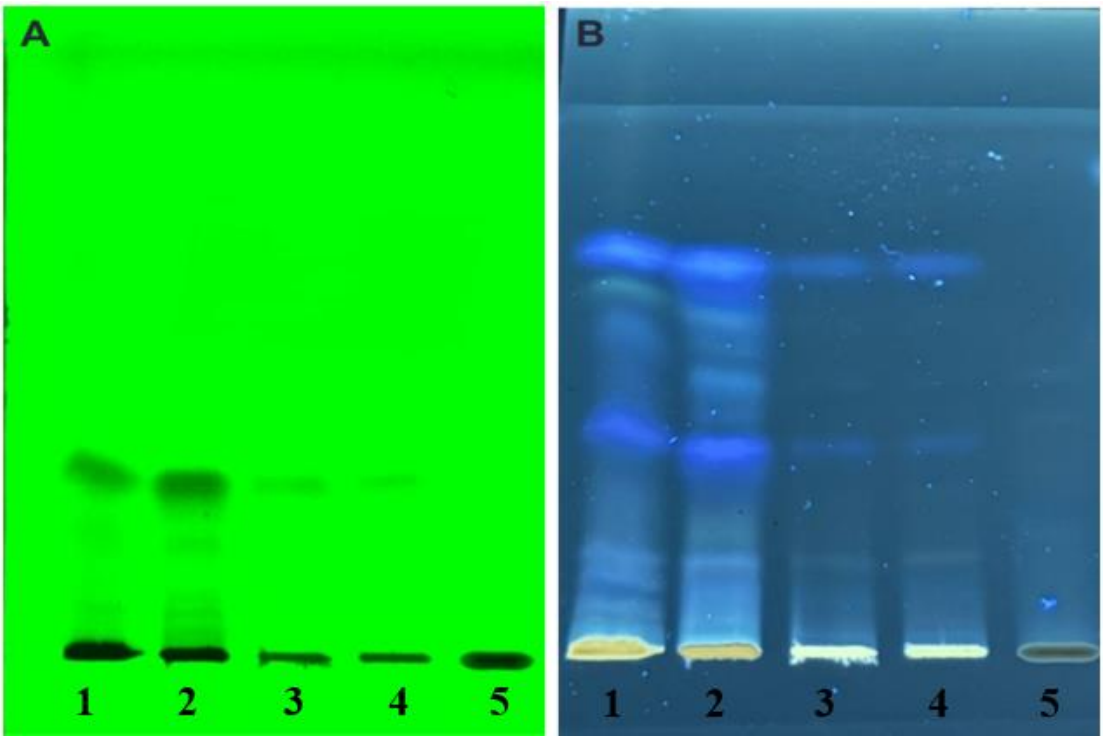

Track 1 - CMEAF, Track 2 – CMBUF, Track 3 – CMPEF, Track 4 - CMBF, Track 5 - CMWF

Figure 5.28: HPTLC fingerprinting of fractions of *citrus medica* A) At 366 nm B) 254 n

Table 5.24 demonstrated that CMBUF and CMBF fractions had eight bands. While CMEAF and CMWF fractions had seven bands. CMPEF had at least six bands at 254nm wavelength. All fractions show different numbers of bands at different Rf values and with different % peak areas.

Table 5.24: HPTLC fingerprinting analysis of fractions of *C.medica*

Track No.	Name of Fraction	Number of Bands at 254 nm
1	CMEAF	07
2	CMBUF	08
3	CMPEF	06
4	CMBF	08
5	CMWF	07

CMPEF – *Citrus medica* petroleum ether fraction, CMBF - *Citrus medica* benzene fraction, CMEAF - *Citrus medica* ethyl acetate fraction, CMBUF - *Citrus medica* butanol fraction, CMWF - *Citrus medica* water fraction.

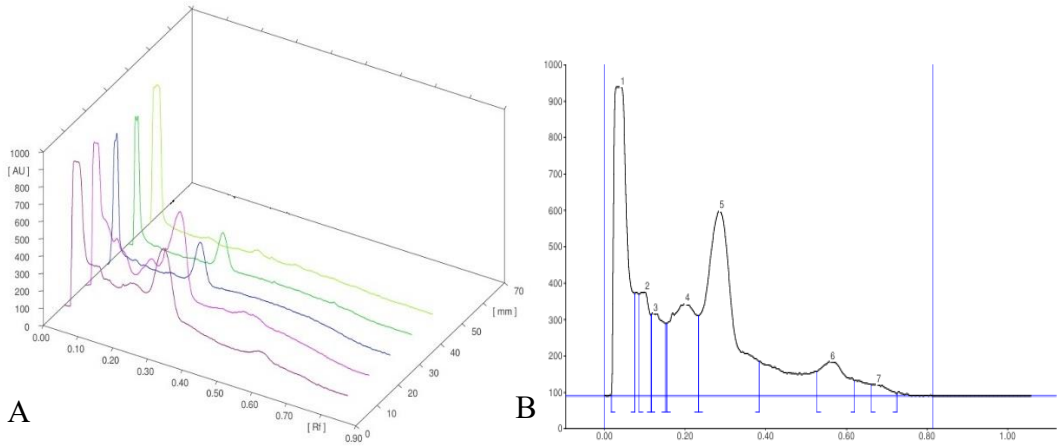

Figure 5.29: A) 3D chromatogram of fractions of *C.medica* B) chromatogram of CMEAF

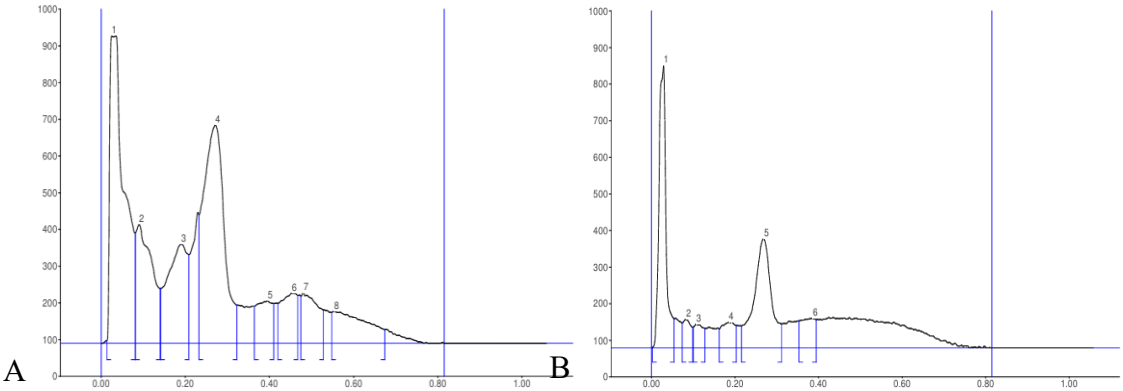

Figure 5.30: Chromatogram of A) CMBUF B) CMPEF

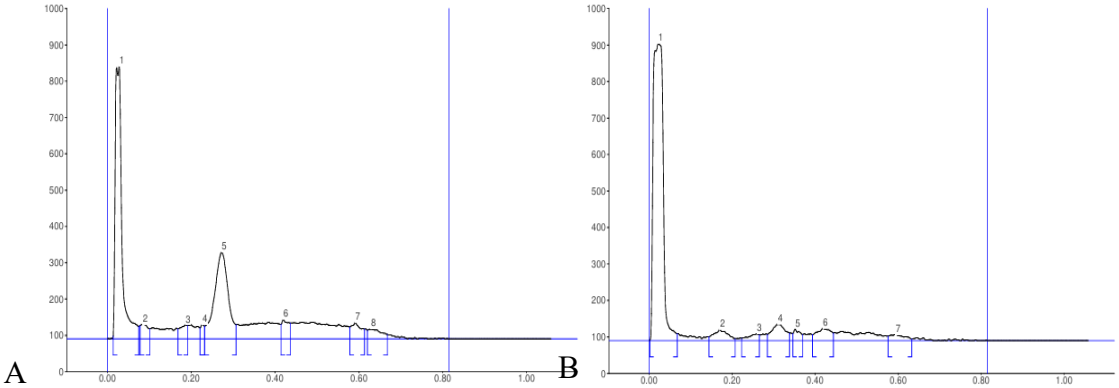

Figure 5.31: Chromatogram of A) CMBF B) CMWF

Table 5.25: Number of bands, Rf value, and percentage of peak area of various fractions of *C.medica*

CMEAF			CMWF			CMPEF			CMBUF			CMBF		
Peak No.	**Rf value**	**% Area**	**Peak No.**	**Rf value**	**% Area**	**Peak No.**	**Rf value**	**% Area**	**Peak No.**	**Rf value**	**% Area**	**Peak No.**	**Rf value**	**% Area**
1	0.07	28.62	1	0.07	78.55	1	0.06	38.87	1	0.05	27.42	1	0.07	49.18
2	0.11	7.05	2	0.21	4.09	2	0.10	4.75	2	0.14	11.78	2	0.10	3.05
3	0.15	6.82	3	0.27	1.98	3	0.13	4.45	3	0.21	12.10	3	0.19	2.88
4	0.23	16.14	4	0.34	6.04	4	0.20	6.99	4	0.32	27.59	4	0.23	1.52
5	0.38	34.12	5	0.37	2.07	5	0.31	36.44	5	0.41	4.22	5	0.31	31.46
6	0.62	5.98	6	0.45	4.75	6	0.40	8.49	6	0.47	4.97	6	0.44	3.92
7	0.72	1.26	7	0.63	2.51				7	0.53	5.14	7	0.61	4.38
									8	0.68	6.77	8	0.67	3.61

CMPEF – *Citrus medica* petroleum ether fraction, CMBF - *Citrus medica* benzene fraction, CMEAF - *Citrus medica* ethyl acetate fraction, CMBUF - *Citrus medica* butanol fraction, CMWF - *Citrus medica* water fraction.

5.13.2 Qualitative HPTLC Fingerprinting of fractions of *T.undulata*

We found that different fractions of *T.undulata* exhibited a wide range of secondary flavonoid metabolites based on HPTLC fingerprinting, as evident by the different colors of the bands at 265 and 365 nm wavelengths (Figure 5.32A and B).

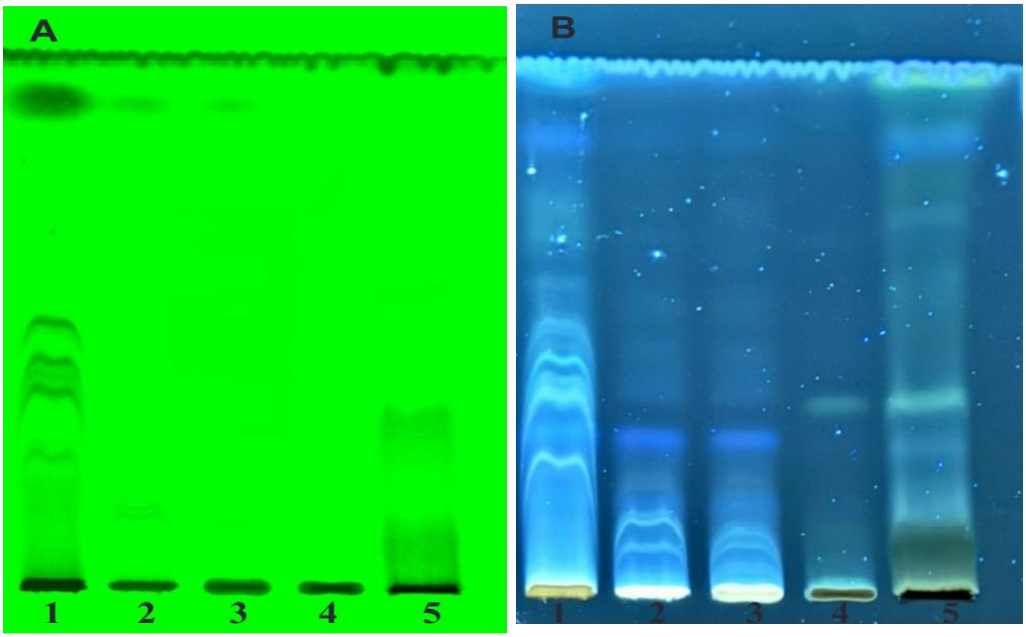

Track 1 - TUEAF, Track 2 – TUBUF, Track 3 – TUPEF, Track 4 - TUBF, Track 5 - TUWF

Figure 5.32: HPTLC fingerprinting of fractions of *citrus medica* A) At 366 nm B) 254 nm

Table 5.26 demonstrated that TMEAF, TUPEF, TUBUF, TUWF, and TUBF fractions had twelve, eleven, ten, seven, and four bands respectively at 254nm wavelength. All fractions show different numbers of bands at different Rf values and with different % peak areas.

Table 5.26: HPTLC fingerprinting analysis of fractions of *T.undulata*

Track No.	Name of Fraction	Number of Bands at 254 nm
1	TUEAF	12
2	TUBUF	10
3	TUPEF	11
4	TUBF	04
5	TUWF	07

TUPEF – *Tecomella undulata* petroleum ether fraction, TUBF - *Tecomella undulata* benzene fraction, TUEAF - *Tecomella undulata* ethyl acetate fraction, TUBUF - *Tecomella undulata* butanol fraction, TUWF - *Tecomella undulata* water fraction.

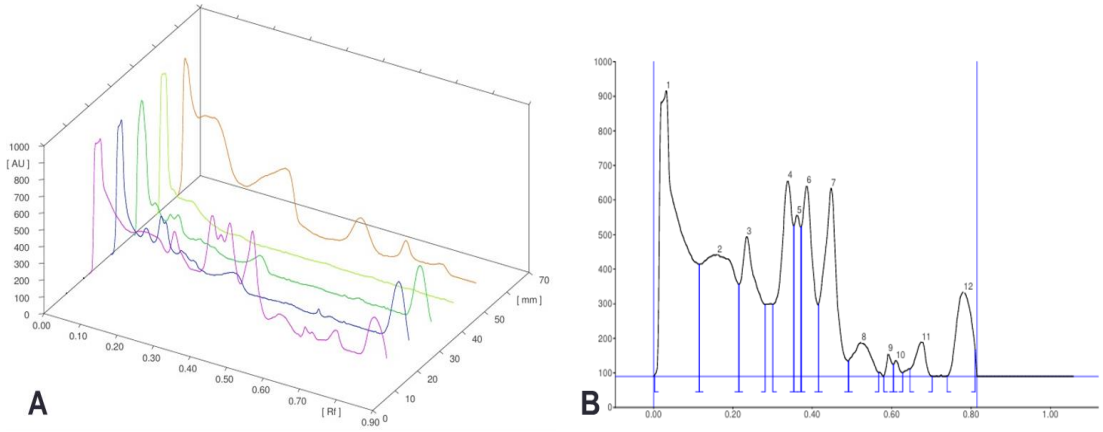

Figure 5.33: A) 3D chromatogram of fractions of *T.undualata* B) chromatogram of TUEAF

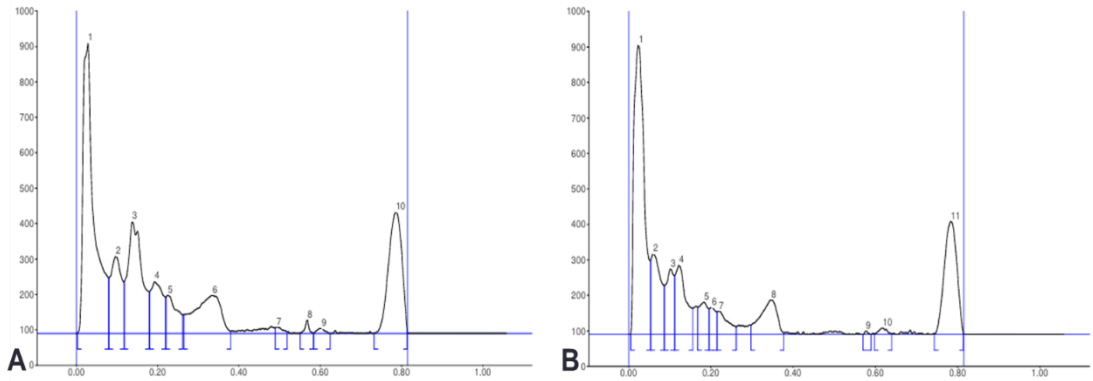

Figure 5.34: Chromatogram of A) TUBUF B) TUPEF

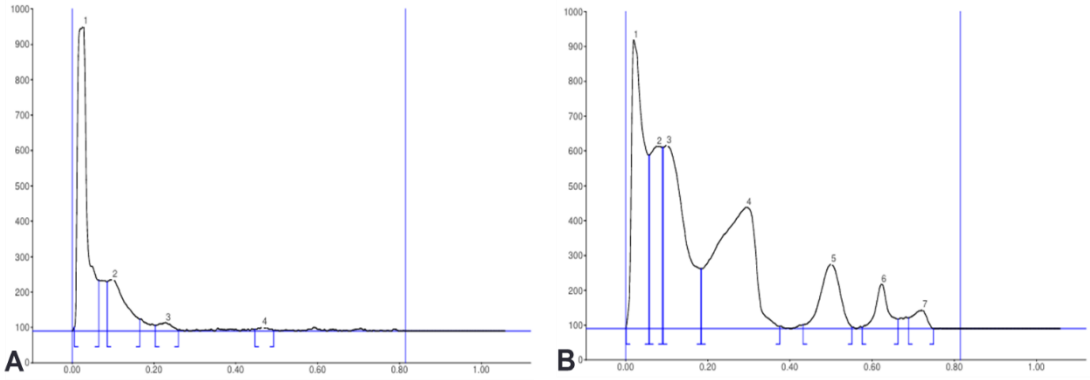

Figure 5.35: Chromatogram of A) TUBF B) TUWF

Table 5.27: Number of bands, Rf value, and percentage of peak area of various fractions of *T.undulata*

TUEAF			TUBUF			TUPEF			TUBF			TUWF		
Peak No.	**Rf value**	**% Area**	**Peak No.**	**Rf value**	**% Area**	**Peak No.**	**Rf value**	**% Area**	**Peak No.**	**Rf value**	**% Area**	**Peak No.**	**Rf value**	**% Area**
1	0.11	26.79	1	0.08	34.10	1	0.05	38.05	1	0.06	73.46	1	0.06	21.93
2	0.21	17.38	2	0.12	8.95	2	0.09	10.32	2	0.17	22.65	2	0.09	12.70
3	0.28	10.33	3	0.18	16.85	3	0.11	6.44	3	0.26	2.84	3	0.18	23.77
4	0.35	10.84	4	0.22	6.64	4	0.16	9.55	4	0.49	1.05	4	0.38	29.02
5	0.37	4.31	5	0.26	4.38	5	0.20	3.73				5	0.55	7.60
6	0.42	9.11	6	0.38	10.55	6	0.21	2.24				6	0.66	3.38
7	0.49	10.72	7	0.52	0.49	7	0.26	3.22				7	0.75	1.61
8	0.57	2.63	8	0.58	0.54	8	0.38	7.29						
9	0.60	0.49	9	0.63	0.42	9	0.59	0.14						
10	0.63	0.38	10	0.82	17.08	10	0.64	0.68						
11	0.70	1.52				11	0.82	18.34						
12	0.81	5.51												

TUPEF – *Tecomella undulata* petroleum ether fraction, TUBF - *Tecomella undulata* benzene fraction, TUEAF - *Tecomella undulata* ethyl acetate fraction, TUBUF - *Tecomella undulata* butanol fraction, TUWF - *Tecomella undulata* water fraction.

5.14 *In-vivo* anticoagulant activity of Fractions

5.14.1 *In-vivo* Blood Clotting Time Measurement

5.14.1.1 *In-vivo* Blood clotting time measurement of ethyl acetate fraction of *C.medica*

Figure 5.36 depicts these observations. This finding indicates the presence of anticoagulant(s) in *C.medica*, implying that they work optimally within a specified concentration range.

Blood clotting time was assessed in this anticoagulant activity model at 3, 5, and 7-day intervals. The amount of time needed for blood clotting was measured in the ethyl acetate fraction of *C. medica*. When compared to the normal group (30.33 ± 1.53), the CMEAF 200 mg/ml (65 ± 3.0) concentration on day 7 had the highest clotting time, on day 3(47 ± 3.0) and day 5 (58.33 ± 3.51) minutes, respectively. The same concentration demonstrated substantial blood clotting time on the third (47 ± 3.0, $p<0.001$) and fifth (58.33 ± 3.51, $p<0.01$) day when compared to the positive control group (36 ± 2.0 and 45.33 ± 3.06).

Table 5.28: *In-vivo* Blood clotting time of ethyl acetate fraction of *C.medica*

Group	Clotting Time (Minutes)		
	3rd day	5th day	7th day
NS	30.33 ± 1.53	30.33 ± 2.08	30.33 ± 1.53
CMEAF 100	42 ± 2.0*	45.67 ± 2.52^{ns}	54.33 ± 2.08^{ns}
CMEAF 200	47 ± 3.0$^{\#}$	58.33 ± 3.51**	65 ± 3.0*
CMEAF 400	44.67 ± 2.08**	56 ± 4.0*	62 ± 2.0^{ns}
Positive Control (Warfarin)	36 ± 2.0	45.33 ± 3.06	53.33 ± 2.08

Results are expressed as Mean ± SE values (n=3). All concentrations of *Citrus medica* ethyl acetate fractions (CMEAF) were suspended in saline. *p<0.05, **p<0.01, #p<0.001 significant when compared with standard (Positive control group), α p<0.05, β p<0.01, γ p<0.001 significant when compared with Normal saline (Vehicle control group) using one way ANOVA analysis (Multiple comparison).

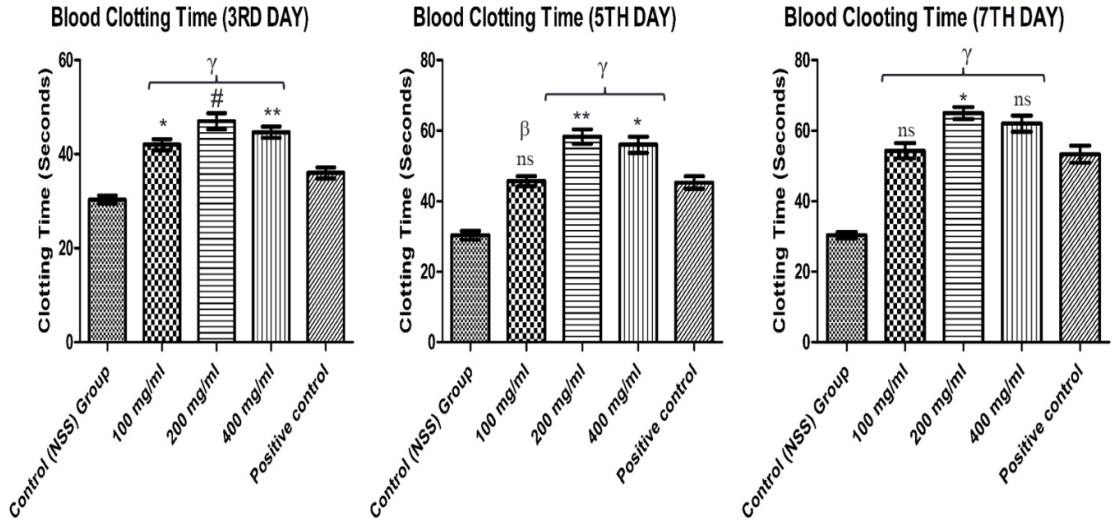

Results are expressed as Mean ± SE values (n=3). All concentrations of fraction were suspended in saline. *p<0.05, **p<0.01, #p<0.001 significant when compared with standard (Positive control group), α p<0.05, β p<0.01, γ p<0.001 significant when compared with Normal saline (Vehicle control group)

Figure 5.36: *In-vivo* Blood clotting time of ethyl acetate fraction of *C.medica*

The blood clotting time on the seventh day is marginally longer (65 ± 3.0, p<0.05) than in the positive control group (53.33 ± 2.08). Comparing CMEAF 100mg/ml (42 ± 2.0, p<0.05) to the positive control group alone on the third day revealed a significant effect on blood clotting. As compared to the positive control group, the CMEAF 500 mg/ml blood clotting effect persisted for 3 days (44.67 ± 2.08, p<0.01), and 5 days (56 ± 4.0, p<0.05), as indicated by Table 5.28 and Figure 5.36. CMEAF 200 mg/ml has a longer half-life than CMEAF 400 mg/ml, however, the effect of CMEAF 400 mg/ml on activated partial thromboplastin time lasted for five days.

5.14.1.2 *In-vivo* Blood clotting time measurement of butanol fraction of *T.undulata*

In this anticoagulant activity model, blood clotting time was measured at 3, 5, and 7-day intervals. The butanol fraction of *T.undulata* was used to measure the time required for blood coagulation. The TUBUF 200 mg/ml (54.67 ± 3.05) concentration on day 7 had the maximum clotting time, on day 3 (45 ± 2.65) and day 5 (52.67 ± 2.08) minutes, respectively, as compared to the normal group (30.33 ± 1.53). When comparing the blood clotting time on the fifth (52.67 ± 2.08, p<0.01) and seventh (54.67 ± 3.05, p<0.001) days to the positive control group (45.33 ± 3.06, and 53.33 ± 2.08) on the same day, the same concentration showed significant differences.

On the seventh day, the positive control group's blood clotting time (53.33 ± 2.08) is marginally shorter than that of the blood clotting time (54.67 ± 3.05, $p<0.01$). TUBUF 100mg/ml (42 ± 2.0, $p<0.05$) did not significantly affect blood coagulation as compared to the positive control group on the third, fifth, and seventh day. Table 5.29 and Figure 5.37 simply show that the TUBUF 400 mg/ml blood coagulation effect lasted for 3 days (43.67 ± 2.52, $p<0.05$) in comparison to the positive control group.

Table 5.29: *In-vivo* Blood clotting time of butanol fraction of *T.undulata*

Group	Clotting Time (Minutes)		
	3rd day	5th day	7th day
NS	30.33 ± 1.53	30.33 ± 2.08	30.33 ± 1.53
TUBUF 100	34.67 ± 2.51^{ns}	36.67 ± 2.51^{ns}	39.33 ± 3.05^{ns}
TUBUF 200	$45 \pm 2.65^{**}$	$52.67 \pm 2.08^{*}$	$54.67 \pm 3.05^{**}$
TUBUF 400	$43.67 \pm 2.52^{*}$	45.67 ± 3.08^{ns}	40.33 ± 3.5^{ns}
Positive Control (Warfarin)	36 ± 2.0	45.33 ± 3.06	53.33 ± 2.08

Results are expressed as Mean ± SE values (n=3). All *Tecomella undulata* butanol fractions (TUBUF) were suspended in saline. *p<0.05, **p<0.01, ***p<0.005, #p<0.001 significant when compared with Normal saline (vehicle control), α p<0.05, β p<0.01, γ p<0.001 significant when compared with Normal saline (Vehicle control group) using one way ANOVA analysis (Multiple comparison).

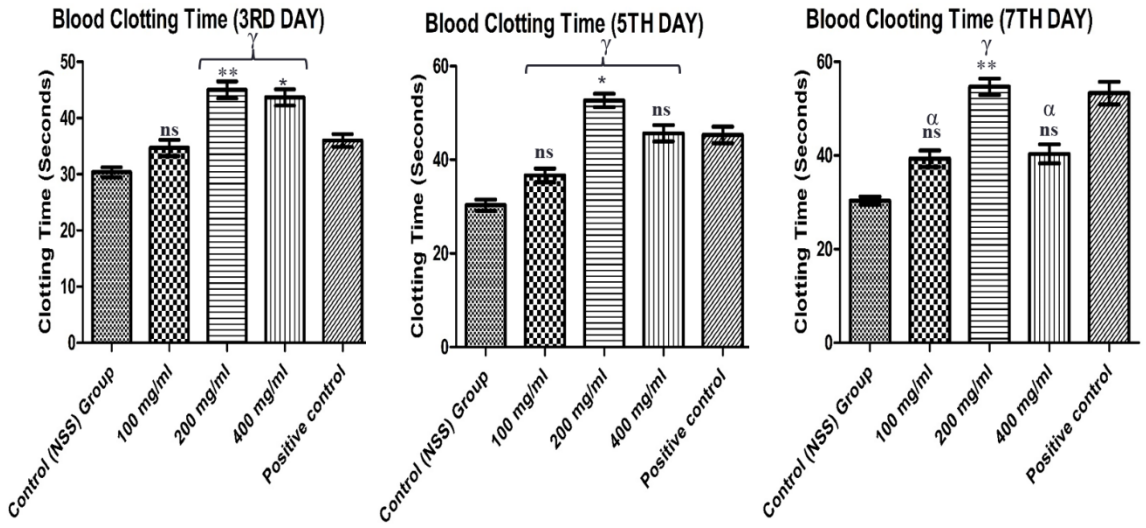

Results are expressed as Mean ± SE values (n=3). All concentrations of fraction were suspended in saline. *p<0.05, **p<0.01, #p<0.001 significant when compared with standard (Positive control group), α p<0.05, β p<0.01, γ p<0.001 significant when compared with Normal saline (Vehicle control group)

Figure 5.37: *In-vivo* Blood clotting time of butanol fraction of *T.undulata*

5.14.2 *In-vivo* Prothrombin time (PT) activity assay

5.14.2.1 *In-vivo* Prothrombin time measurement of ethyl acetate fraction of *C.medica*

In this anticoagulant activity model, prothrombin time was measured at 3, 5, and 7-day intervals. The Prothrombin time was determined in the *C. medica* ethyl acetate fraction. Day 3 CMEAF 200 mg/ml (36 ± 2.0) had the maximum prothrombin time on day 5 (26.67 ± 2.52) and day 7 (27.33 ± 2.52) seconds, respectively, as compared to the normal group (16 ± 1.0). Comparing the prothrombin time on the fifth (26.67 ± 2.52, $p<0.01$) and seventh (27.33 ± 2.52, $p<0.001$) days to the positive control group (19.67 ± 1.43 and 19.33 ± 1.53), the same concentration showed significant differences.

On the third day, there was a greater duration of Prothrombin time (36 ± 2.0, $p<0.001$) compared to the positive control group's 53.33 ± 2.08. A marginally significant effect on prothrombin time was seen on the third day (26.67 ± 3.06, $p<0.05$) and fifth day (22.33 ± 1.53, $p<0.05$) when CMEAF 100mg/ml was compared to the positive control group alone. Table 5.30 and Figure 5.38 show the CMEAF 400 mg/ml shows a significant increase in prothrombin time as compared to the positive control group on the third (31 ± 3.61, $p<0.01$), fifth (24 ± 1.0, $p<0.05$), and seventh day (25.33 ± 2.08, $p<0.05$).

Table 5.30: *In-vivo* Prothrombin time of ethyl acetate fraction of *C.medica*

Group	**Prothrombin Time (Seconds)**		
	3rd day	**5th day**	**7th day**
NS	16 ± 1.0	14.93 ± 1.93	14.83 ± 1.42
CMEAF 100	26.67 ± 3.06*	22.33 ± 1.53*	17.67 ± 1.53^{ns}
CMEAF 200	36 ± 2.0$^{\#}$	26.67 ± 2.52**	27.33 ± 2.52**
CMEAF 400	31 ± 3.61**	24 ± 1.0*	25.33 ± 2.08*
Positive Control (Warfarin)	22.67 ± 1.53	19.67 ± 1.43	19.33 ± 1.53

Results are expressed as Mean ± SE values (n=3). All concentrations of *Citrus medica* ethyl acetate fractions were suspended in saline. *p<0.05, **p<0.01, #p<0.001 significant when compared with standard (Positive control group) using one way ANOVA analysis (Multiple comparison).

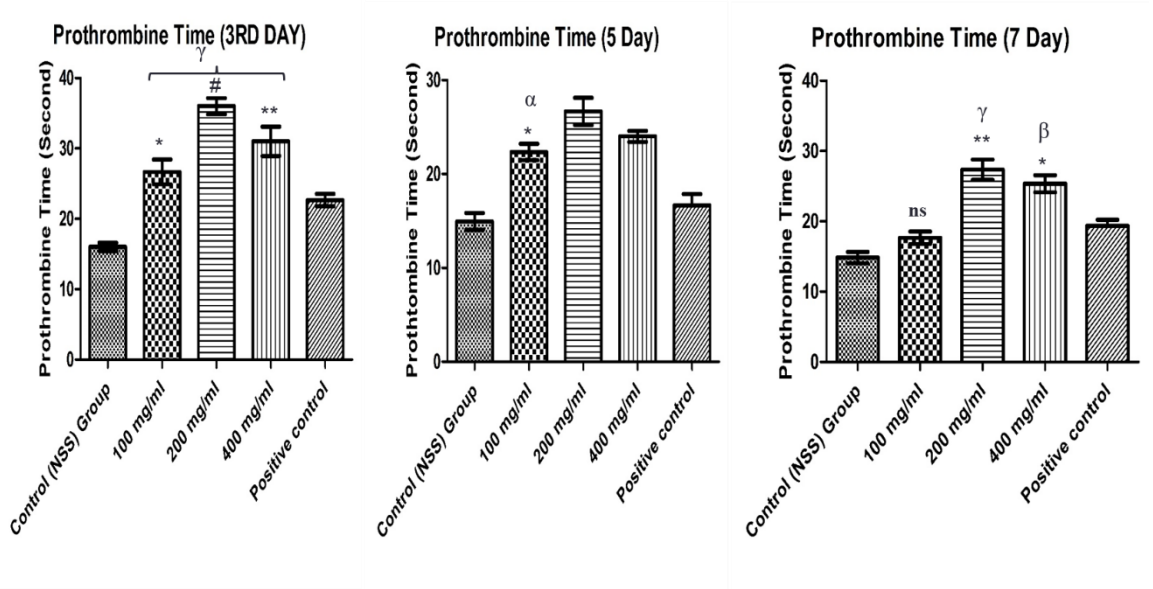

Results are expressed as Mean ± SE values (n=3). All concentrations of fraction were suspended in saline. *p<0.05, **p<0.01, #p<0.001 significant when compared with standard (Positive control group), α p<0.05, β p<0.01, γ p<0.001 significant when compared with Normal saline (Vehicle control group)

Figure 5.38: *In-vivo* Prothrombin time of ethyl acetate fraction of *C.medica*

5.14.2.2 *In-vivo* Prothrombin time measurement of butanol fraction of *T.undulata*

In this anticoagulant activity model, prothrombin time was measured at 3, 5, and 7-day intervals. The Prothrombin time was determined in the *T.undulata* butanol fraction. Day 3 TUBUF 200 mg/ml (29 ± 2.0) had the maximum prothrombin time on day 5 (23.67 ± 1.52) and day 7 (25 ± 2.0) seconds, respectively, as compared to the normal group (16 ± 1.0). Comparing the prothrombin time on the third day (29 ± 2.0, p<0.01), the fifth (23.67 ± 1.52, p<0.05) and seventh (25 ± 2.0, p<0.05) days showed significant differences to the positive control group (19.67 ± 1.43 and 19.33 ± 1.53) at TUBUF 200 mg/ml concentration.

Table 5.31: *In-vivo* Prothrombin time of butanol fraction of *T.undulata*

Group	Prothrombin Time (Seconds)		
	3rd day	5th day	7th day
NS	16 ± 1.0	14.93 ± 1.93	14.83 ± 1.42
TUBUF 100	20.33 ± 1.5^{ns}	22.33 ± 1.53^{ns}	19 ± 2.0 ^{ns}
TUBUF 200	29 ± 2.0**	23.67 ± 1.52*	25 ± 2.0*
TUBUF 400	23 ± 1.75^{ns}	22.33 ± 3.05^{ns}	20.33 ± 1.52 ^{ns}
Positive Control	22.67 ± 1.53	19.67 ± 1.43	19.33 ± 1.53

(Warfarin)

Results are expressed as Mean ± SE values (n=3). All *Tecomella undulata* butanol fractions (TUBUF) were suspended in saline. *p<0.05, **p<0.01, ***p<0.005, #p<0.001 significant when compared with Normal saline (vehicle control) using one way ANOVA analysis (Multiple comparison).

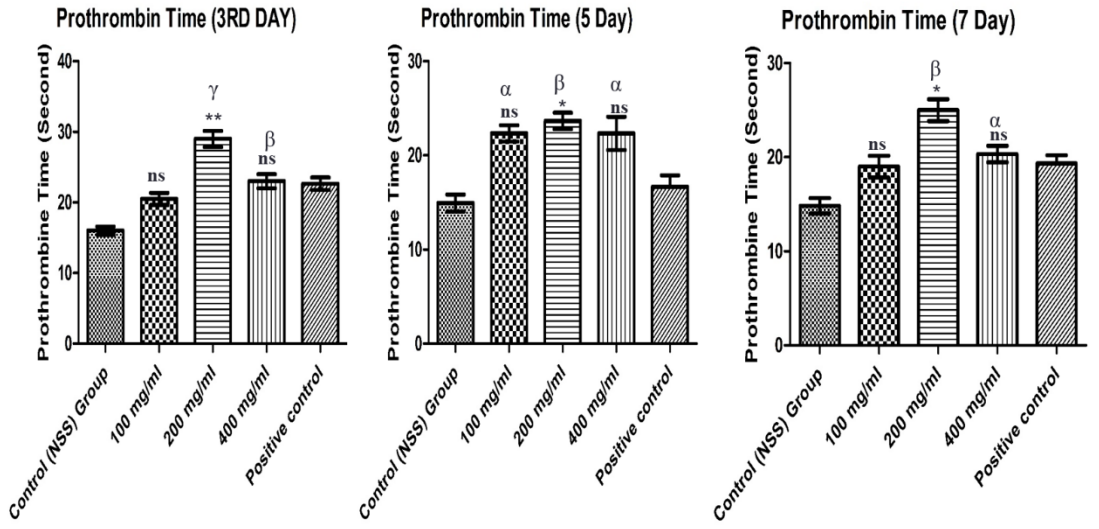

Results are expressed as Mean ± SE values (n=3). All concentrations of fraction were suspended in saline. *p<0.05, **p<0.01, #p<0.001 significant when compared with standard (Positive control group), α p<0.05, β p<0.01, γ p<0.001 significant when compared with Normal saline (Vehicle control group)

Figure 5.39: *In-vivo* Prothrombin time of butanol fraction of *T.undulata*

In comparison to the positive control group on the third (20.33 ± 1.5, 23 ± 1.75), fifth (22.33 ± 1.5, 22.33 ± 3.05), and seventh day (20.33 ± 1.52), Table 5.31 and Figure 5.39 demonstrate that CMEAF 100 and 400 mg/ml had no discernible impact on prothrombin time. For seven days, TUBUF 200 mg/ml had an impact on prothrombin time.

5.14.3 *In-vivo* Activated Partial Thromboplastin time (APTT) activity assay

5.14.3.1 *In-vivo* Activated Partial Thromboplastin time measurement of ethyl acetate fraction of *C.medica*

In this anticoagulant activity model, activated partial thromboplastin time was measured at 3, 5, and 7-day intervals. The activated partial thromboplastin time was determined in the *C. medica* ethyl acetate fraction. Day 3 CMEAF 200 mg/ml (30.33 ± 2.08) had the maximum activated partial thromboplastin time and on day 5 (30.33 ± 1.53) and day 7 (30 ± 2.00) seconds, respectively, as compared to the normal group (15.33 ± 0.58). At CMEAF 200mg/ml when comparing the activated partial thromboplastin on the third (30.33 ± 2.08, p<0.001) the fifth (30.33 ± 1.53,

p<0.01), and seventh (30 ± 2.00, p<0.01) days to the positive control group (20.67 ± 1.53, 19.67 ± 2.52, and 22.67 ± 1.53), the same concentration showed significant differences. The effect of CMEAF 200mg/ml on activated partial thromboplastin time persisted for 7 days.

Table 5.32: *In-vivo* Activated Partial Thromboplastin time of ethyl acetate fraction of *C.medica*

Group	Activated Partial Thromboplastin Time (Seconds)		
	3rd day	5th day	7th day
NS	15.33 ± 0.58	15.13 ± 1.21	15.67 ± 1.15
CMEAF 100	25.33 ± 2.52*	21.33 ± 2.53ns	20.67 ± 2.53 ns
CMEAF 200	30.33 ± 2.08#	30.33 ± 1.53**	30 ± 2.00**
CMEAF 400	27.67 ± 2.52**	29.67 ± 2.0**	28.33 ± 1.53*
Positive Control (Warfarin)	20.67 ± 1.53	19.67 ± 2.52	22.67 ± 1.53

Results are expressed as Mean ± SE values (n=3). All concentrations of *Citrus medica* ethyl acetate fractions were suspended in saline. *p<0.05, **p<0.01, #p<0.001 significant when compared with standard (Positive control group) using one way ANOVA analysis (Multiple comparison).

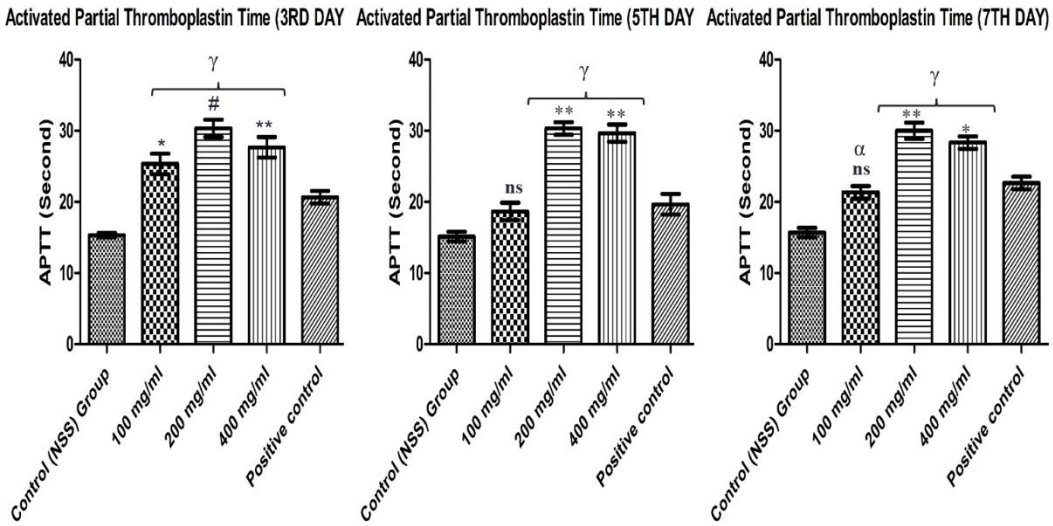

Results are expressed as Mean ± SE values (n=3). All concentrations of fraction were suspended in saline. *p<0.05, **p<0.01, #p<0.001 significant when compared with standard (Positive control group), α p<0.05, β p<0.01, γ p<0.001 significant when compared with Normal saline (Vehicle control group)

Figure 5.40: *In-vivo* Activated Partial Thromboplastin time of ethyl acetate fraction of *C.medica*

In comparison to the positive control group (20.67 ± 1.53), CMEAF 100mg/ml had a marginally significant effect on activated partial thromboplastin time seen on the third day (25.33 ± 2.52, $p<0.05$). It was unable to demonstrate the noteworthy impact of activated partial thromboplastin time on the fifth and seventh days. As compared to the positive control group, the CMEAF 400 mg/ml significantly increased the activated partial thromboplastin time on the third (27.67 ± 2.52, $p<0.01$), fifth (29.67 ± 2.0, $p<0.01$), and seventh days (28.33 ± 1.53, $p<0.01$) (Table 5.32 and Figure 5.40). CMEAF 200 mg/ml has a longer half-life than CMEAF 400 mg/ml, however, the effect of CMEAF 400 mg/ml on activated partial thromboplastin time lasted for seven days.

5.14.3.2 *In-vivo* Activated Partial Thromboplastin time measurement of butanol fraction of *T.undulata*

Activated partial thromboplastin time was assessed in this anticoagulant activity model at 3, 5, and 7-day intervals. Activated partial thromboplastin time was measured in the butanol fraction of *T.undulata*. When compared to the normal group (15.33 ± 0.58), day 3 TUBUF 200 mg/ml (27.67 ± 1.52) had the largest activated partial thromboplastin time on day 5 (26.33 ± 2.30) and day 7 (26.67 ± 2.51) seconds, respectively. When comparing the activated partial thromboplastin time at TUBUF 200 mg/ml concentration to the positive control group, the results on the third day (27.67 ± 1.52, $p<0.01$), the fifth day (26.33 ± 2.30, $p<0.05$), and the seventh day (26.67 ± 2.51, $p<0.05$) showed significant differences. In comparison to the positive control group on the third (19.67 ± 2.08), fifth (18.33 ± 1.52), and seventh day (17.67 ± 1.52). Table 5.33 and Figure 5.41 show that TUBUF 100 mg/ml had no significant effect on activated partial thromboplastin time when compared to the positive control group on the third (19.67 ± 2.08), fifth (18.33 ± 1.52), and seventh day (17.67 ± 1.52). On the third day alone, TUBUF 400 mg/ml was found to influence activated partial thromboplastin time. TUBUF 400 mg/ml had no effect on activated partial thromboplastin time on the fifth or seventh day. TUBUF 200 mg/ml affected activated partial thromboplastin time for seven days.

Table 5.33: *In-vivo* Activated Partial Thromboplastin time of butanol fraction of *T.undulata*

Group	Activated Partial Thromboplastin Time (Seconds)

	3rd day	5th day	7th day
NS	15.33 ± 0.58	15.13 ± 1.21	15.67 ± 1.15
TUBUF 100	19.67 ± 2.08^{ns}	18.33 ± 1.52^{ns}	17.67 ± 1.52^{ns}
TUBUF 200	27.67 ± 1.52**	26.33 ± 2.30*	26.67 ± 2.51*
TUBUF 400	25.33 ± 1.52*	24.33 ± 1.52^{ns}	24.67 ± 3.60^{ns}
Positive Control (Warfarin)	20.67 ± 1.53^{ns}	19.67 ± 2.52^{ns}	22.67 ± 1.53^{ns}

Results are expressed as Mean ± SE values (n=3). All *Tecomella undulata* butanol fractions (TUBUF) were suspended in saline. *p<0.05, **p<0.01, ***p<0.005, #p<0.001 significant when compared with Normal saline (vehicle control), α p<0.05, β p<0.01, γ p<0.001 significant when compared with Normal saline (Vehicle control group) using one way ANOVA analysis (Multiple comparison).

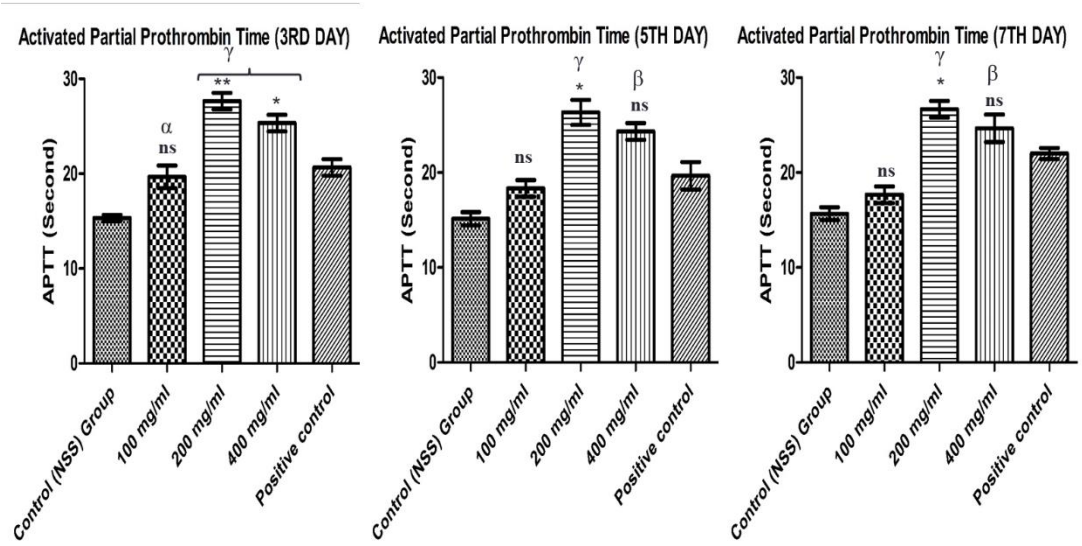

Results are expressed as Mean ± SE values (n=3). All concentrations of fraction were suspended in saline. *p<0.05, **p<0.01, #p<0.001 significant when compared with standard (Positive control group), α p<0.05, β p<0.01, γ p<0.001 significant when compared with Normal saline (Vehicle control group)

Figure 5.41: *In-vivo* Activated Partial Thromboplastin time of butanol fraction of *T.undulata*

The coagulation system functions by a complex cascade of processes involving multiple unique protein pathways (Palta et al., 2014). Through these mechanisms, fibrinogen is converted into fibrin, which joins platelets to create a thrombus. The two elements that start coagulation cascades are intrinsic and extrinsic coagulation pathways. The extrinsic coagulation pathway produces the first generation of activated factor X (Factor Xa), which is induced by the factor VIIa/tissue factor complex. The intrinsic route is influenced by factors XI, XII, IX, and VIII. When

the intrinsic pathway is triggered, Factor Xa, a crucial part of the coagulation cascade known as the common pathway, is enhanced (Palta et al., 2014). The APTT and PT tests measure the ability to form a blood clot in a reasonable amount of time; if any of these components are compromised, the test results will be prolonged. Coagulation factors VIII, IX, XI, and XII in the intrinsic coagulation pathway are evaluated by the APTT, while the extrinsic clotting factors, such as coagulation factor VII, are evaluated by the PT test. These two tests also evaluate a common route comprising factors I, II, V, and X of the clotting cascade. According to the experiment's findings, both CMEAF and TUBUF prolonged blood clotting time, PT, and aPPT for seven days in a dose-dependent manner. However, when compared to warfarin as the norm, the 200 mg/ml concentrations of TUBUF and CMEAF prolong the PT and aPTT times by 7 days. Consequently, the inhibition of factors V, X, and prothrombin in the common coagulation pathway is implied by the prolonged PT and aPTT that follow therapy with CMEAF and TUBUF. To identify the precise mechanism underlying this inhibition, more research is required. Nonetheless, direct inhibition of the same coagulation pathway may be one possible mode of action for both fractions (CMEAF & TUBUF). Multiple mechanisms may be involved in this suppression. For example, factor Xa and its cofactor Va may reduce thrombin (factor IIa) production, or thrombin and fibrinogen may interact less effectively, preventing fibrin formation. These findings imply that the butanol and ethyl acetate fractions of *T.undulata* and *C.medica* contain a protease inhibitor that may be able to efficiently block these proteases. As a result, there would be no zymogen conversion into active factors Xa, Va, and thrombin. Furthermore, by binding to Antithrombin III and causing a conformational change that converts protein C (PC) into activated protein C (APC), the active component(s) of *C.medica* and *T.undulata* may activate the natural anticoagulant cascade. Factors Va and VIIIa are essential cofactors for the activation of factors Xa and IIa, and APC suppresses them together with protein S, its cofactor.

This combined action ultimately prevents thrombin and factor Xa from being activated in the common coagulation pathway, which may account for the anticoagulant effects. Common anticoagulant medications such as heparin, warfarin, all-trans retinoic acid, and new anticoagulants (NOACs) are frequently

used in the treatment of thrombotic disorders. Regarding reversibility and duration of action, these medications differ from one another. Warfarin is a long-acting, slow-acting action that is also reversible, whereas heparin is a fast-acting anticoagulant. While NOACs operate quickly but cannot be reversed, all-trans retinoic acid acts slowly (Rajesh 2011, Bryan, 2013).

Heparin binds to a specific place on Antithrombin to produce a conformational shift that exposes the binding site for thrombin (IIa) and inactivating factor Xa, which is how it exerts its anticoagulant effects. This considerably increases Antithrombin's anticoagulant activity by a factor of 1,000 (Blann & Khoo 2009). The coagulation pathway's vitamin K-dependent proteins are neither activated or synthesized when taking warfarin, a vitamin K antagonist. Factors X, IX, VII, and prothrombin are among these proteins. For these proteins to be able to bind calcium and be physiologically activated, certain glutamic acid residues must be carboxylated, which requires vitamin K (Truong & Booth 2011, Ross, A. C et al. 2012). According to studies (Ghaffari et al., 2019, Aoshima et al., 1998, Koyama et al., 1994), all-trans retinoic acid increases the antithrombotic potential of microvascular endothelial cells by downregulating Tissue Factor and upregulating thrombomodulin expression. The butanol fraction of *T.undulata* and the ethyl acetate fraction of *C.medica* both exhibit anticoagulant activity, and their mechanisms of action are similar to those of warfarin, with a narrow concentration range of activity peak indicating quick action and reversibility.

5.15 GC-MS ANALYSIS:

5.15.1 GCMA Analysis of ethyl acetate fraction of *C.medica*

The running duration for the *C. medica* ethyl acetate fractions in the gas chromatography-mass spectrometry (GC-MS) analysis was forty minutes. It turned up fifteen peaks in all (Figure 5.42). By comparing the peak retention duration, peak area (%), height (%), and mass spectral fragmentation patterns of these peaks with those of recognized compounds listed in the National Institute of Standards and Technology (NIST) library, the bioactive compounds were discovered. The ethyl acetate fraction of *C. medica* included 15 recognized chemicals, according to the analysis (Table 5.34). The major phytoconstituents present in the ethyl acetate fraction of *C.medica* were Sucrose (22.58) (Figure 5.49), 5-Hydroxymethylfurfural

(21.21) (Figure 5.45), Lup-20(29)-en-3-ol, acetate, (3.beta.)- (18.83) (Figure 5.56), Olean-12-en-3-ol, acetate, (3.beta.)- (9.77) (Figure 5.55), 3-Deoxy-d-mannoic lactone (7.7) (Figure 5.50).

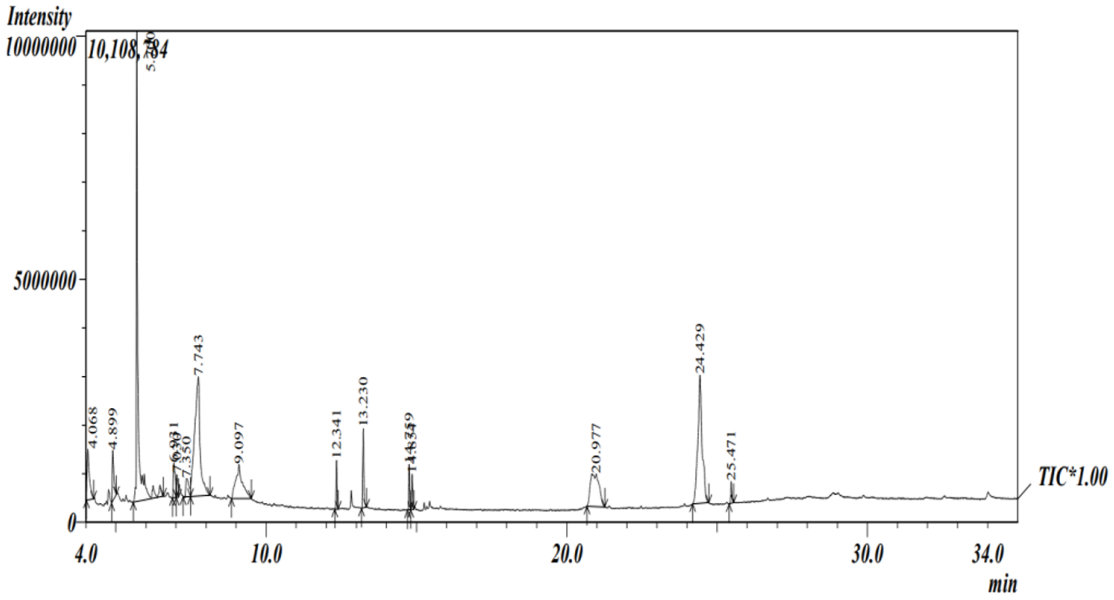

Figure 5.42: GC-MS chromatogram of ethyl acetate fraction of *C.medica*

Table 5.34: Retention time, peak area, name of compound present in CMEAF

S/N	Retention time	Name of compound	Molecular Formula	Peak Area (%)	Reported biological activity
1	4.068	Maltol	C6H6O3	3.95	Antioxidant activity (Han et. al., 2015) (Kang et. al., 2008), Diabetic Neuroprotective (Guo et. al., 2018), Liver & kidney (Sha et. al., 2021), Anti-inflammatory activity (Ahn et. al., 2022)

2	4.899	4H-Pyran-4-one, 2,3-dihydro-3,5-dihydroxy-6-methyl-	C6H8O4	2.85	Antioxidant activity (Kim et. al., 2022), α-glucosidase inhibitability (Van Chen et. al., 2022), Antifungal activity (Hamid et. al., 2016), Antimutagenic activity (Berhow et. al., 2000), Antitumor activity (Ban et. al., 2007), Anti-plasmodial activity (Amlabu et. al., 2018) Antioxidant Activity (Zhao et. al., 2013), Antiproliferative activities, Anti-ischemic, and Anti-tyrosine enzyme effects, Improving blood rheology and Protective in hypoxic brain injury (Li et. al., 2011), Anti-sickling (Abdulmalik et. al., 2005), Anti-inflammatory (Yamada et.al.,2011), Hepatoprotective (Ding et. al., 2010), Antiarthritic (Feng et. al., 2011), Anti-
3	5.7	5-Hydroxymethylfurfural	C6H6O3	21.21	

					allergen (Alizadeh et. al., 2017)
4	6.931	Sulfurous acid, cyclohexylmethyl hexadecyl ester	C23H46O3S	2.31	Antioxidant activity (Soleha et. al., 2020)
5	7.03	Butane, 1,1'-[methylenebis(oxy)] bis[3-methyl- / Furazan-3-ol, 4-amino / 2-Pyrrolidinone, 3-hydroxy-3,4-dimethyl	C11H24O2	1.11	No activity reported
6	7.35	Pyrazole, 3-methylaminomethyl-5-propyl-	C8H15N3	1.99	No activity reported
7	7.743	Sucrose	C12H22O11	22.58	No activity reported
8	9.097	3-Deoxy-d-mannoic lactone	C6H10O5	7.7	No activity reported
9	12.341	Hexadecanoic acid, methyl ester	C17H34O2	1.36	Immunosuppressive (Saeidinia et. al., 2004), Antioxidant & Antibacterial activity (Ganesan et. al., 2022), Antifungal, Anti-inflammatory, Hypocholesterolaemia and Cancer prevention activities (Kalpana et. al., 2012)
10	13.23	2H-1-Benzopyran-2-one, 5,7-dimethoxy-	C11H10O4	2.78	No activity reported
11	14.759	9,12-Octadecadienoic acid (Z,Z)-, methyl ester	C19H34O2	1.42	Anti-inflammatory, Antibacterial, Hypocholesterolemic,

12	14.854	8,11,14-Docosatrienoic acid, methyl ester	C23H40O2	1.29	Hepatoprotective activities, Antioxidant & Antimicrobial properties (Rahman et. al., 2014), Anti-arthritic, Antihistamine (Henry et al., 2002) Antitumor, Antioxidant & Anti-Inflammatory Activities (Chen et al., 2021) Antibacterial activity (Lazreg-Aref et al., 2012), Anti-inflammatory, Antitumor, Antifungal, Anti-diabetic, Anti-hyperlipidemic activities (Okoye et al., 2014), Antioxidative & Antiviral activity (Parvez et al.,2018), Antiallergic, Antiulcer, Antinociceptive activity (Oliveira et al., 2004), Antiplatelet Activity (Aragão et al., 2007),
13	20.977	Olean-12-en-3-ol, acetate, (3.beta.)-	C32H52O2	9.77	

					Sedative, Anticonvulsant and Anxiolytic activity (Aragão et al., 2009)
14	24.429	Lup-20(29)-en-3-ol, acetate, (3.beta.)-	C32H52O2	18.83	Antiprotozoal, Anti-inflammatory, Antitumor, Anti-prostate cancer, Anti-head and neck squamous cell carcinoma, Anti-melanoma, Cancer chemopreventive, Cardioprotective, Hepatoprotective, Antimicrobial, Anti-urolithiatic, Antiallergic, Antidiabetic, Anti-aging, Snake venom Antiserum activity, Antifertility agents, Gastroprotective, protect in neurodegenerative disorder (Sharma et al., 2020), Antiplatelet Activity (Saputri et al., 2012)

15	25.471	Squalene	C30H50	0.85	Hypolipidemic, Hepatoprotective, Cardioprotective, Antioxidant, Antitumor & Anti-toxicant activity (Muzalevskaya et al., 2015), Antimicrobial efficacy (Toh et al., 2023), Antidiabetic activity (Widyawati et al., 2023), Healing agent (Wołosik et al., 2013), Anti-cancer properties (Gunes 2013), Cardioprotective & Antioxidant effect (Ibrahim et al., 2020), Anti-inflammatory activity (Lou-Bonafonte et al., 2018)

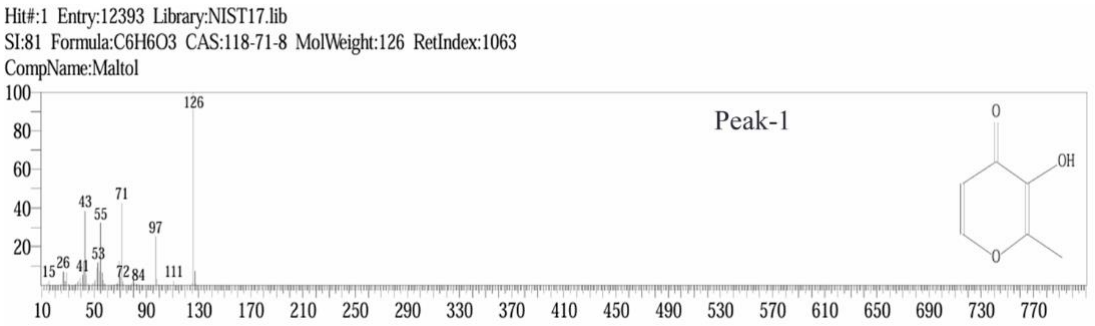

Figure 5.43: Mass fragmentation pattern of peak 1 of CMEAF

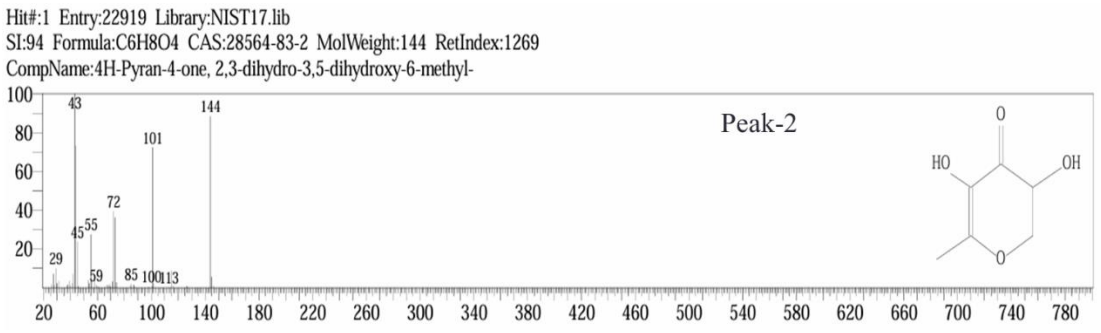

Figure 5.44: Mass fragmentation pattern of peak 2 of CMEAF

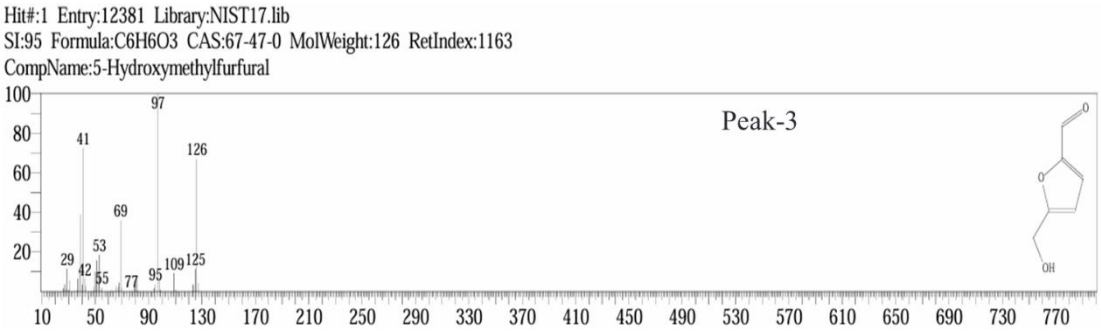

Figure 5.45: Mass fragmentation pattern of peak 3 of CMEAF

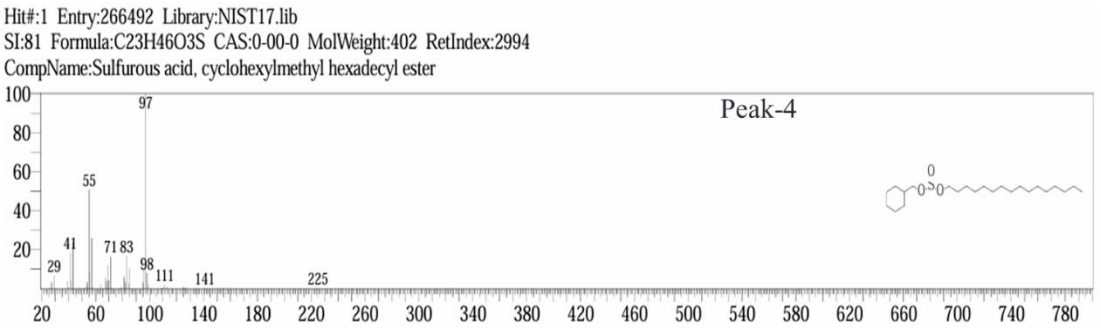

Figure 5.46: Mass fragmentation pattern of peak 4 of CMEAF

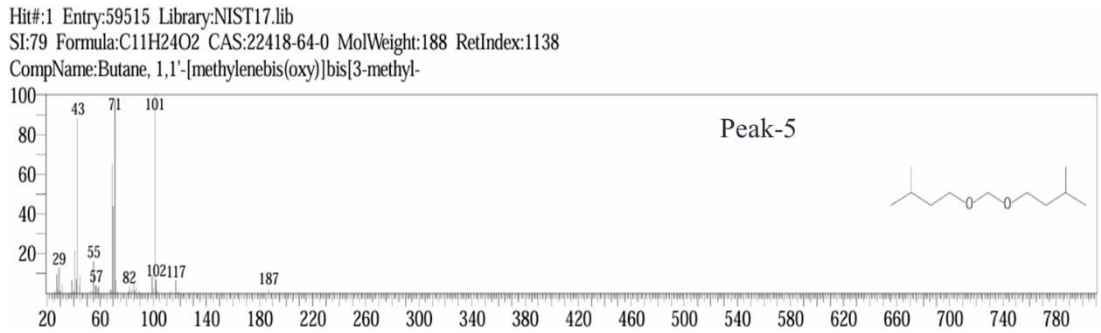

Figure 5.47: Mass fragmentation pattern of peak 5 of CMEAF

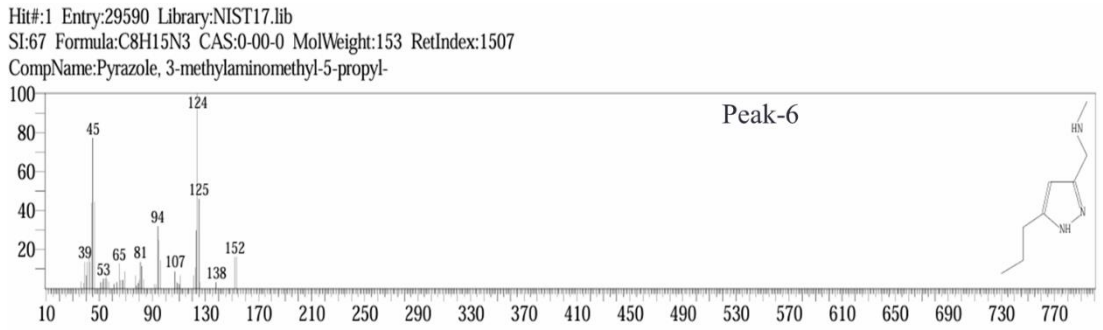

Figure 5.48: Mass fragmentation pattern of peak 6 of CMEAF

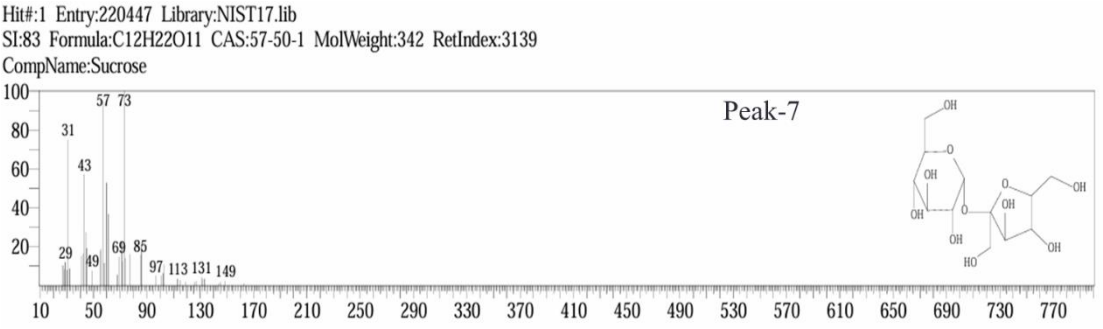

Figure 5.49: Mass fragmentation pattern of peak 7 of CMEAF

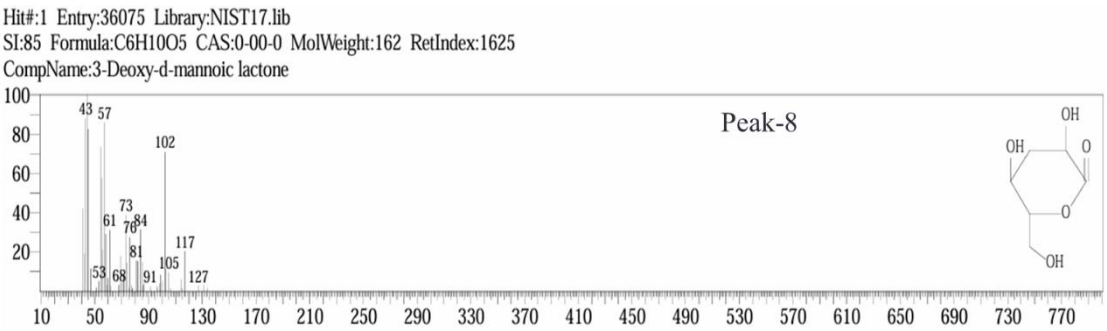

Figure 5.50: Mass fragmentation pattern of peak 8 of CMEAF

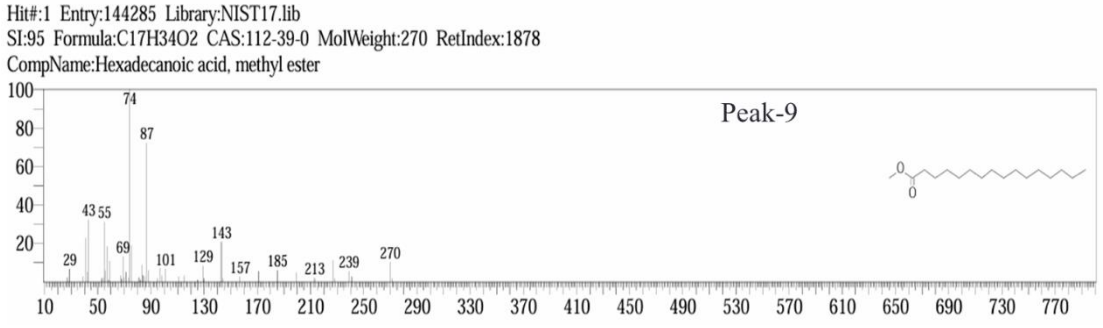

Figure 5.51: Mass fragmentation pattern of peak 9 of CMEAF

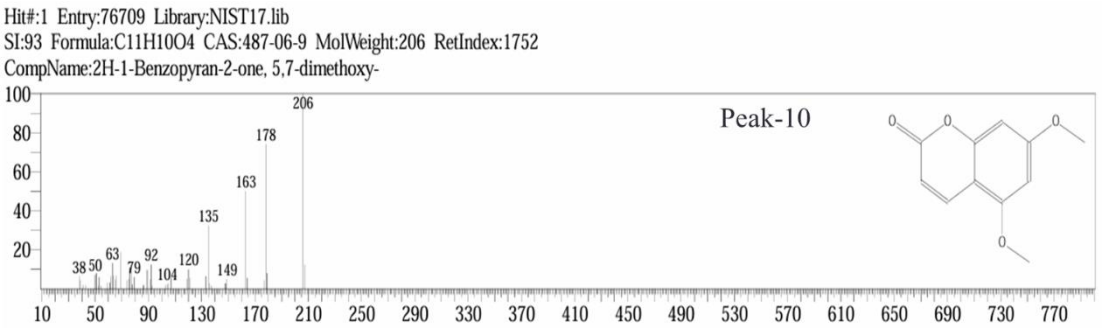

Figure 5.52: Mass fragmentation pattern of peak 10 of CMEAF

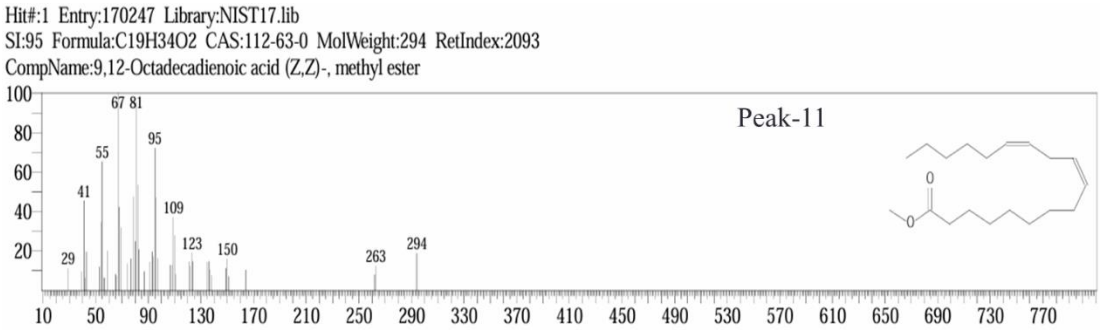

Figure 5.53: Mass fragmentation pattern of peak 11 of CMEAF

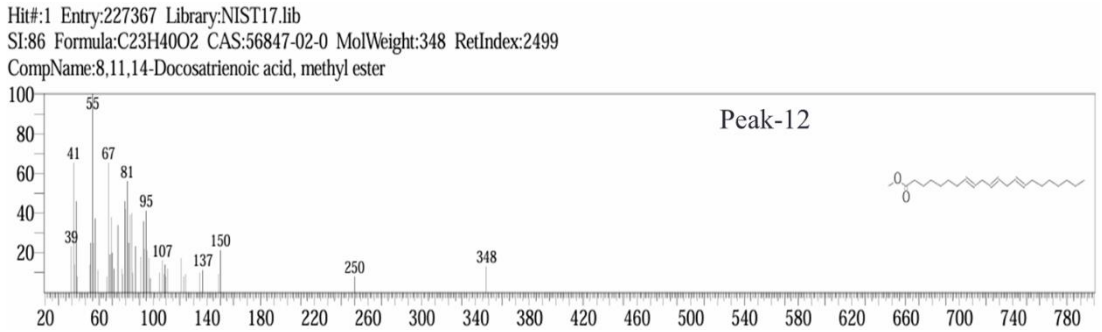

Figure 5.54: Mass fragmentation pattern of peak 12 of CMEAF

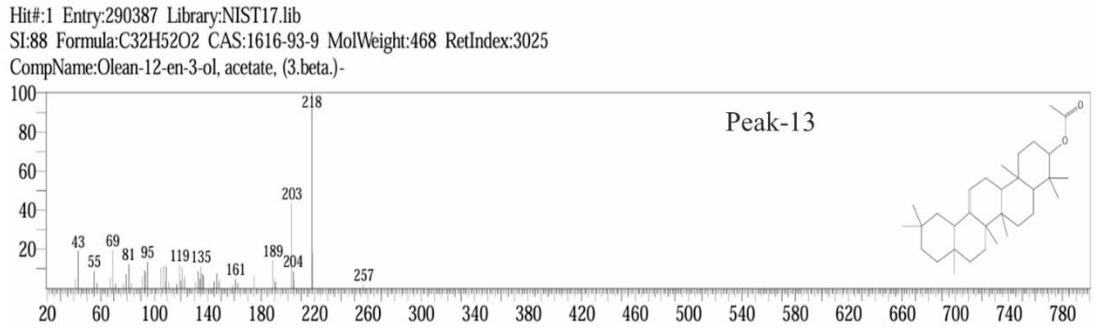

Figure 5.55: Mass fragmentation pattern of peak 13 of CMEAF

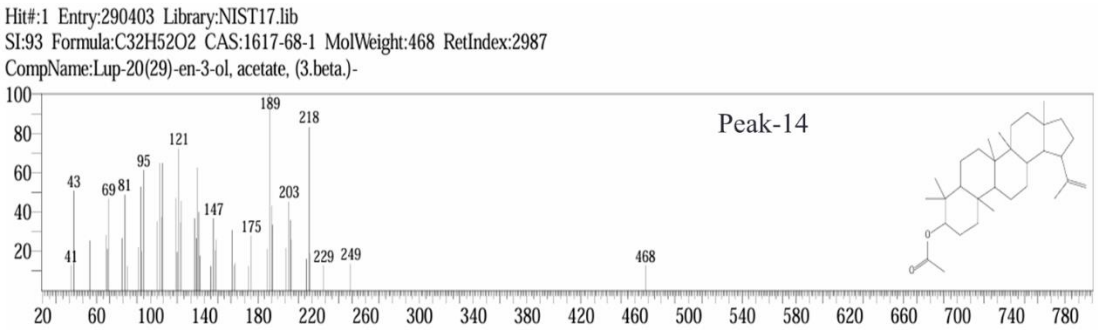

Figure 5.56: Mass fragmentation pattern of peak 14 of CMEAF

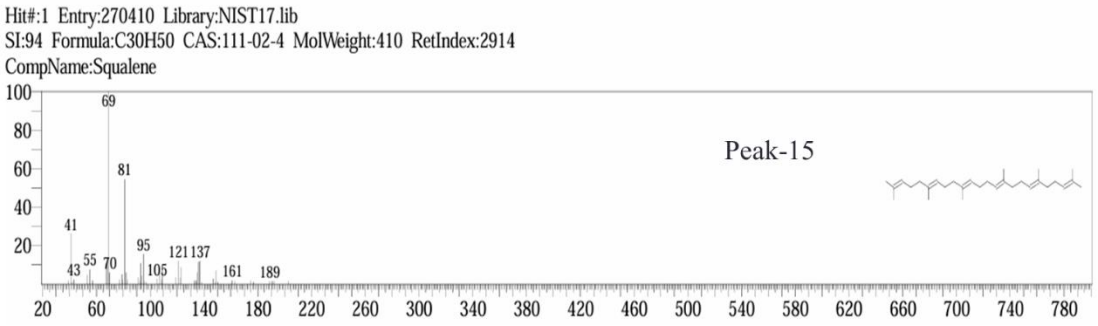

Figure 5.57: Mass fragmentation pattern of peak 15 of CMEAF

The ethyl acetate fraction of *C.medica* fruit underwent GC-MS analysis, which identified the presence of a variety of bioactive chemicals with varying biological activity. 5-Hydroxymethylfurfural (Zhao et al., 2013), Olean-12-en-3-ol, acetate, (3.beta.) (Parvez et al., 2018), Lup-20(29)-en-3-ol, acetate, (3.beta.) (Saputri et al., 2012), Maltol (Han et al., 2015), 8,11,14-Docosatrienoic acid, methyl ester (Chen et al., 2021), 9,12-Octadecadienoic acid (Z,Z)-, methyl ester (Rahman et al., 2014), Hexadecanoic acid, methyl ester (Ganesan et al., 2022), 4H-Pyran-4-one, 2,3-dihydro-3,5-dihydroxy-6-methyl (Kim et al., 2022), and Squalene (Muzalevskaya et al., 2015) all showed antioxidant activity. Numerous researchers have reported on the anticoagulant, anti-thrombotic, and antiplatelet activity of naringin (Huang et al., 2021), narirutin, hesperidin (Kuntić et al., 2011), quercetin (Manjunath & Thimmulappa 2022), rutin (Kuntić et al., 2011), kaempferol (Choi et al., 2015), etc.), caffeic acid (Nam et al., 2020), chlorogenic acid (Choi et al., 2017), salicylic acid (Roncaglioni et al., 1988), gallic acid (Chang et al., 2012), benzoic acid (Yun-Choi et al., 1996), trans-cinnamic acid (Wang et al., 2018), p-coumaric acid (Luceri et al. 2007), and trans-ferulic acid (Choi et al. 2018). The results of this investigation suggest that *C.medica* could contain bioactive compounds with anticoagulant

properties, providing a potential pathway for the development of novel anticoagulant drugs.

5.15.2 GCMA Analysis of ethyl acetate fraction of *T.undulata*

The running duration for the *T.undualta* butanol fractions in the gas chromatography-mass spectrometry (GC-MS) analysis was fifty minutes. It turned up 10 peaks in all (Figure 5.58). By comparing the peak retention duration, peak area (%), height (%), and mass spectral fragmentation patterns of these peaks with those of recognized compounds listed in the National Institute of Standards and Technology (NIST) library, the bioactive compounds were discovered. The butanol fraction of *T.undulata* included 10 recognized chemicals, according to the analysis (Table 5.35). The major phytoconstituents present in butanol fraction of *T.undulata* were Tetratetracontane (14.09) (Figure 5.66), 1-Octanol, 2,2-dimethyl- (13.7) (Figure 5.61), Triacontane, 1-iodo- (13.6) (Figure 5.67), Tetracontane (12.46) (Figure 5.65), Octacosane, 1-iodo / Hexacosane, 1-iodo (10.4) (Figure 5.68).

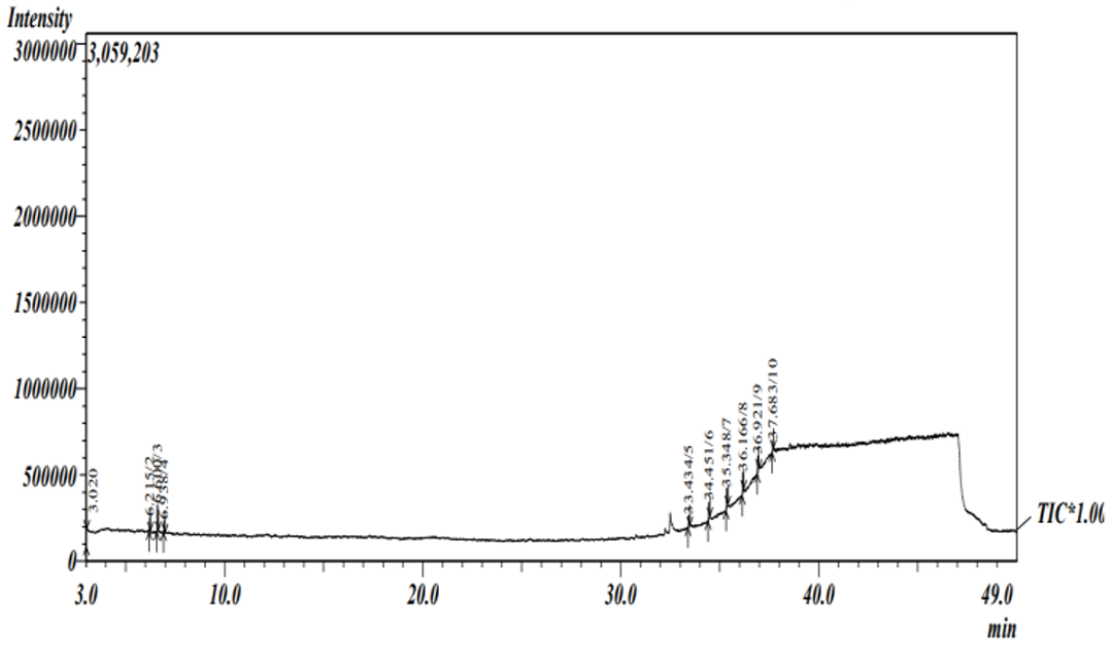

Figure 5.58: GC-MS chromatogram of butanol fraction of *T.undulata*

Table 5.35: Retention time, peak area, name of compound present in TUBUF

S/N	Retention time	Name of compound	Molecular Formula	Peak Area (%)	Reported biological activity
1	3.02	2-Trifluoroacetoxydodecane	C14H25F3O2	6.95	Antioxidant (Zagulyaeva et.al 2010)
2	6.215	Pentanedioic acid, 2-oxo-, dimethyl ester	C7H10O5	7.24	Antioxidant, Antiplatelet, Anticoagulant activity (Skorik et.al 2017, Shao et.al 2014)
3	6.6	1-Octanol, 2,2-dimethyl-	C10H22O	13.7	Anti-inflammatory & Analgesic activities (Li et.al 2016), Antimicrobial (Indrayan et.al 2010), Antioxidant (Coêlho et. Al 2022, Khodaie et.al 2015), Cytotoxic activity (Coêlho et. Al 2022)
4	6.938	3,3,6-Trimethyl-2,5-heptanedione	C10H18O2	7.14	Antimicrobial activity (Fazal et.al 2023)
5	33.434	Pentacosane	C25H52	8.28	Antibacterial Activity (Aboutabla et.al 2023, Chen et.al 2011, Aboaba et.al 2009), Antifungal activity (Zhang et.al 2014),

					Antiproliferative Activity (Gyawali et.al 2012), Antioxidant activity (Shao et.al 2014), Insecticidal efficacy (Benelli et.al 2019), Antibacterial Activity (Shukla et.al 2017), Antidiabetic activity (Selim & Sakeran 2014)
	34.451	Tetracontane	C40H82	12.46	Antifungal activity (Zhang et.al 2014), Antioxidant activity (Shao et.al 2014), Antiproliferative Activity (Gyawali et.al 2012), Insecticidal efficacy (Benelli et.al 2019), Antibacterial Activity (Shukla et.al 2017), Anticholinesterase Activities (Ertas et.al 2014), Breast cancer (Hussein et.al 2020)
7	35.348	Tetratetracontane	C44H90	14.09	Anticholinesterase Activities (Ertas et.al 2014), Antimicrobial

					activity (Kayode et.al 2018) Insecticidal efficacy (Benelli et.al 2019),
8	36.166	Triacontane, 1-iodo-	C30H61I	13.6	Antibacterial Activity (Shukla et.al 2017)
9	36.921	Octacosane, 1-iodo / Hexacosane, 1-iodo	C28H57I / C26H53I	10.4	Anti-α-glucosidase & Anti-cyclooxygenase activity (Harrabi et.al 2021)
10	37.683	Dotriacontane	C32H66	6.13	Antimicrobial, Antioxidant, Antispasmodic, Antibacterial, & Antiviral (Devi et. Al 2014), Anticandidal Activity (Oladosu et.al 2009), Antifungal anti-inflammatory, Cytotoxic activity (Harris 1992)., Anti-α-glucosidase& Anti-cyclooxygenase activities (Harrabi et.al 2021)

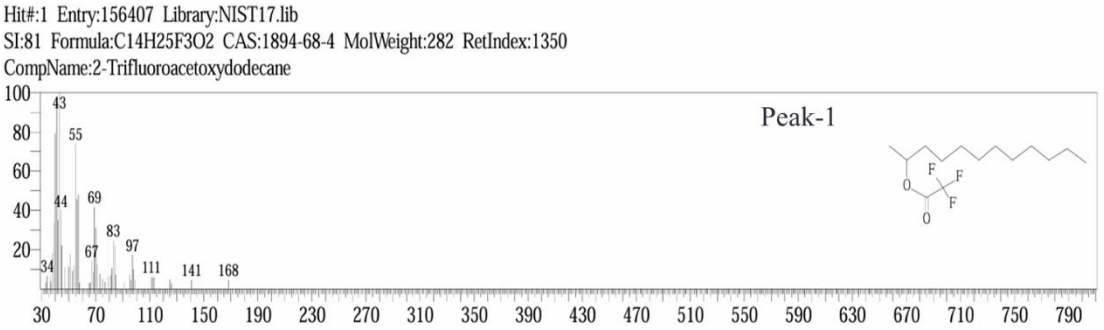

Figure 5.59: Mass fragmentation pattern of peak 1 of TUBUF

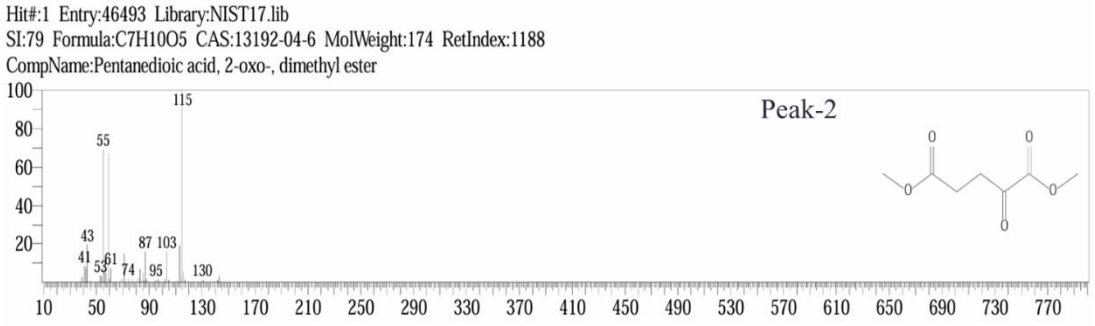

Figure 5.60: Mass fragmentation pattern of peak 2 of TUBUF

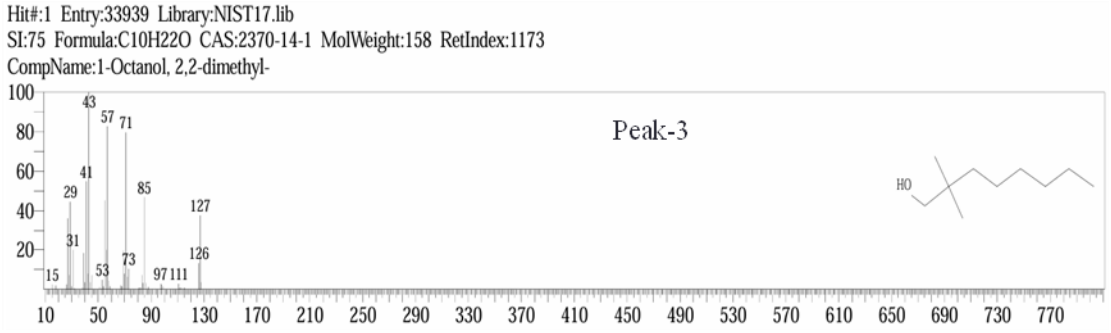

Figure 5.61: Mass fragmentation pattern of peak 3 of TUBUF

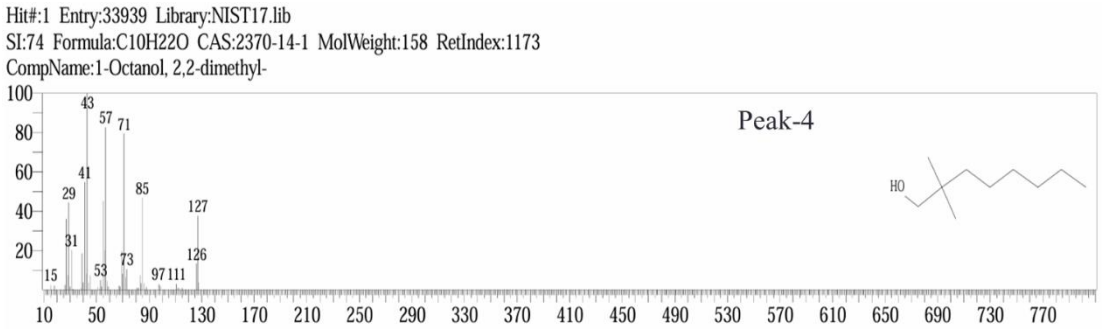

Figure 5.62: Mass fragmentation pattern of peak 4 of TUBUF

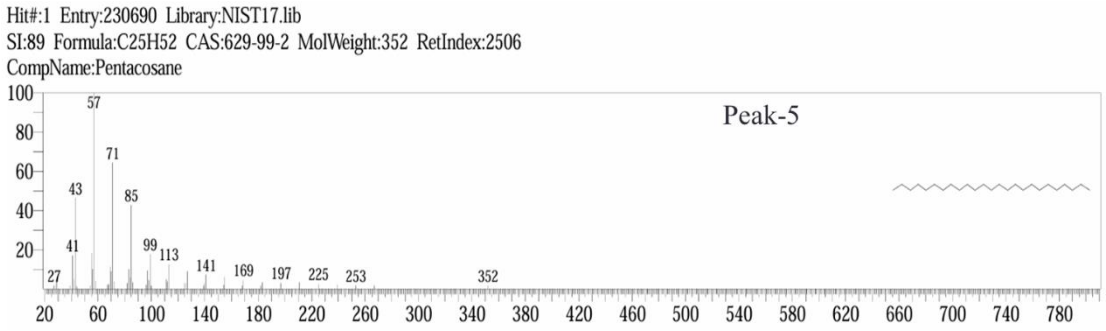

Figure 5.63: Mass fragmentation pattern of peak 5 of TUBUF

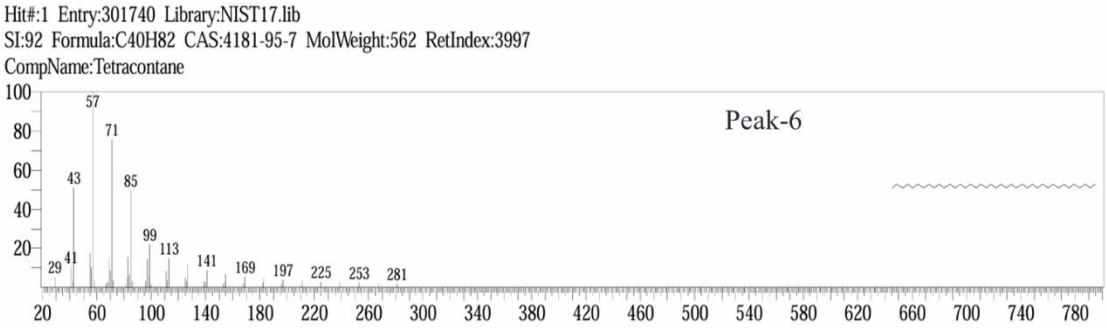

Figure 5.64: Mass fragmentation pattern of peak 6 of TUBUF

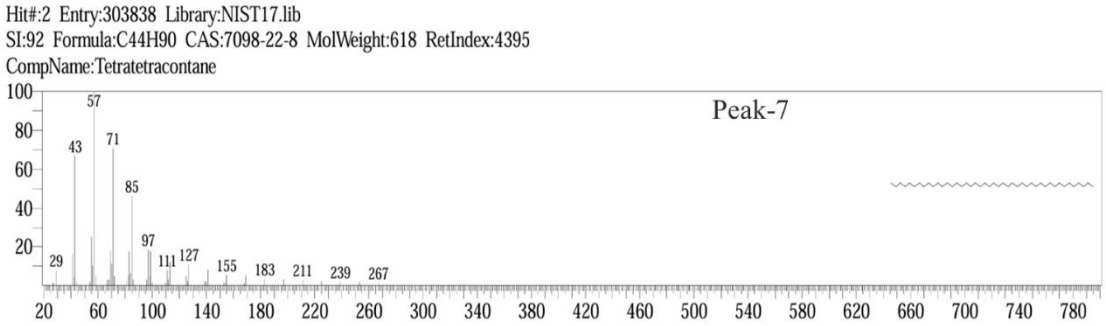

Figure 5.65: Mass fragmentation pattern of peak 7 of TUBUF

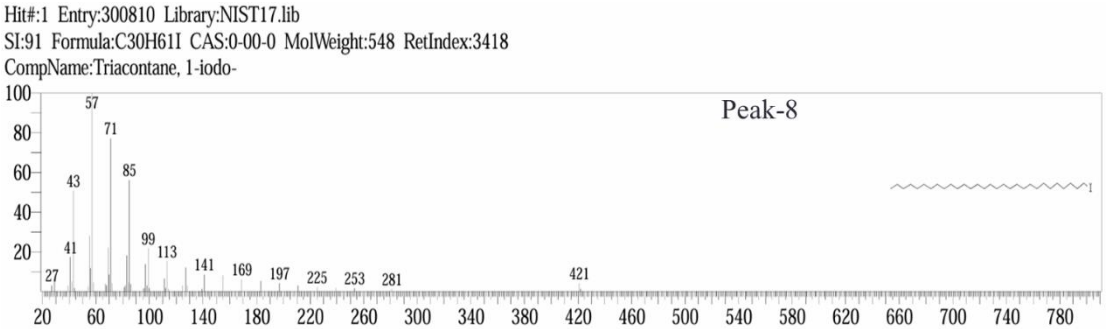

Figure 5.66: Mass fragmentation pattern of peak 8 of TUBUF

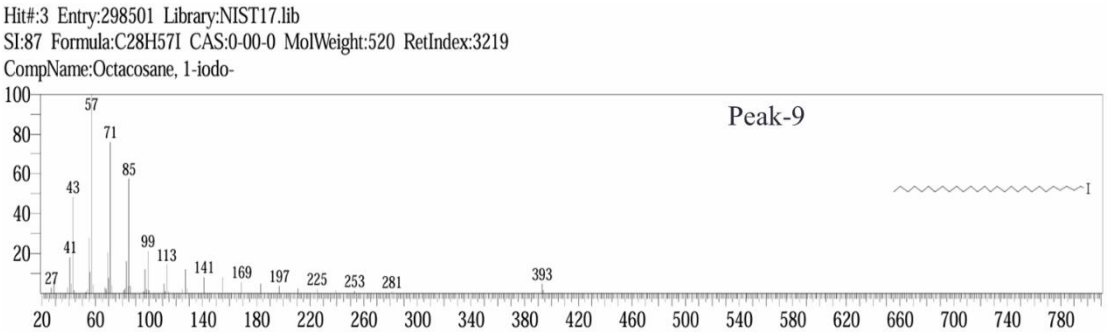

Figure 5.67: Mass fragmentation pattern of peak 9 of TUBUF

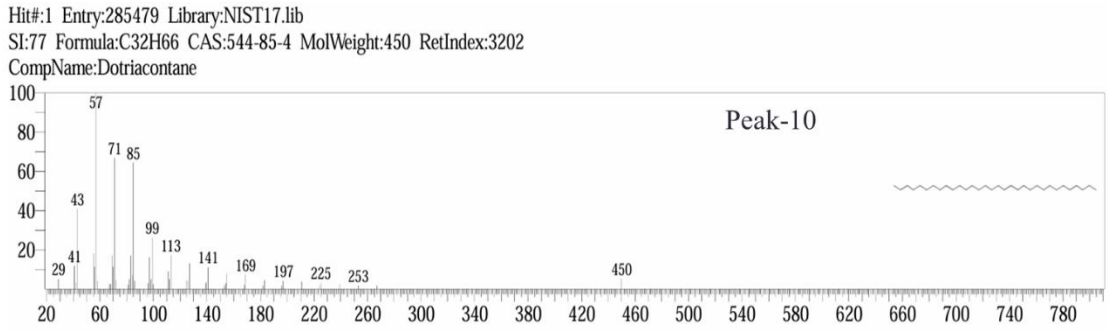

Figure 5.68: Mass fragmentation pattern of peak 10 of TUBUF

The butanol fraction of *T.undulata* bark underwent GC-MS analysis, which identified the presence of a variety of bioactive chemicals with varying biological activity. Antioxidant activity was found in Pentanedioic acid, 2-oxo-dimethyl ester, 2-Trifluoroacetoxydodecane, 1-Octanol, 2,2-dimethyl, Pentacosane, Tetracontane, and Dotriacontane (Add Reference). Furthermore, it has been found that pentanedioic acid, 2-oxo-dimethyl ester, has antiplatelet and anticoagulant properties (Skorik et al., 2017, Shao et al., 2014). Heptacosane, Tecoside, Lapachol, Dehydrotectol, Undulatoside A, 1-Triacontanol, 3,4-Dimethoxybenzoic acid, 1-Octacosanol, Triacontane, Nonacosane, Tecomelloside, Ferulic acid, beta-Sitosterol, Daucosterol, Rutin, and beta-Sitosterol-beta-D-glucoside are just a few of the compounds in *T.undulata* bark that have been identified in earlier studies by Karthikeyan Mohanraj et al. Ferulic acid and its derivatives have been shown to have antithrombotic and anticoagulant effect by studies by Shuai & Yue 2018, Jun-Hui Choi et al, and Laibin Zhang et al. Choi et al. 2018, Zhang & Lv 2018. Furthermore, research by Gogoi et al. (2018) and Salunkhe et al. (2018) has shown that beta sitosterol has antithrombotic and anticoagulant properties. Vitamin K quinone reductase and vitamin K epoxide reductase is inhibited by lapacol (Preusch & Suttie 1984). Moreover, longer PT and APTT times have been linked to 1-Triacontanol,

3,4-dihydroxybenzoic acid, and rutin (Ganeshpurkar & Saluja 2017, Xu et.al 2016). The findings of this study indicate that *T.undulata* may contain bioactive substances with anticoagulant qualities, offering a possible avenue for the creation of new anticoagulant medications.

5.16 LCMS/MS ANALYSIS:

5.16.1 LCMS/MS analysis of ethyl acetate fraction of *C.medica*

After individually injecting the standard solutions of the analytes (rutin, quercetin, and gallic acid) and CMEAF into the mass spectrometer, the optimal mass parameters (CE) were discovered. For the quantification studies, the transitions m/z 611.30/300.0 for rutin, 303.10/153.0 for quercetin, and 169.0/125.10 for gallic acid were selected. Figure 5.69 displays the analytes' product ion mass spectrum.

Ammonium formate and formic acid were two of the mobile phase additions that were evaluated to boost the analytes' signal response. Ammonium formate did not significantly affect these flavonoids, however, 0.2% formic acid in the mobile phase was shown to be able to decrease the chromatographic time and improve the peak shape of the analytes. Using Kintex PFP (50mm x 4.6mm, 2.6 μ) column, a straightforward elution method produced a satisfactory separation in 3 minutes. Using the mobile phase prevented any endogenous components from interfering with the analytes, as Figure 5.66 illustrates. Gallic acid, quercetin, and rutin had retention times of 0.602, 0.625, and 0.598 minutes, respectively.

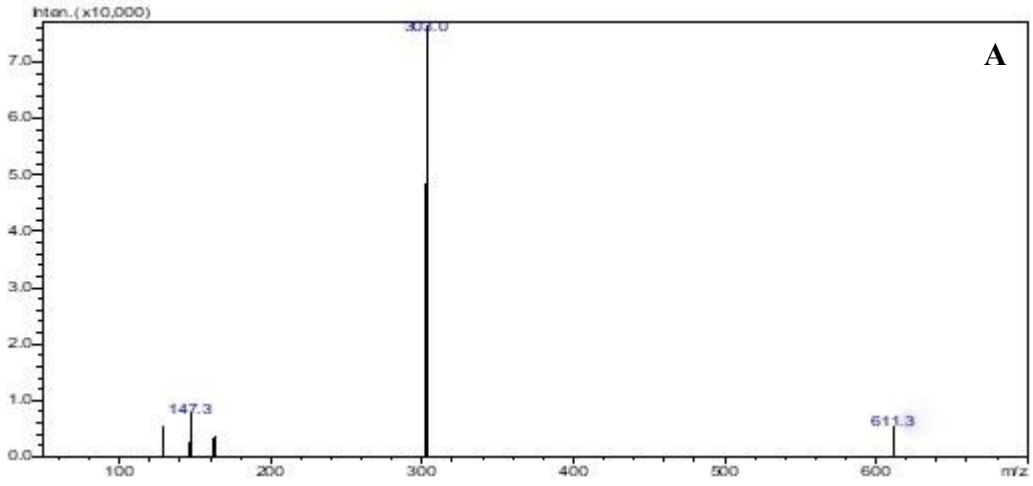

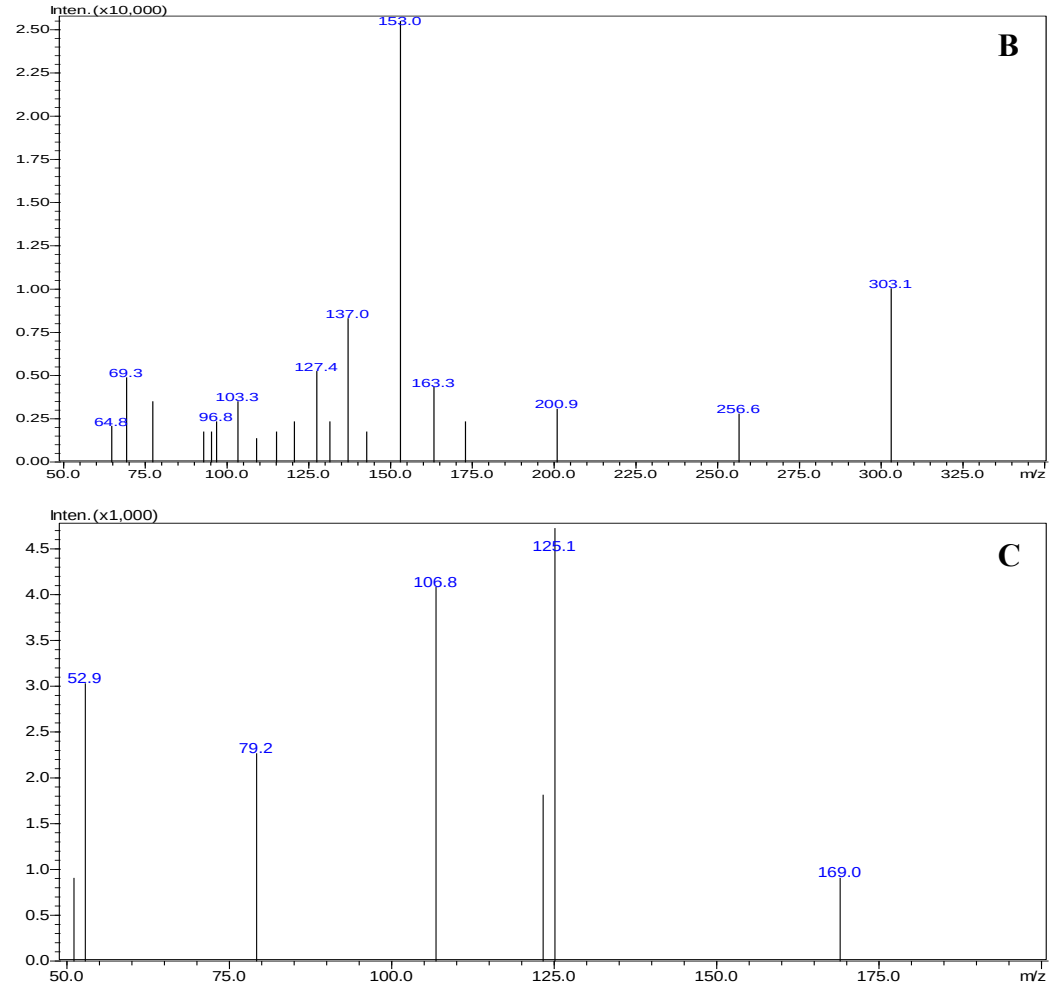

Figure 5.69: Representative MRM chromatograms of rutin (A), quercetin (B), gallic acid (C)

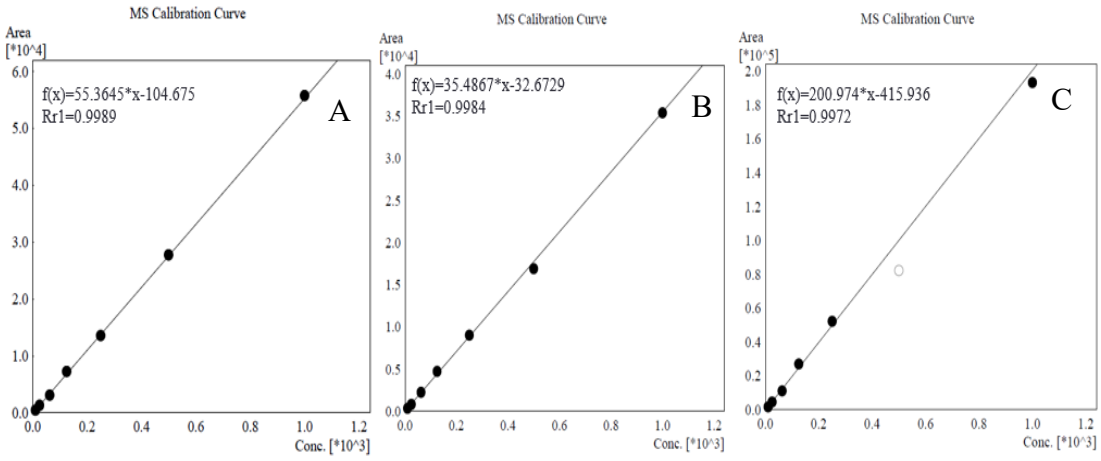

Figure 5.70: MS Calibration Curve of A) Gallic Acid B) Quercetin C) Rutin

Table 5.36 displays the regression equations, linear ranges, correlation coefficients (r), and LLOQ. Within the verified concentration range, good linearity was attained.

Table 5.36: The calibration curves, linear ranges, and LLOQs of the rutin, quercetin, and gallic acid

Compound	Regression equation	*r*	Linear range (ng mL^{-1})	LLOQ (ng mL^{-1})
Rutin	y=200.974*x-415.936	0.9972	200-25000	1
Quercetin	y=35.4867*x-32.6729	0.9984	200-25000	1
Gallic acid	y=55.3645*x-104.675	0.9989	200-25000	1

The concentrations of gallic acid, quercetin, and rutin in CMEAF were determined to514.543 ng, 67.839 ng, and 53.691 ng, respectively.

5.17 Isolation and Characterization of Bioactive Compound from ethyl acetate fraction of *Citrus medica*

5.17.1 Isolation of bioactive compound from ethyl acetate fraction of *C.medica*

The TLC analysis was performed for a potent ethyl acetate fraction of *C.medica* by using Toluene: Ethyl acetate: Formic acid (07:03:0.5) solvent system. The plate was scanned at 255 and 366 nm using CAMAG TLC Scanner-3 and LINOMAT-V. The peak area of each compound separated on the plate was recorded and the highest peak area compound (34.12 %, 16.14 %, and 8.98%) was marked with the pencil as shown in Figure 5.71 and Table 5.37.

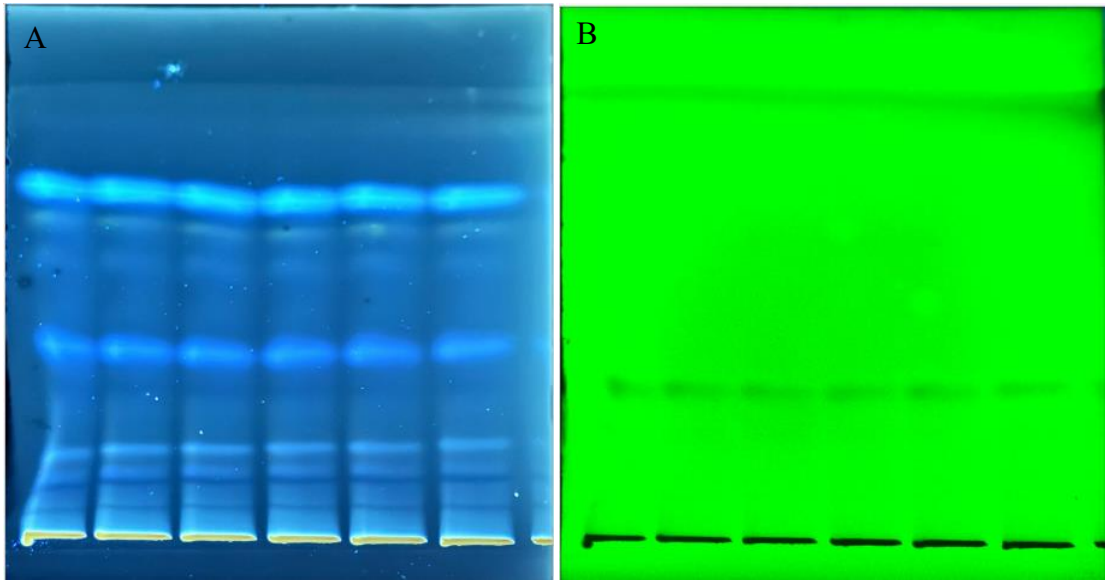

All Track - CMEAF (1 mg/ml concentration)

Figure 5.71: HPTLC of Ethyl acetate fraction of *C.medica* A) at 254 nm B) at 365 nm

Table 5.37: Rf value and percentage peak area of ethyl acetate of *C.medica*

Isolated Compound number	Rf value	% Area
1	0.23	16.14
2	0.38	34.12
3	0.62	8.98

5.17.2 Characterization of bioactive compound from ethyl acetate fraction of *C.medica*

5.17.2.1 HPTLC analysis

Based on HPTLC fingerprinting, we discovered that the three isolated compounds of *C.medica* ethyl acetate have different Rf values as shown in Table 5.38. Among these, compound 2 has the same Rf value (0.52) as the ferulic acid standard (Rf = 0.54) at 254 and 365 nm wavelengths (Figure 5.72A and B) with the highest peak area of 78.06% as shown in Table 5.38 which might be responsible for anticoagulant activity. Using HPTLC to further purify and confirm the identity of compound 2 ensures that we accurately identify and validate ferulic acid in the *Citrus medica* ethyl acetate fraction. This approach corroborates the findings from HPTLC and strengthens the evidence supporting the presence of ferulic acid in the fraction.

Table 5.38: Rf value and percentage peak area of isolated compounds from CMEAF and ferulic acid

Isolated Compound number	Track No	Rf value	% Area
1	1	0.23	16.14
2	2	0.54	78.12
3	3	0.62	28.98
Std (Ferulic Acid)	4	0.56	90

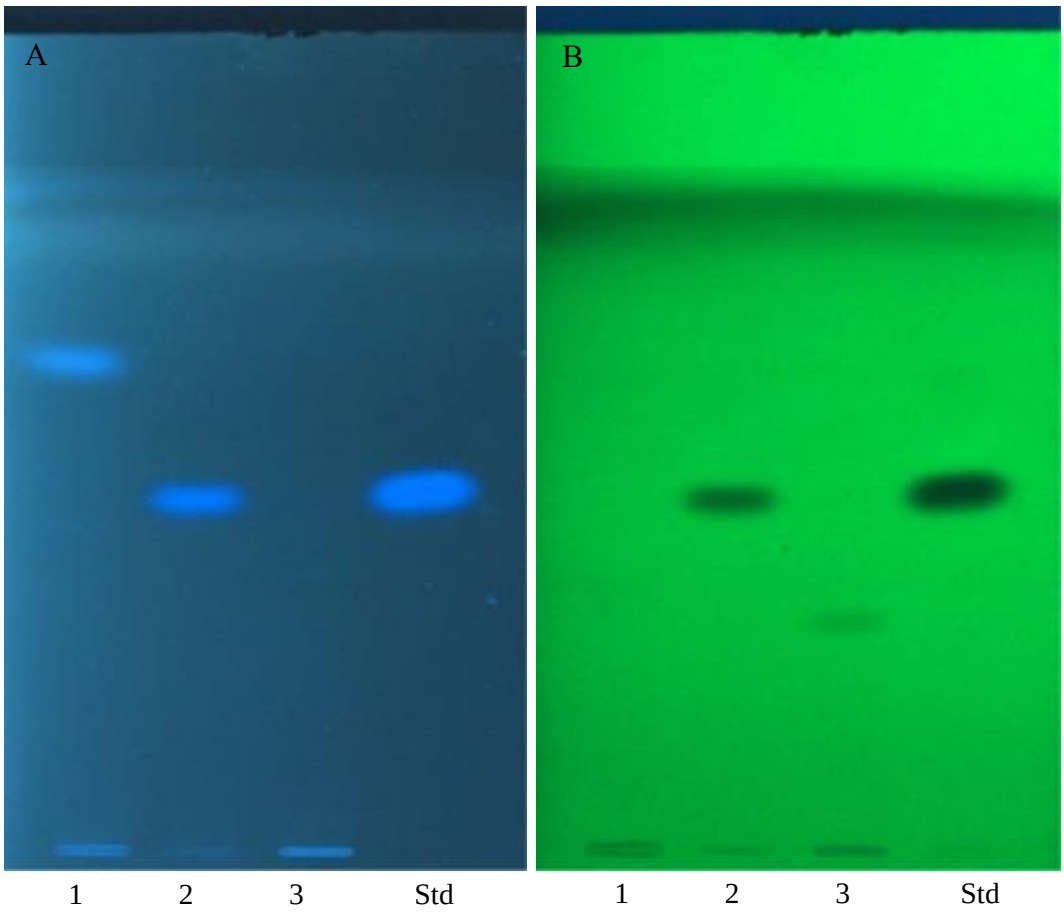

Track 1-Isolated Compound-1, Track 2- isolated Compound-2, Track 3- isolated Compound-3, Track 4 -Standard (Ferulic acid)

Figure 5.72: HPTLC of isolated compounds from CMEAF and ferulic acid A) at 254 nm B) at 365 nm

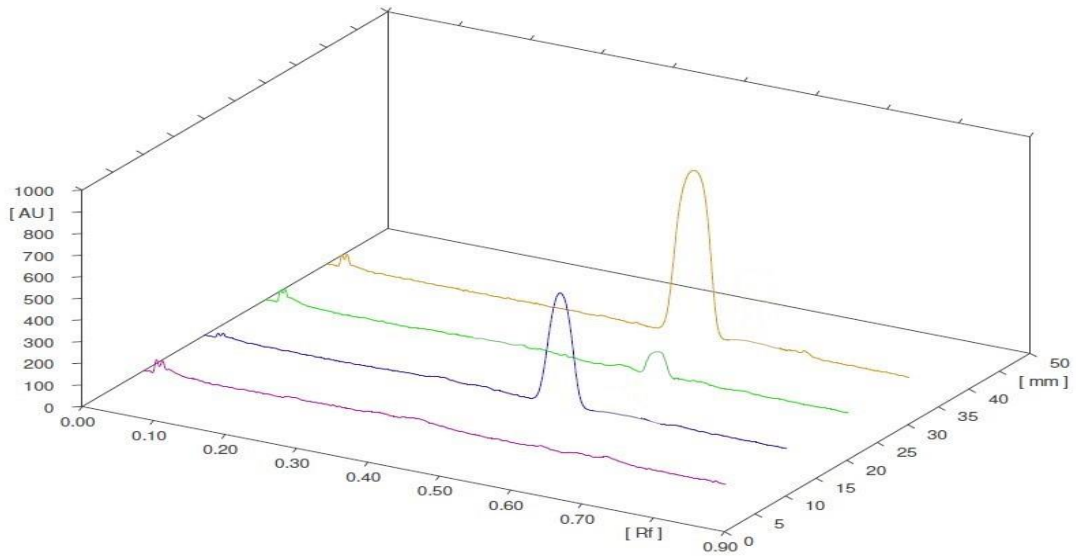

Figure 5.73: 3D chromatogram of isolated compounds from CMEAF and ferulic acid

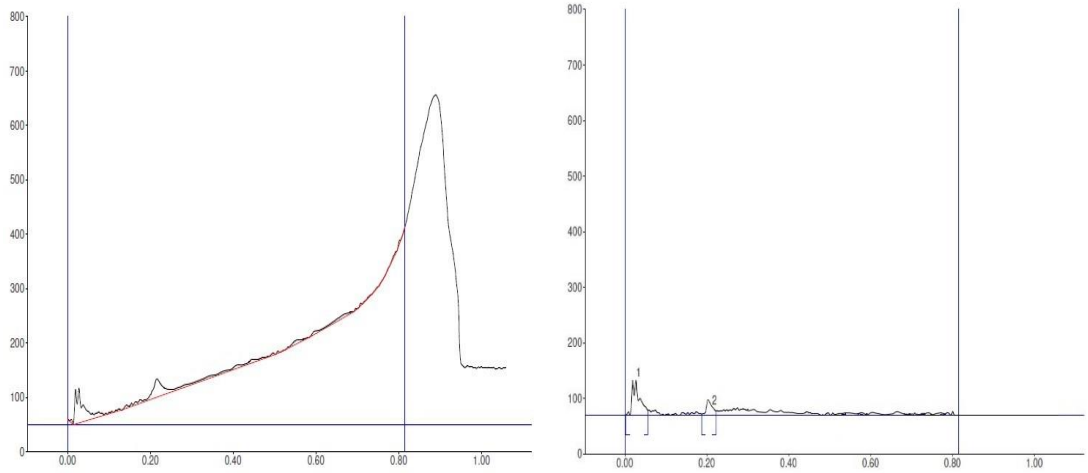

Figure 5.74: Chromatogram of Isolated compound 1 from CMEAF

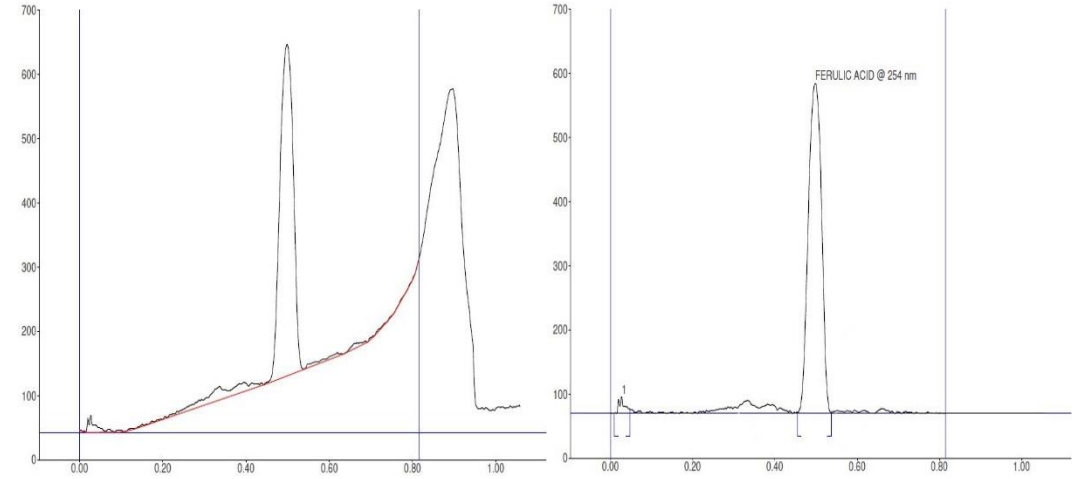

Figure 5.75: Chromatogram of Isolated compound 2 from CMEAF

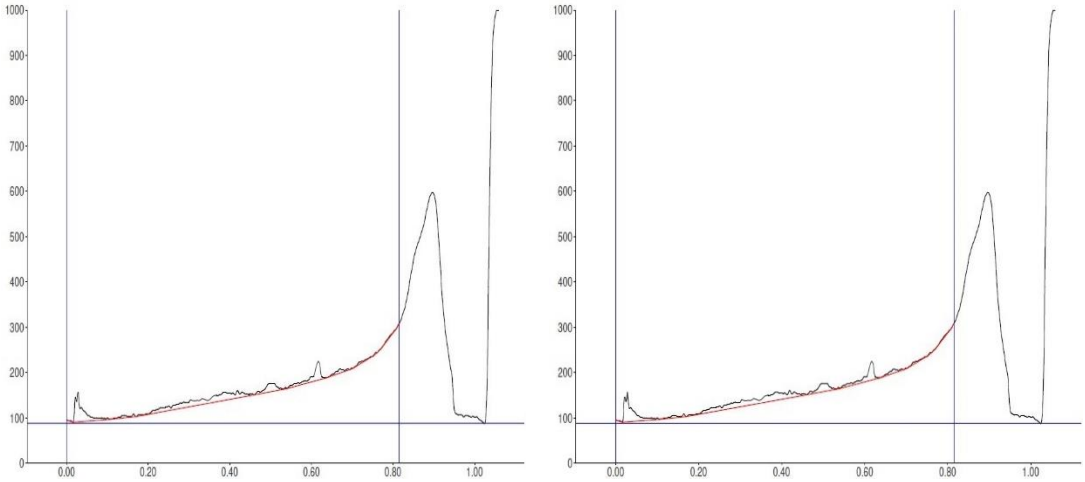

Figure 5.76: Chromatogram of Isolated compound 3 from CMEAF

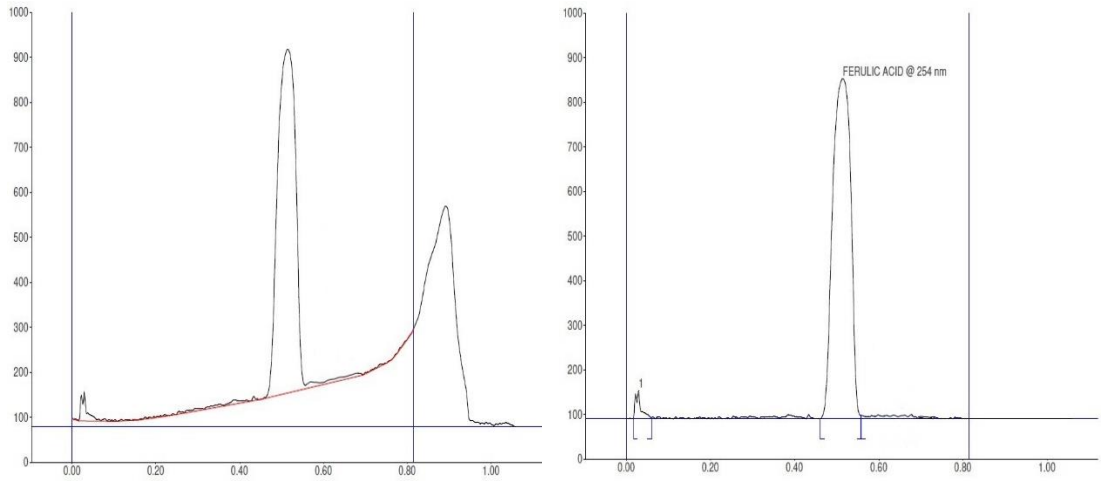

Figure 5.77: Chromatogram of Ferulic acid standard

5.17.2.2 FTIR analysis

The % yield of compound 2 were found to be highest among other two compounds. Hence, Only compound 2 was selected for further characterization. The FTIR spectrum of the isolated compound 2 from ethyl acetate fraction of *Citrus medica* exhibited characteristic absorption bands indicative of various functional groups present in the sample (Figure 5.78). The spectrum revealed prominent peaks at specific wavenumbers, corresponding to the vibrational modes of the molecular bonds within the compounds.

Absorption bands in the FTIR spectrum were indicative of different functional groups found in the ethyl acetate fraction. The stretching vibrations of C-H bonds in alkyl groups were identified as the cause of bands seen at about 2950-2850 cm^-1, which suggested the existence of aromatic organic substances. The signal located approximately at 3400 cm^-1 suggested the existence of hydroxyl (-OH) groups, which are frequently seen in phenolic substances such as ferulic acid. The distinctive peaks seen in the FTIR spectrum verified that ferulic acid was present in the ethyl acetate fraction of *Citrus medica*. Absorption bands are commonly observed in ferulic acid at approximately 1740 cm^-1, which is associated with the stretching vibration of the carbonyl group (C=O) within the phenolic ring. Ferulic acid is further confirmed by attributing peaks between 1600 and 1650 cm^-1 to the stretching vibrations of aromatic rings (Silverstein et.al 2014, Aarabi et.al 2016).

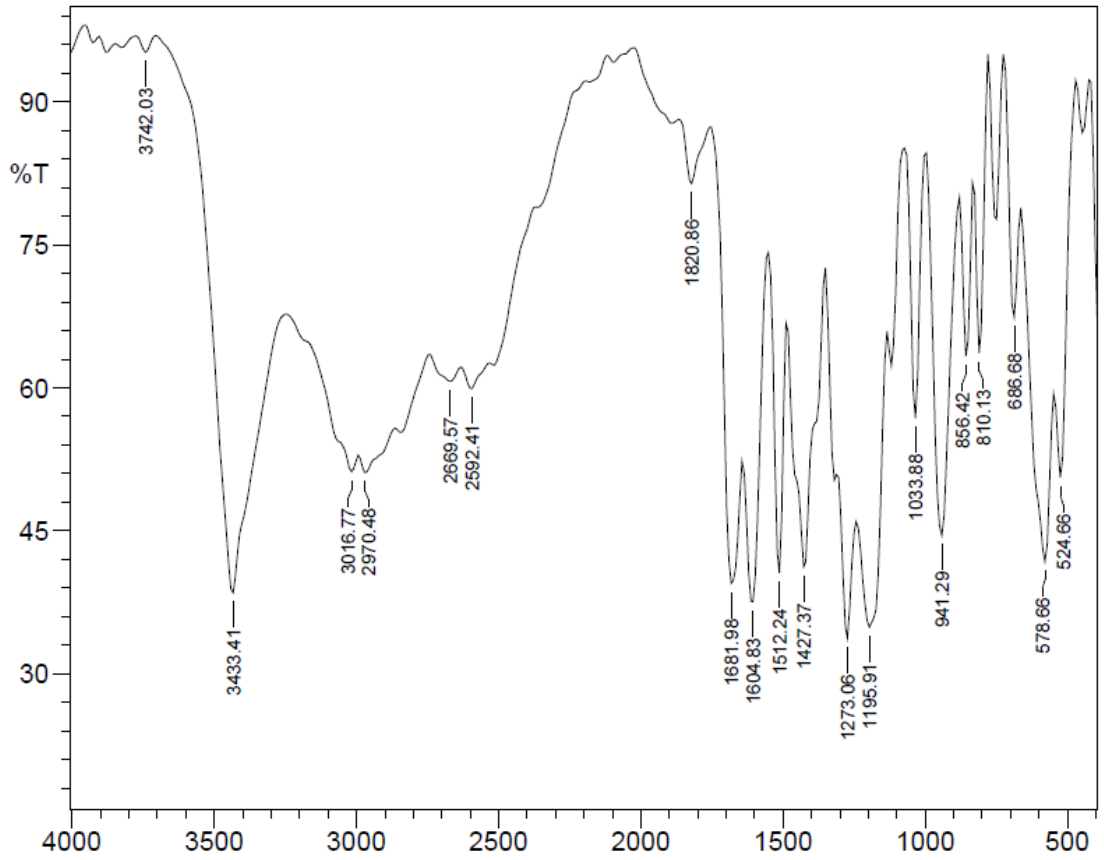

Figure 5.78: FTIR of isolated compound 1 from ethyl acetate fraction of *C.medica*

The ethyl acetate fraction of *C.medica* FTIR spectrum was compared to reference spectra of ferulic acid and other well-known *Citrus medica* compounds. Based on the similarity of the absorption bands and peak positions, this comparison assisted in the identification and confirmation of ferulic acid in the sample.

Important ramifications for *Citrus medica's* possible pharmacological and therapeutic qualities result from the presence of ferulic acid. *Citrus medica* extracts may be therapeutically beneficial because of ferulic acid, which is known to have hypoglycemic, anti-inflammatory, antioxidant (Roghani et.al 2020), Anti-apoptotic activities (Chowdhury et.al 2019), anticoagulant (Zhang & Lv 2018), anti-platelets (Li et.al 2021), and neuroprotective activities (Thapliyal et.al 2021).